치의과학박사 학위논문

The role of Pin1-mediated prolyl isomerization in bone formation

뼈 형성에서 Pin1 매개 프롤린 이성질화의 역할

2018년 2월

서울대학교 대학원

치의과학과 분자유전학 전공

신 혜 림

Abstract

The role of Pin1-mediated isomerization in bone formation

Hye-Rim Shin

Department of Molecular Genetics

The Graduate School

Seoul National University

(Directed by Prof. Hyun-Mo Ryoo, D.D.S., Ph.D.)

One of the most reported post-translational modifications (PTMs) regulation of protein in the cell is prolin-directed phosphorylation, these phosphorylated resides also can be the targets of enzyme for other PTMs. Pin1 is an isomerase that recognizes phosphorylated Ser/Thr-Pro residues and causes the structural change of protein. Our previous studies have shown that Pin1 deficient exhibited a wide range of abnormal bone phenotypes. Moreover, in the signaling pathways such as FGF, BMP and PTH, which are responsible for osteoblast differentiation, isomerization of the molecule by Pin1 plays important role.

Wnt/β-catenin signaling pathway, in which β-catenin nuclear localization is a critical step, also plays a major role in the control of

osteoblast differentiation. However, the association of Pin1 with Wnt/β-catenin signaling pathway during bone development and detailed mechanism is not clear. In Part 1, we observed a marked reduction of β-catenin in osteoblasts of Pin1 null mice tibia. From MC3T3-E1 cells, transcription activity, the nucleus β-catenin level and the target gene expression of β-catenin were all decreased when the activity of Pin1 was reduced by si RNA or by inhibitor. We also demonstrated that Pin1 directly interacted with β-catenin, and the isomerized β-catenin which could not bind to nuclear adenomatous polyposis coli (APC) only can be retention and act as a transcription factor in the nucleus. These results might explain the decrease of β-catenin ubiquitination and showed that Pin1 is a critical factor that can regulate bone formation regulated by Wnt/β-catenin signaling pathway.

In part 2, the importance of Pin1 in osteogenesis was confirmed in craniosynostosis (CS) disease animal model. CS is characterized by the premature closure of craniofacial sutures. It is follows autosomal dominant inheritance pattern, and the mutation of the FGFR2 gene is mainly the genetic cause of it. This study focused on the change of coronal suture fusion which is the major phenotype of Apert syndrome (AS) using S252W gain of function mutation of FGFR2. We aimed to treat CS caused by over-

activated FGF/FGFR signal, and it was targeted that inhibiting Pin1-induced isomerization of Runx2 in FGF signaling pathway. As a result, we showed that fusion of coronal suture can be restored to close to the normal phenotype when the $FGFR^{2S252W+}$ and the $Pin1^{+/-}$ genotype are present simultaneously. The similar results were obtained when juglone, Pin1 inhibitor, was administered to the fetus of $FGFR2^{S252W/+}$ mice for drug therapy.

Collectively, we demonstrated here that isomerization of β-catenin through direct interaction of β-catenin with Pin1 during osteoblast differentiation is an important factor controlling nuclear β-catenin retention and stability. In addition, we demonstrated the drug target of CS by proving that the inactivation of Pin1 causes the recovery of disease through gain of function mutation in FGFR2.

Keyword : Isomerization, Pin1, Wnt/β-catenin signaling, fibroblast growth factor receptor (FGFR), bone formation, craniosynostosis**.**

Student Number : 2011-23826

Table of Contents

List of Figures

Part 1. Pin1-mediated modification prolongs the nuclear retention of β-catenin in Wnt3a-induced osteoblast differentiation

Part 2. Pin1 is a new therapeutic target of craniosynostosis

List of Tables

Part 1. Pin1-mediated modification prolongs the nuclear retention of β-catenin in Wnt3a-induced osteoblast differentiation

Part 2. Pin1 is a new therapeutic target of craniosynostosis

I. Abbreviations

PTM post-translational modification

CDK cyclin-dependent kinase

MAPK mitogen-activated protein kinase

GSK3 glycogen synthase kinase 3

PLK polo-like kinase

PPIase peptidyl-prolyl cis-trans isomerase

Pin1 peptidyl-prolyl cis-trans isomerase NIMA-interacting 1

Pro proline

Ser serine

Thr threonine

MSC mesenchymal stem cell

BMP bone morphogenetic protein

FGFR fibroblast growth factor receptor

PTH parathyroid hormone

TGF-β transforming growth factor-β

Runx2 Runt-related transcription factor 2

ERK extracellular signal-regulated kinase

LEF/TCF lymphoid-enhancer factor/T cell factor

LRP lipoprotein-receptor-related protein

APC adenomatous polyposis coli

CHX cycloheximide

WT wild type

MEF mouse embryonic fibroblast

HEK293 human embryonic kidney 293

FBS fetal bovine serum

LMB leptomycin B

CRM1 chromosomal region maintenance)/exportin 1 protein

ALP alkaline phosphatase

IHC immunohistochemistry

IP immunoprecipitation

IF immunofluorescence

GST-PD glutathione-S-transferase pulldown

DTM dependentamethylene thiuram monosulfide

NLS nuclear localization signal

NES nuclear export signal

CsA cyclosporine A

CS craniosynostosis

AS apert syndrome

IgII immunoglobulin-like domain II

H&E staining hematoxylin and eosin staining

Dusp dual specificity phosphatase

Spry sprouty RTK signaling antagonist

IC50 inhibitory concentration 50

II. Literature review

II-1. Post-translational modifications (PTMs)

PTMs are alterations that occur in a protein, which are catalyzed by enzymes after its translation by ribosomes (Jensen, 2006). PTM generally represents that functional groups such as phosphorylation and acetylation are added to the protein covalently, but also represents proteolytic processing and folding processes essential for a protein to mature functionally (Snider and Omary, 2014).

These PTMs orchestrate every activity of a protein over its total lifespan-from subcellular localization to protein-protein interaction, activity and protein stability (Hansen and O'Shea, 2015). Chemical alterations that usually occur during the PTM of protein include phosphorylation, methylation, acetylation, ubiquitination, nitrosylation, glycosylation, and lipidation (Duan and Walther, 2015). This modification modulates protein levels and functions to constitute a central mechanism that allows cells to respond quickly to developmental or environmental impetuses. Thus, PTMs are important steps leading to cell biology such as signal transduction, development, cell structure, mitosis, DNA repair, and others (Duan and

Walther, 2015). Many previous reports have studied on these varied PTMs effects. In this study, we focus on protein phosphorylation and consequent isomerization PTM process.

Protein phosphorylation is the first PTM to be researched when observing the control of protein activity. It regulates activation of the signaling pathway in response to extracellular and intracellular impetuses to adjust cell growth, proliferation and survival (Brognard and Hunter, 2011). These signaling actions frequently involve structural modifications in protein kinases and their substrates (Filtz et al., 2014). Such conformational changes act for s signal transduction mechanisms that can control both the spatial and temporal activity of proteins in physiological processes and diseases such as cancer (Lu and Hunter, 2014). Structural interconversions of protein involved in signaling pathway a key part in many aspects of cell functioning, which is mainly controlled by peptidyl prolyl cis-trans isomerization (Lu and Hunter, 2014).

Pro-directed protein phosphorylation is a shared and crucial signaling mechanism that plays an essential roles in various cellular progressions (Lu and Hunter, 2014). Enzymes that induce such phosphorylation belong to a large superfamily of Pro-directed protein kinases, which include CDKs, MAPKs, GSK3 and PLKs (Lu and Hunter, 2014). Pro exists as two different

conformers, cis and trans isoforms, which is fundamentally slow intertransformed by PPIase enzymes (Creese and Cooper, 2016; Lu et al., 2007).

II-2. Peptidyl-prolyl cis-trans isomerase NIMA-interacting 1, Pin1

PPIases are enzymes that catalyze the cis-trans isomerization and have the three conserved PPIase families such as cyclophilins, FK506-binding proteins and parvulins (Bell et al., 1994). Pin1 is the parvulin subfamily of several PPIases that recognizes and isomerizes specific phosphorylated Ser or Thr residues in pSer/Thr-Pro peptide sequences (Thorpe et al., 2001). The cis-trans conversion is much more thermodynamically disturbed when Pro is located after the phosphorylated Ser or Thr residue. Thus, common PPIase such as cyclophilins and FK506-binding proteins become inaccessible and only Pin1 specifically recognizes and isomerizes pSer/Thr-Pro residues (Lu and Hunter, 2014).

Pin1 binds specifically to phosphorylated Ser/Thr-Pro motifs through its WW domain of the N-terminal and causes cis/trans isomerization through its PPIase domain of the C-terminal (Lu and Zhou, 2007). The conformational change of the protein induced by Pin1 following

phosphorylation is a key step to control diverse intracellular processes as well as functioning as a molecular timer (Lu and Zhou, 2007). In addition, Pin1 has to be tightly regulated at several levels, and if not properly regulated, is known to increase the risk of developing diseases such as cancer and Alzheimer's disease (Balastik et al., 2007).

II-3. Role of Pin1 in osteoblast differentiation signaling pathways

Osteoblasts are differentiated from MSCs which are multipotent progenitors that can commit to osteoblast, chondrocyte, adipocyte, and several other lineages (Lindner et al., 2010). Osteoblasts may form bone through two pathways. One of them is directly via intramembranous bone formation and the other is from a chondrocyte-derived cartilage template during endochondral bone formation (Long and Ornitz, 2013). These processes are very carefully controlled through several signaling pathways. Remarkable paracrine signaling pathways include BMP signaling, FGF/FGFR signaling and PTH signaling pathway (Ornitz and Marie, 2015).

BMPs were first purified from bovine bone and is one of the as members of the TGF-β superfamily of multifunctional cytokines (Kirkbride et al., 2008). In our previous paper, canonical BMP signaling

pathway through Smad 1/5 was shown to be regulated by Pin1. Smad 1/5 are isomerized and stabilized by Pin1, and results in promotes osteoblast differentiation and bone mineralization (Yoon et al., 2015).

FGF/FGFR signaling pathway is an critical process for osteoblast differentiation and bone formation. FGF2 is one of the most important FGFs and has been reported to be mainly expressed in bone cells and tissues (Islam et al., 2017). Our previous papers showed that Runx2, one of the most significant factors in the bone development, is transcriptionally activated through FGF2 signaling pathway, and Erk/MAP Kinase-mediated phosphorylation of Runx2 is critical (Park et al., 2010). Based on this, we observed that inhibition of Pin1 resulted in destabilization of Runx2 in vitro and Pin1-mediated isomerization of Runx2 is crucial for the transactivation activity of Runx2 (Yoon et al., 2014; Yoon et al., 2013). Hence, prolyl isomerization event is part of a cascade of consecutive PTMs that determine osteoblastic cell differentiation.

Wnt signaling pathway is also important in osteoblast differentiation and Wnt signaling pathway is historically catagorized as a canonical or non-canonical signaling (Widelitz, 2005). Canonical Wnts signal through β-catenin, and it is important that β-catenin acts as a transcription factor in the nucleus with TCF/LEF (Shin et al., 2016). Genetic studies of the LRP in

both humans and mice showed that Wnt is a effective anabolic stimulus for bone (Gong et al., 2001; Little et al., 2002; Shin et al., 2016). Especially, Wnt signaling stimulates osteoblast differentiation, proliferation, and survival through stabilization of β-catenin (Westendorf et al., 2004). However, it is not known whether Pin1 is related to the regulation of osteoblast differentiation by β-catenin modulation or, if so, which detailed molecular mechanisms control this process.

II-4. Craniosynostosis (CS)

The mammalian skull vault is made up of five major flat bones combined by structures known as the cranial sutures (Moazen et al., 2015). These sutures are the most important part of the skull growth during development (Morriss-Kay and Wilkie, 2005). The cranial sutures offer pliable joints for passage through the birth canal, act as shock absorbers, prevent dissociation of the cranial bones, and allow space for the brain to grow (Jin et al., 2016). CS represents a defection of the skull that occurs when one or more of the cranial sutures are early fused than normal (Heuze et al., 2010). The alteration in the shape of the cranial vault varies depends on the fused sutures, and compensatory development occurs in dimensions not restricted by sutures (Delashaw et al., 1989). CS may be classified

according to the number of sutures included, etiology, and presence or absence of syndrome (Delashaw et al., 1989; Greenwood et al., 2014).

Particularly, when CS is divided depending on whether it is syndromic or nonsyndromic, nonsyndromic CS is generally classified according to the included suture(s) (Greenwood et al., 2014). Syndromic CS is associated with numerous dysplasia, including the face, bone, nervous system, and over 180 different syndromes are involved in CS (Kimonis et al., 2007). So, the syndromes of CS patients are clinically heterogeneous with coinciding two or more features, and, sometimes it is difficult to diagnose them precisely (Kimonis et al., 2007). The following clinical descriptions illustrate the various features of syndromic CS.

Crouzon syndrome (MIM123500) was first pronounced in 1912. Inheritance is autosomal dominant, which is also known as ‘branchial arch syndrome’, accompanying secondary changes of the facial bones and structure (Belludi et al., 2012; Kreiborg and Cohen, 2010; Samatha et al., 2010). The most prominent characteristic of Crouzon syndrome is CS, which features a short and broad head (Mohan et al., 2012). Other general features include hypertelorism, exophthalmos and external strabismus, parrot-beaked nose, short upper lip, and hypoplastic maxilla results in relative mandibular prognathism (Kreiborg and Cohen, 2010; Mohan et al.,

2012).

Pfeiffer syndrome (MIM101600) also has an autosomal dominant inheritance (Ciurea and Toader, 2009). This CS syndrome shows characteristic anomalies of the hands and feet (Ciurea and Toader, 2009). Three clinical subtypes have been established, which are critical for accurate diagnosis and prognosis (Ciurea and Toader, 2009; Vogels and Fryns, 2006). Type 1, the classic Pfeiffer syndrome, is associated with standard level of intelligence and good outcome, midface hypoplasia, finger and toe abnormalities, brachydcephaly, and variable syndactyly (Ciurea and Toader, 2009; Park et al., 2006; Vogels and Fryns, 2006). The features of type 2 and type 3 appear to overlap partially. Type 2 is more severe and consists of cloverleaf skull with acute ocular proptosis, broad hands and feet, together with ankylosis of the elbows (Ciurea and Toader, 2009; Park et al., 2006; Vogels and Fryns, 2006). Type 3 is similar to type 2, but has no cloverleaf skull (Ciurea and Toader, 2009; Park et al., 2006; Vogels and Fryns, 2006). Type 1 patients have the best long-term outcome, while patients with type 2 and 3 have neurological damage and die at an early age (Cohen, 1993).

Now known as Apert syndrome (AS) (MIM101200), this disorder is characterized by coronal CS, midface hypoplasia, exorbitism, syndactyly of the hands and feet with a tendency to fusion of bony structures, and variable

mental retardation (Akram et al., 2015; Ciurea and Toader, 2009). The clinical organization of children with AS includes surgical improvement of the CS, midfacial hypoplasia and syndactyly (Akram et al., 2015). Almost all patients with AS are caused by mutation in FGFR2, including FGFR2 Ser252Trp or FGFR2 Ser253Arg mutations (Suzuki et al., 2012). Approximately 50% of cases are random, but autosomal dominant inheritance also has been described (Akram et al., 2015; Suzuki et al., 2012).

The FGFR mutations in CS syndromes can be parted into four groups: 1) Ig like domain II–III linker region mutations, 2) Ig-like domain III mutations, 3) transmembrane domain mutations, and 4) tyrosine kinase domain mutations (Cunningham et al., 2007). In addition, it can be classified into three according to the activation mechanism by the mutation of FGFRs: 1) dimerization by unpaired cysteines, 2) enhanced affinity for the ligand, 3) stimulation by eliminating the inhibition in the activating loop of the kinase domain (Kannan and Givol, 2000). These gain-of-function mutations in FGFR1 to 3 have been connected with several CS syndromes (Kannan and Givol, 2000). Thus, the FGFR2 S252W mutant mouse was used as a CS model in this paper, this mutation leads to excessive FGF/FGFR signaling, resulting in faster calvaria suture fusion than normal. According to this and our previous paper (Islam et al., 2017; Park et al.,

2010; Yoon et al., 2014; Yoon et al., 2013), we examined whether inactivation of Pin1 can rescue increased FGF/FGFR signaling and CS phenotype or not in vivo model.

II-5. Juglone, a Pin1 inhibitor

PPIases are enzymes that cause the cis/trans isomerization of peptide bond that precedes prolyl residue (Hanes, 2015). PPIases can be classified into three families depending on amino acid sequence homology and on the characteristics of inhibition by drugs (Hanes, 2015; Hennig et al., 1998). Two of these families were directly inhibitable by immunosuppressive gents as primary targets (Hanes, 2015; Hennig et al., 1998). For example, the cyclophilins, which are reversibly inhibited by CsA, and FK506, ramanycin, many other α-dicarbonyl amides bind to most of the FKBPs and inhibit its function (Hanes, 2015; Hennig et al., 1998). While an inhibitor of parvulin was investigated and improved until recently. In many previous papers, the natural compound juglone was discovered to exactly inactivate PPIase activity of the parvulin from E. coli, which means that it can inhibit the human parvulin, Pin1 (Hennig et al., 1998).

Juglone (5-hydroxy-1,4-naphthoquinone) is a brown color separated from fruit shells and leaves of black walnut trees (Juglans), which is a

phenolic compound that has allelopathic qualities belonging to the naphthoquinones class (Chen et al., 2005; Hennig et al., 1998; Saling et al., 2011). When exposed to the air, the α-hydrojuglone is spontaneously oxidized and becomes juglone, which is closely related to the developmental procedures and defense systems of the nuts (Chen et al., 2005; Hennig et al., 1998; Saling et al., 2011). Pin1, inactivated by juglone, includes two juglone molecules linked by a covalent bone in the side chains because of a Michael addition of the thiol groups to juglone (Hennig et al., 1998). Thus, partial unfolding of the active site following thiol group alteration was supposed to be the reason of the aggravation of PPIase activity (Hennig et al., 1998).

Juglone experiences biotransformation in the liver to form various metabolites, which can be detected mainly in the urine (Saling et al., 2011). Thus, the compound has obviously access to the liver cells and several metabolites are created such as 1,4,5-trihydroxynaphthalene di-glucuronide, 1,4,5-trihydroxynaphthalene mono-glucuronide mono-sulfate, 2-sulfo-2,3-dihydrojuglone, 4,8-dihydroxy-1-tetralone mono-glucuronide and 1,4,5-trihydroxynaphthalene mono-glucuronide (Chen et al., 2005; Saling et al., 2011). For this reason, juglone is a very interesting substance as a drug, with the potential to regulate liver function or to be used for medicinal purpose in other parts of the body (Chen et al., 2005; Hennig et al., 1998; Saling et al.,

2011). On the other hand, pure juglone is used only for a study chemical purposes and black walnut hull creations are registered as 'Unapproved Herbs' in the German Commission E Monographs due to probable mutagenic and carcinogenic properties (Chen et al., 2005). And, because of the metabolism and temper of juglone, it has been designated as a potentially toxic natural product by the National Toxicology Program in USA (Chen et al., 2005; Saling et al., 2011). In addition, it has been found that juglone is a potent inhibitor not only Pin1 but also other enzyme such as RNA polymerase II (Hanes, 2015). In this study, when we treated juglone for inhibition of Pin1 in vitro and in vivo, it is necessary to carry out experiments with the concentration and specificity of juglone. The part 2 results showed that control of Pin1 is important for target of CS therapy and Pin1 inhibitor such as juglone needs to be modified to be more valuable as a drug.

III. Purpose of study

The critical role of Pin1 in osteoblast differentiation has been reported. In addition, the importance of Pin1 and Wnt/β-catenin in breast cancer and neuronal differentiation was also described. However, it is not known whether Pin1 is related to the regulation of osteoblast differentiation by β-catenin modulation or, if so, which detailed molecular mechanisms control this process. In addition, the importance of Pin1 in FGF/FGFR2 signaling was described. We hypothesized that suppression of Pin1 would normalized hyper activated FGFR2 signaling, and then subsequently rescue premature obliteration of coronal sutures by gain-of-function mutation of FGFR2. Therefore, the purpose of this study is to investigate the relationships between Pin1 and Wnt/β-catenin signaling in osteoblast differentiation, and suggest Pin1 could be a promising molecular target to overcome CS by non-surgical approaches.

PART 1: Effect and molecular mechanisms of Pin1 on Wnt/β-catenin signaling in osteoblasts

PART 2: Therapeutic effect of Pin1 inhibition by genetic and chemical approaches on CS

IV. Part 1.

Pin1-mediated Modification Prolongs the Nuclear Retention of β-catenin in Wnt3a-induced Osteoblast Differentiation

This research was originally published in the Journal of Biological Chemistry. *J. Biol. Chem.* VOL. 291, NO.11, pp. 5555-5565, March 11, 2016

Abstract

Canonical Wnt signaling pathway in which β-catenin nuclear localization is a crucial step plays an important role in osteoblast differentiation. Pin1, a prolyl isomerase, is also known as a key enzyme in osteogenesis, however, the association of Pin1 in canonical Wnt signal-induced osteoblast differentiation is poorly understood. We found Pin1 deficiency caused osteopenia and reduction of β-catenin in bone lining cells. Similarly, Pin1 knock-down or the treatment of Pin1 inhibitors strongly decreased nuclear β-catenin level, the TOP flash activity and the expression of bone marker genes induced by canonical Wnt activation, and vice versa in Pin1 overexpression. Pin1 directly interacts with and isomerizesβ-catenin in the nucleus. The isomerized β-catenin could not bind to nuclear APC that drives β-catenin out of nucleus for proteasomal degradation, which consequently increases the retention of β-catenin in the nucleus and might explain the decrease of β-catenin ubiquitination. These results indicate that Pin1 could be a critical target to modulate β-catenin-mediated osteogenesis.

Introduction

Wnt signaling is critical for the regulation of genes involved in normal embryonic development, cellular proliferation and differentiation (Holland et al., 2013; Logan and Nusse, 2004). In the canonical pathway, in the absence of Wnt, β-catenin is subjected to proteasome-mediated degradation by a destruction complex, which predominantly includes GSK3β, Axin, and the APC protein (Bikkavilli et al., 2008). In the presence of Wnt signaling, there is reduced GSK3β kinase activity and increased accumulation of β-catenin in the nucleus, which is followed by stimulation of LEF/TCF transcriptional activation (Behrens et al., 1996; MacDonald et al., 2009; Molenaar et al., 1996). The well-established canonical Wnt/β-catenin pathway is a key signaling pathway in bone development (Westendorf et al., 2004). For example, genetic studies in humans and mice have determined that low-density LRP5/Wnt signaling plays a major role in the control of bone mass (Gong et al., 2001; Hill et al., 2005; Kolpakova and Olsen, 2005; Little et al., 2002).

The nuclear localization of β-catenin in response to Wnt is an essential event of the canonical Wnt signaling pathway for communicating with the transcription factor TCF/LEF (Behrens et al., 1996; Huber et al., 1996). Aberrant accumulation of β-catenin contributes to abnormal

development and tumorigenesis; therefore, it requires strict regulation. Previous reports have suggested that BCL9 (Townsley et al., 2004), Smad3(Jian et al., 2006; Zhang et al., 2010) and glucose-induced β-catenin and LEF1 interaction (Chocarro-Calvo et al., 2013) actively import β-catenin to the nucleus, whereas APC (Henderson, 2000; Neufeld et al., 2000; Rosin-Arbesfeld et al., 2000) and Axin (Cong and Varmus, 2004) export it to the cytoplasm. Specifically, APC has two major mechanisms by which it modulates the concentration of β-catenin in the nucleus. First, APC promotes the degradation of β-catenin by combining it with the degradation complex, and second, APC binds nuclear β-catenin and exports it to the cytoplasm for degradation (Ryo et al., 2001).

The pSer/Thr-Pro motifs in certain proteins exist in either cis- or trans- conformation, and conversion between these states is catalyzed by the unique prolyl isomerase Pin1 (Lu et al., 1996; Nakamura et al., 2012). Pin1-catalyzed post-phosphorylation conformational regulation often functions as a molecular timer (Liou et al., 2011). Previously, we found that the interaction of Pin1 with Runx2, the major transcription factor for osteoblast differentiation, is critical for bone development (Yoon et al., 2014a; Yoon et al., 2013a). We showed that Pin1 hetero and KO mice exhibit reduced mineralization at birth. Pin1 mutation causes short stature with

hypomineralization throughout the skeleton. Pin1 is known to bind and modulate β-catenin stability and subcellular localization at the post-translational level by regulating its interaction with APC in breast cancer (Ryo et al., 2001) and neuronal differentiation (Nakamura et al., 2012). However, it is not known whether Pin1 is related to the regulation of osteoblast differentiation by β-catenin modulation or, if so, which detailed molecular mechanisms control this process.

In this study, we found that Pin1 is required for the transcriptional activity of β-catenin and demonstrated that interaction between Pin1 and β-catenin is critical in the osteogenic pathway. Furthermore, our data showed that Pin1-directed conformational changes in nuclear β-catenin are critical for the nuclear retention of β-catenin, which modulates the export of β-catenin to the cytosol by regulating the interaction of β-catenin with APC in the nucleus. Taken together, our results reveal that Pin1 is a novel regulator that promotes osteoblast differentiation through structural modification and stabilization of β-catenin in the nucleus.

Materials and methods

Animal experiments

Pin1-deficient mice have been described previously (Fujimori et al.,

1999) and were kindly given by Dr. Takafumi Uchida (Tohuku University). Pin1 KO mice were generated from heterozygous mating (Islam et al., 2014a). All mice have maintained in the Specific-pathogen-free (SPF) condition, and were approved by the Special Committee on Animal Welfare, Seoul National University, Seoul, Republic of Korea.

Antibodies and reagents

The antibodies and reagents are described in detail in Tables 1.1. and 1.2.

DNA construction and site-directed mutagenesis

Construction of the Pin1 (HA-pcDNA3.1-Pin1) WT and mutant (Y23A, W34A and C113A) expression vectors has been described previously (Yoon et al., 2013a). Ds-Red Pin1 WT and mutant constructs have also have been described previously (Yoon et al., 2014a). Full-length β-catenin cDNAs were generated by PCR and subcloned between BamH1 and Not1 sites in pcDNA3.1, respectively, to create FLAG-epitope fusion proteins. All mutant constructs of Pin1 binding sites were generated by serial mutagenesis from the single and double binding site mutants with PCR, and the fragments were ligated using an In-Fusion HD cloning kit per

the user manual. PCR primers (Table 1.3.) were synthesized and purchased from Integrated DNA Technology. PrimeSTAR DNA Polymerase (Takara, Shiga, Japan) was used, and PCR was performed using the manufacturer's protocol.

Cell culture and nuclear–cytoplasmic fractionation

All cell culture media and antibiotics were from Hyclone (GE Healthcare, Little Chalfont, UK). Cells used in this study were cultured at 37℃, in 5% CO_2. Mouse myogenic C2C12, HEK293, and MEF cells were maintained in Dulbecco's modified Eagle's medium (DMEM) with 10% heat-inactivated FBS containing 1% penicillin and streptomycin antibiotics. And pre-osteoblast MC3T3-E1 and multipotent ST2 mesenchymal progenitor cells were cultured in alpha-Minimunm Essential Medium (α-MEM) with 10% FBS and 1% antibiotics (Cho et al., 2014; Yoon et al., 2013a). Nuclear–cytoplasmic fractionation was conducted using the NE-PER Nuclear and Cytoplasmic Extraction Reagent kit (Thermo Fisher Scientific, Massachusetts, USA) according to the manufacturer's protocol.

ALP staining

For ALP staining, cells were washed twice with phosphate-buffered

saline, fixed with 2% paraformaldehyde, and stained for ALP-induced chromophores according to the manufacturer's instructions (Sigma, St. Louis, MO, USA).

Luciferase reporter assay

The transcriptional activity of TCF/LEF was measured with the TOP/FOPflash reporter plasmid vectors (Molenaar et al., 1996). For luciferase assay, cells were lysis with passive lysis buffer (Promega, WC, USA). After treatment of substrate using a Bright- Glo™ Luciferase assay system (Promega, WC, USA), luciferase activity was detected with a GloMax-Multi Detection System reader (Promega, WC, USA).

Extraction of total RNAs, reverse transcription polymerase chain reaction (RT-PCR) and Real time PCR (qPCR)

Total RNA was extracted from cultured cell using the QIAzol® (QIAGEN, Hilden, Germany). RNA samples were reverse-transcribed by using the PrimeScript RT kit (Takara Bio, Shiga, Japan). Quantitative real-time PCR was performed by using Takara SYBR premix Ex Taq (Takara, Shiga, Japan) on an Applied Biosystems 7500 Real Time PCR system (Foster city, CA). Primers were synthesized by Integrated DNA technology

(IDT, Coralville, IA) and the primer sets were well explained previously (Islam et al., 2014a; Yoon et al., 2013a)

GST-PD assay, IP, and immunoblot analyses

Cellular proteins and GST-PD assays were prepared in a lysis buffer of 50mM HEPES (pH 7.5), 150mM NaCl, 100mM NaF, 1mM DTT, 1mM EDTA, 0.25% Na-deoxycholate, 0.25% CHAPS, 1% NP-40 and 10% glycerol added with protease and phosphatase inhibitors, including Na_3VO_4 (Yoon et al., 2013a). For the immunoblot assays, the cells were lysed in buffer containing 0.1% SDS. Recombinant GST or GST-Pin1 proteins (1ug) were incubated with cell lysates for 2hr at 4℃. After incubation, glutathione agaroses beads were added, and incubated for 30min. The precipitated proteins were analyzed by immunoblot with specific antibodies (Supplemental Table. S3). For the IP, the cell lysates were incubated with antibody for 1h, IgG beads were added, and the mixture was incubated for 2h in 4℃.

IF and IHC

For the detection of Pin1 and β-catenin by IF, cells were fixed in 4% formaldehyde. The cells were then treated with the primary antibody or only

IgG as a negative control, and stained with fluorescent-conjugated secondary antibody (Islam et al., 2014a; Yoon et al., 2014b). Imagining was conducted with a Carl Zeiss LSM700 confocal microscope, and analyzed with associated software program, ZEN2011 (Carl Zeiss, Oberkochen, Germany). For the IHC, tissues were fixed in 4% paraformaldehyde solution for 2h and dehydrated, and then embedded in paraffin. Serial paraffin sections (5um thicknesses) were made, and analyses of samples were performed with the Dako Cytomtion Envision System (Dako, Glostrup, Denmark). The tissue samples were observed with a DP72 digital camera (Olympus, Tokyo, Japa).

Knock-down assay with siRNA and transfection

To knockdown Pin1 expression, siRNAs against Pin1 were purchased from Dharmacon (Lafayette, CO), siGENOME SMART pool. siGENOME non-targeting siRNA #2 was used as a control (scramble siRNA). Forty pmol of siRNA was transfected**.** MC3T3-E1, ST2, and C2C12 cells were transfected by electroporation using the Neon Transfection system (Invitrogen) according to the manufacturer's instructions. Transfection of the HEK293 cells was performed using PolyJet reagent (SignaGen Laboratory) according to the manufacturer’s instructions.

Statistical analysis

The results are presented as mean ± SD. Each experiment was performed at least three times, and the results of one representative experiment are shown. The significance of the difference was evaluated using the Student's t test.

Table 1.1. Antibodies used in this study.

Antigen	Clone	Cat.#	Host	Appl.	Source
β-catenin	-	#9562	Rb, pAb	WB, IP, IHC	Cell signlaing
Pin1	-	#3722	Rb, pAb	IB	Cell Signaling
	H-123	sc-15340	Rb, pAb	IF, IP	Santa Cruz
	-	NBP1-05424	Ch, pAb	IF	Novus
FLAG	-	PM020	Rb, pAb	WB, IP, IHC	MBL
β-actin	C-4	Sc-47779	M, mAb	WB, IHC	Santa Cruz
GAPDH	FL-335	sc-25778	Rb, pAb	WB, IP, IF, IHC	Santa Cruz
Lamin A/C	N-18	Sc-6215	G, pAb	WB,IP,IF	Santa Cruz
HA	16B12	MMS-101P	M, mAb	IP,IB	Covance
APC	CC-1	OP80	M, pAb	WB,ICC, IHC	Calbiochem®
GST	-	RPN1236V	pAb	WB	GE Health

M, mouse; Rb, rabbit; G, goat
mAb, monoclonal antibody; pAb, polyclonal antibody

Table 1.2. Chemical reagents used in this study.

Chemical reagents	Application	Source
Juglone	Pin1 inhibitor	Calbiochem
DTM	Pin1 inhibitor	Calbiochem
Wnt3a	Wnt signaling pathway ligand	R&D Systems
CHX	Protein synthesis inhibitor	Sigma-Aldrich
SB216763	GSK3β inhibitor	Sigma-Aldrich
LMB	Inhibitor of nuclear export signal	Sigma-Aldrich

Juglone, 5-hydroxy-1,4-naphthalenedione; DTM, Dipentamethylene thiuram monosulfide; CHX, Cycloheximide; LMB, Leptomycin B

Table 1.3. Primer sequences for the generation of β-catetnin mutant constructs. The lowercase letters indicate the substitution of nucleotide for site-directed mutagenesis of β-catenin.

Name	*Oligonucleotide Sequence*
S191A (forward)	*5′-GACACGCTATCATGCGTGCCCCTCAGATGGTGTCTGC-3′*
S191A (reverse)	*5′-GCAGACACCATCTGAGGGGCACGCATGATAGCGTGTC-3′*
S246A (forward)	*5′-CTGGTGAAAATGCTTGGTGCCCCAGTGGATTCTGTGTTG-3′*
S246A (reverse)	*5′-CAACACAGAATCCACTGGGGCACCAAGCATTTTCACCAG-3′*
S605A (forward)	*5′-GTTTGTGCAGCTGCTTTATGCCCCCATTGAAAACATCCAAAG-3′*
S605A (reverse)	*5′-CTTTGGATGTTTTCAATGGGGGCATAAAGCAGCTGCACAAAC-3′*
In fusion primer F	*5’-TACCGAGCTCGGATCCATGGCTACTCA-3’*
In fusion primer R	*5’-TAGACTCGAGCGGCCGCGACGACGAT-3’*

Results

Pin1 controls β-catenin protein stability and Wnt3a-induced transactivation activity

In this context, we aimed to characterize the role of Pin1 in adult bone metabolism through canonical Wnt signaling. For this purpose, β-catenin protein level in the proximal tibial metaphysis of WT and Pin1 KO mice was determined by IHC. Brown-colored β-catenin expression spots were easily identified in the osteoblasts of WT, while spots were difficult to identify in the Pin1 KO counterpart (Fig. 1.1). Since previous reports have indicated that Pin1 action influences substrate protein stability, we suspected that the decrease in β-catenin protein level in Pin1 KO mice was a result of decreased protein stability. For this purpose, we confirmed that mRNA level of β-catenin was not changed by Wnt3a treatment or not in WT and Pin1 KO MEF cells (Fig. 1.2A). We determined β-catenin stability after blocking de novo protein synthesis by treatment with CHX. WT Pin1 overexpression strongly enhanced β-catenin stability, and the level was sustained 5 h after CHX treatment. However, C113A Pin1, an enzyme-defect mutant, overexpression did not enhance β-catenin stability (Figs. 1.2B, C). The TCF reporter gene (TOP Flash) activity in WT MEF cells was increased more than 5-fold by Wnt3a treatment, while that in Pin1 KO MEF cells was

increased about 2-fold (Fig. 1.2D). In addition, overexpression of Pin1 WT enhanced TOP Flash activity by about 5-fold. On the other hand, overexpression of Pin1 mutants did not demonstrate a comparable enhancement of TOP Flash activity (Fig. 1.2E). Collectively, these results indicate that Pin1 action on β-catenin enhances its protein stability and Wnt3a-induced transactivation activity.

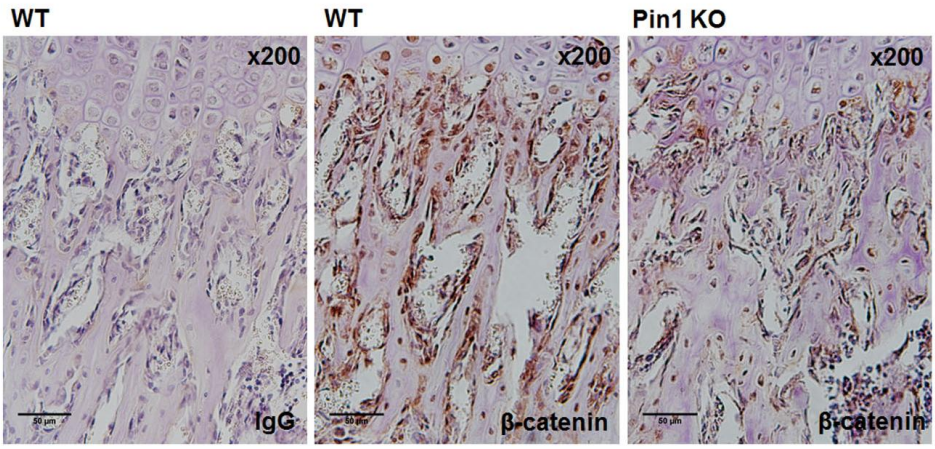

Figure 1.1. Reduced β-catenin levels in the proximal tibia of P40 Pin1-deficient mice.

IHC for β-catenin protein in histological sections of the proximal tibia. Coronal sections of the proximal tibia of P40 Pin1 WT and KO mice were stained with anti-β-catenin antibody (brown coloration) and anti-IgG (n=3 in each group).

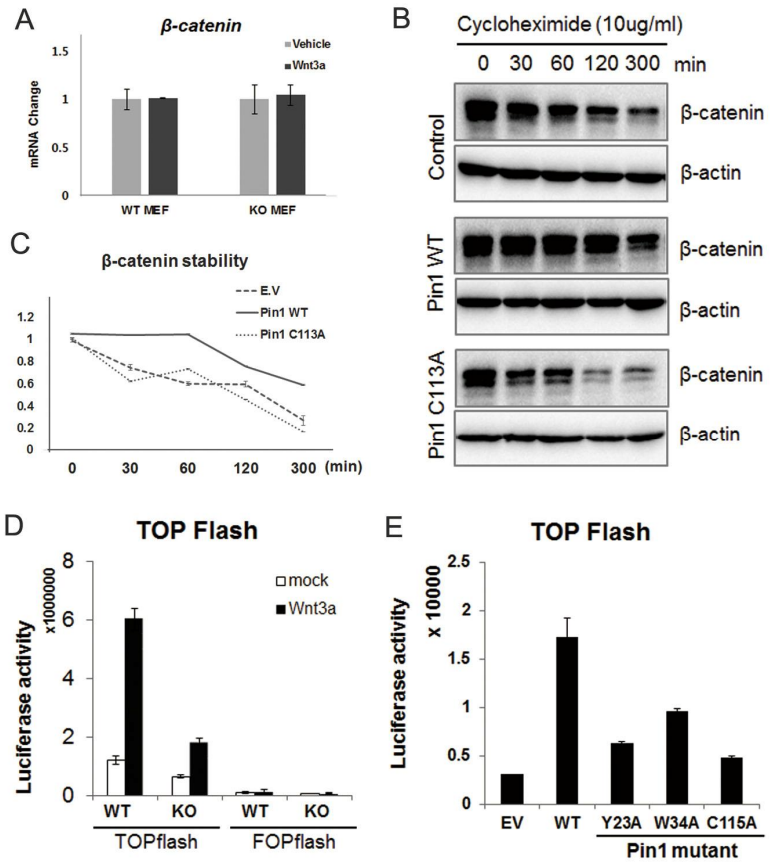

Figure 1.2. Abnormal Pin1 expression reduces β-catenin level and stability and controls Wnt-induced transactivation activity.

A. Confluent WT and Pin1 KO MEF cells were treated with Wnt3a for 3 days. mRNA level of β-catenin was quantitatively analyzed (n=3). **B.** Degradation of β-catenin with CHX treatment was observed in the presence of WT and mutant (C113A) Pin1. HEK293 cells were transfected with control or WT or C113A Pin1 mutant expression plasmids. The cell lysates

were collected at 0, 30, 60, 120, or 300 min after CHX treatment (10 μg/ml), and the β-catenin protein level was detected by immunoblot (left). **C**. Protein blot bands were quantified and normalized against β-actin level (graph on the right) (n=3). **D**. MEF from WT and Pin1 KO mice were transfected with a TCF reporter gene (TOP Flash) or a control reporter gene (FOP Flash). After 24 h, cells were treated with 100 ng/ml Wnt3a for an additional 24 h, and luciferase activity was analyzed from cell lysates (n=3). **E.** TOP Flash activity was also verified in MC3T3-E1 cells that were transfected with an expression vector for WT Pin1 or functionally inactive Pin1 mutants including Y23A, W34A, C113A, or empty vector (EV) (n=3).

Pin1 is indispensable for Wnt3a-induced osteoblast differentiation

In order to understand the Pin1 contribution to Wnt3a-induced osteoblast differentiation, we performed cytochemical analysis of ALP activity and analysis of typical bone marker mRNA expression. Wnt3a-induced ALP staining was almost completely abrogated (Fig. 1.3A) by Pin1 knockdown (Fig. 1.3B) in MC3T3-E1 cells. On the contrary, ALP activity stimulated by minimal Wnt3a treatment was further enhanced (Fig. 1.3D) by Pin1 overexpression (Fig. 1.3D). Similarly, Wnt3a-stimulated mRNA level of several bone marker genes was almost completely blocked by knockdown of Pin1 in the cells (Figs. 1.4A-D). These results clearly indicate that Pin1 action is indispensable for Wnt3a-induced osteoblast differentiation. In addition, Pin1 knockdown also suppressed some bone marker gene expression and ALP staining even in the absence of Wnt3a treatment, suggesting a possibility of Pin1 involvement in β-catenin-independent osteogenic signaling pathways.

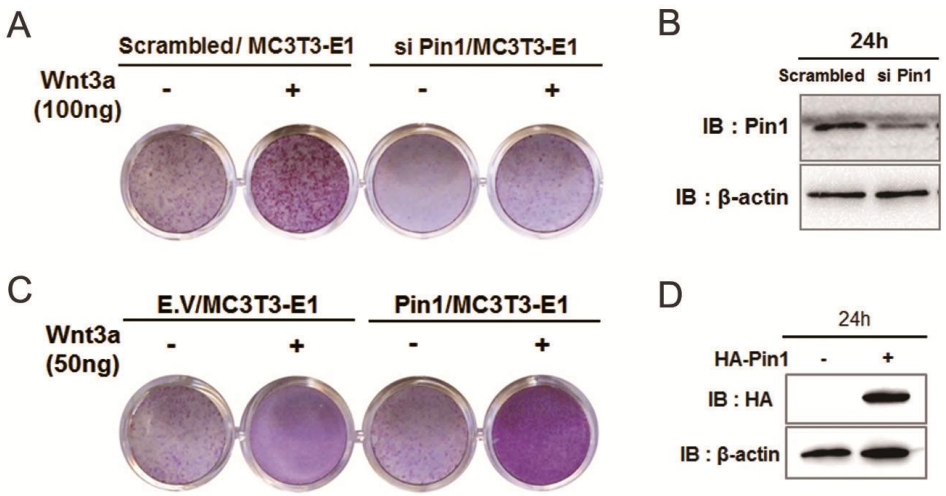

Figure 1.3. Pin1 is critical for osteoblast differentiation on Wnt3a signaling pathway.

A. Confluent MC3T3-E1 cells were transfected with scramble (control) or siPin1 of siRNA. After 24 h, cells were treated with 100ng/ml Wnt3a for an additional 3 days, and ALP activity was cytochemically analyzed. **B.** Pin1 expression level was confirmed by immunoblot assay at 24 h after transfection of siPin1 in MC3T3-E1 cells. **C.** MC3T3-E1 cells overexpressing Pin1 were treated with 50ng/ml Wnt3a for 3 days. ALP activity was cytochemically analyzed. **D.** HA expression level was confirmed by immunoblot assay at 24h after transfection of HA-Pin1 in MC3T3-E1 cells.

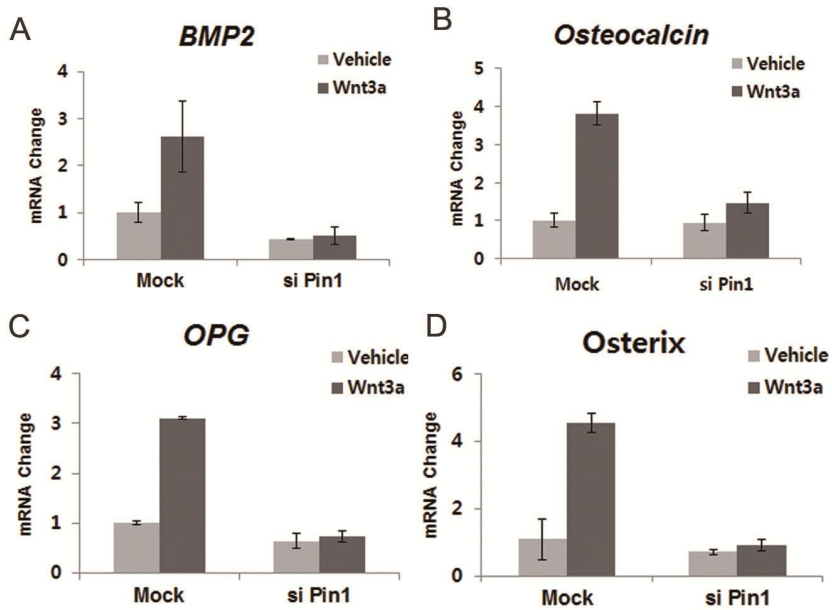

Figure 1.4. Pin1 is indispensable for Wnt3a-induced osteoblast differentiation.

A-D. Confluent MC3T3-E1 cells were transfected with scramble siRNA or siPin1. After 24 h, cells were treated with or without 50ng/ml Wnt3a for 3 days. mRNA levels of bone marker genes such as osteocalcin, Bmp2, OPG, and osterix were quantitatively analyzed (n=3).

β-Catenin is the target of Pin1 in the Wnt3a signaling pathway

β-Catenin is the bottleneck molecule in the canonical Wnt signaling pathway, and Wnt3a-induced signal suppresses GSK3-β activity, which in turn increases β-catenin levels in the cytosol and nucleus (Bikkavilli et al., 2008). Transcriptional activity such as TOP Flash (Fig. 1.5A) and *ALP* promoter (Fig. 1.5B) stimulated by β-catenin was further enhanced by overexpression of Pin1 in MC3T3-E1 cells. As β-catenin was suspected as a candidate target for Pin1 substrate, we tested the molecular interaction in MC3T3-E1 cells. Endogenously expressed β-catenin protein co-precipitated with GST-Pin1 recombinant protein. Moreover, β-catenin extracted from Wnt3a-treated cells showed greater binding than Wnt3a not treated cells because nuclear β-catenin is increased by Wnt3a (Fig. 1.6A). To investigate the endogenous interaction between these two proteins, β-catenin protein was identified in the immunoprecipitate (IP) of anti-Pin1 antibody (Fig. 1.6B). When we observed localization of Pin1 in our previous reports (Yoon et al., 2015b; Yoon et al., 2013b), expressed Pin1 was localized to a nuclear substructure. We examined GST-PD and IP of nuclear β-catenin with anti-Pin1 in nuclear fraction (Figs. 1.6C, D). Pin1 bound to nuclear β-catenin and the interactions were increased with Wnt3a treatment. In order to confirm the biochemical interaction between these two molecules, MC3T3-E1 cells

were transfected with Ds-Red Pin1 expression vectors, and endogenous β-catenin (green) and Ds-Red Pin1 (red) were analyzed using confocal microscopy. In the absence of Wnt3a treatment, most of the Pin1 and β-catenin molecules were independently localized in the nucleus. Only a small fraction of Pin1 molecules were co-localized with endogenous β-catenin (yellow) molecules (Fig. 1.6E, first row). With Wnt3a treatment, nuclear β-catenin increased, and co-localization with the Pin1 molecule also increased (Fig. 1.6E, second row). The co-localization intensity was quantified and is shown in the graph in Fig. 1.6F. These results clearly demonstrate that Pin1 target of the canonical Wnt signaling pathway is β-catenin, and the interaction of Pin1 and β-catenin becomes stronger following an increase in nuclear β-catenin by Wnt3a.

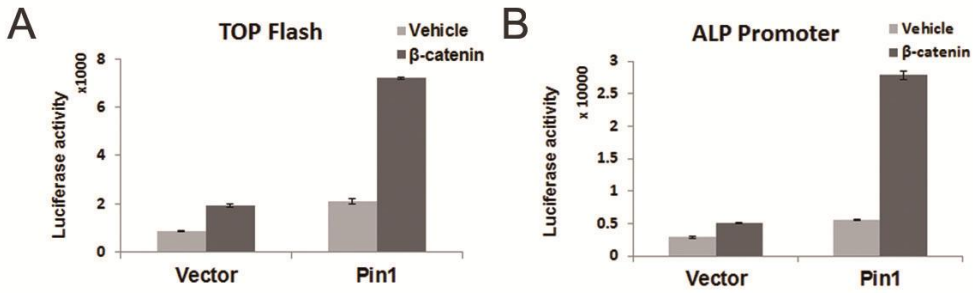

Figure 1.5. Pin1 activates Wnt/β-catenin-induced transacting activity

A-B. MC3T3-E1 cells were transfected with the TOP Flash reporter (A) or mouse Alp promoter reporter (B) and β-catenin expression vector. Reporter activity was analyzed using chemiluminescence assays (n=3).

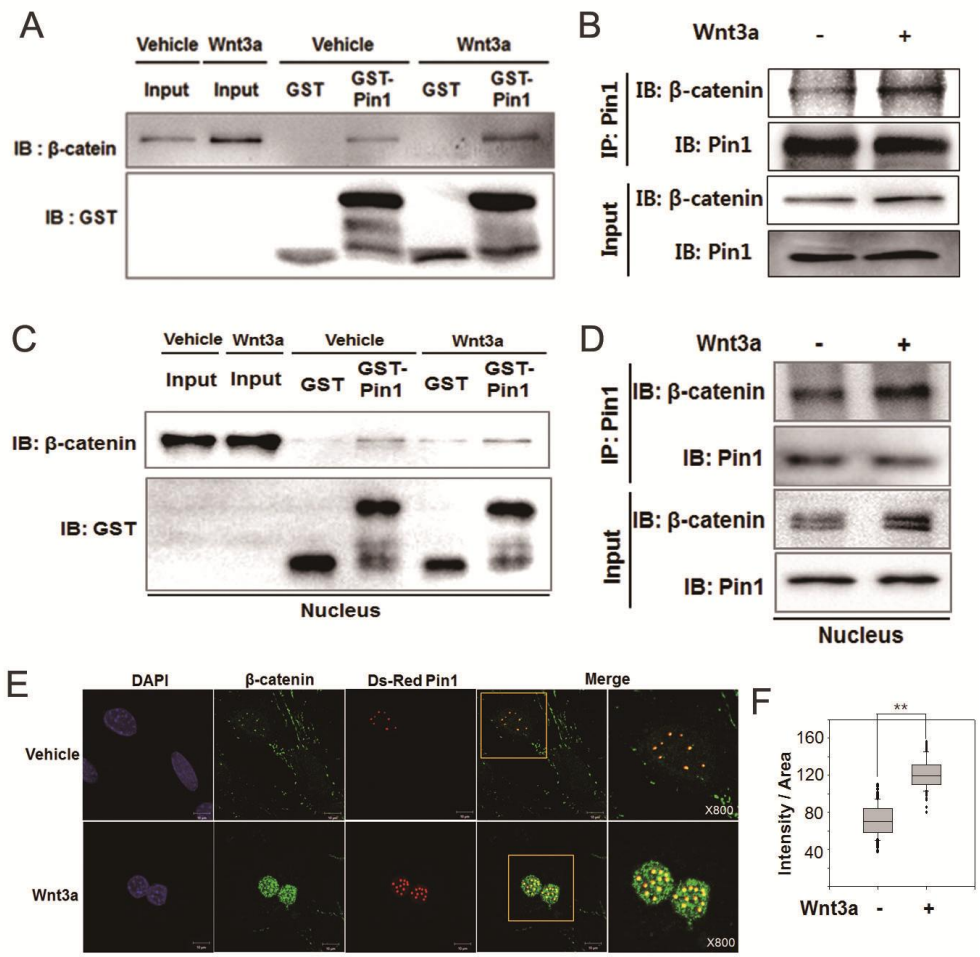

Figure 1.6. The Pin1 target of the canonical Wnt signaling pathway is β-catenin.

A, B. Confluent MC3T3-E1 cells were treated with or without 100 ng/ml Wnt3a for 24 h. Endogenous β-catenin level was determined with immunoblots after GST-PD assays (Fig. 1.6A) or IP (Fig. 1.6B) (n=3). **C, D.** After MC3T3-E1 cells were treated with or without 50ng/ml Wnt3a for 24 h,

nuclear fractions were isolated from cell lysates. Endogenous β-catenin interaction with Pin1 was determined by GST-PD (Fig. 1.6C) and IP (Fig. 1.6D) (n=3). **E.** MC3T3-E1 cells were transfected with Ds-Red Pin1 (red) expression vectors. After 6 h of transfection, cells were treated without or with 100 ng/ml Wnt3a for an additional 24 h. Cells were fixed and stained for endogenous β-catenin using anti-β-catenin antibody. In the merged image, β-catenin and Pin1 co-localization (yellow) was observed with confocal microscopy, and the nucleus was counterstained with 4',6-diamidino-2-phenylindole (DAPI, blue). **F.** Yellow intensity per nuclear area was quantified and is shown as a sigma plot (n=20 in each group, ** indicates $p<0.01$).

Pin1 is crucial for β-catenin accumulation in the nucleus upon stabilization by Wnt3a

To evaluate whether Pin1 regulates the subcellular distribution of endogenous β-catenin, we performed IF analysis in MC3T3-E1 cells. In the absence of Wnt3a, endogenous β-catenin staining was almost exclusively localized to the cell membrane (Figs. 1.7A, B first row). However, upon Wnt3a stimulation, β-catenin is accumulated in the nucleus where it can stimulate transcription of osteogenic marker genes (Figs. 1.7A, B second row). The addition of Pin1 inhibitors, juglone or DTM (Islam et al., 2014b), with Wnt3a resulted in reduced accumulation of β-catenin in the nucleus (Fig. 1.7A, third and fourth rows). Knockdown of Pin1 also showed reduction in nuclear β-catenin accumulation (Fig. 1.7B, third row). To confirm that Pin1 deficiency causes a strong decrease in nuclear β-catenin, we transfected WT or C113A, a dominant negative mutant, Pin1 constructs to examine the localization of endogenous β-catenin after treatment with Wnt3a. Almost all β-catenin was localized in the nucleus by Wnt3a (Fig. 1.8A, arrow). In particular, in WT Pin1-transfected cells, most of the β-catenin was strongly observed in the nucleus (Fig. 1.8A, arrowhead). In C113A Pin1-transfected cells, the amount of nuclear β-catenin was dramatically reduced (Fig. 1.8B, arrowhead), and most β-catenin of un-

transfected cells was observed in the nucleus, which is consistent with the finding that Pin1 determines the localization of β-catenin (Figs. 1.7A, B). To biochemically confirm this localization pattern, an immunoblot of β-catenin was performed. SB216763, a potent inhibitor of GSK3 isozymes, is used to mimic Wnt3a effect (Inoue et al., 2006). Treatment with DTM abolished nuclear β-catenin that was increased by SB216763 (Fig. 1.9). We also determined whether β-catenin mislocalization can be rescued by overexpression of Pin1 in Pin1 KO primary osteoblast cells (Fig. 1.8B). Nuclear β-catenin was increased in WT osteoblast cells when treated with Wnt3a. However, in Pin KO osteoblasts, the nuclear β-catenin was absent even after Wnt3a treatment. We determined the nuclear β-catenin localization change after Pin1 was overexpressed. In Pin1 KO primary osteoblasts, when Pin1 was overexpressed, nuclear β-catenin was slightly increased. Furthermore, when Pin1 was overexpressed in Pin1 KO primary osteoblasts, nuclear β-catenin was highly increased by Wnt3a. This shows that the defect of nuclear β-catenin in Pin1 KO primary osteoblasts can be rescued by reinstatement of Pin1. These results indicate that Pin1 is crucial for nuclear localization of β-catenin.

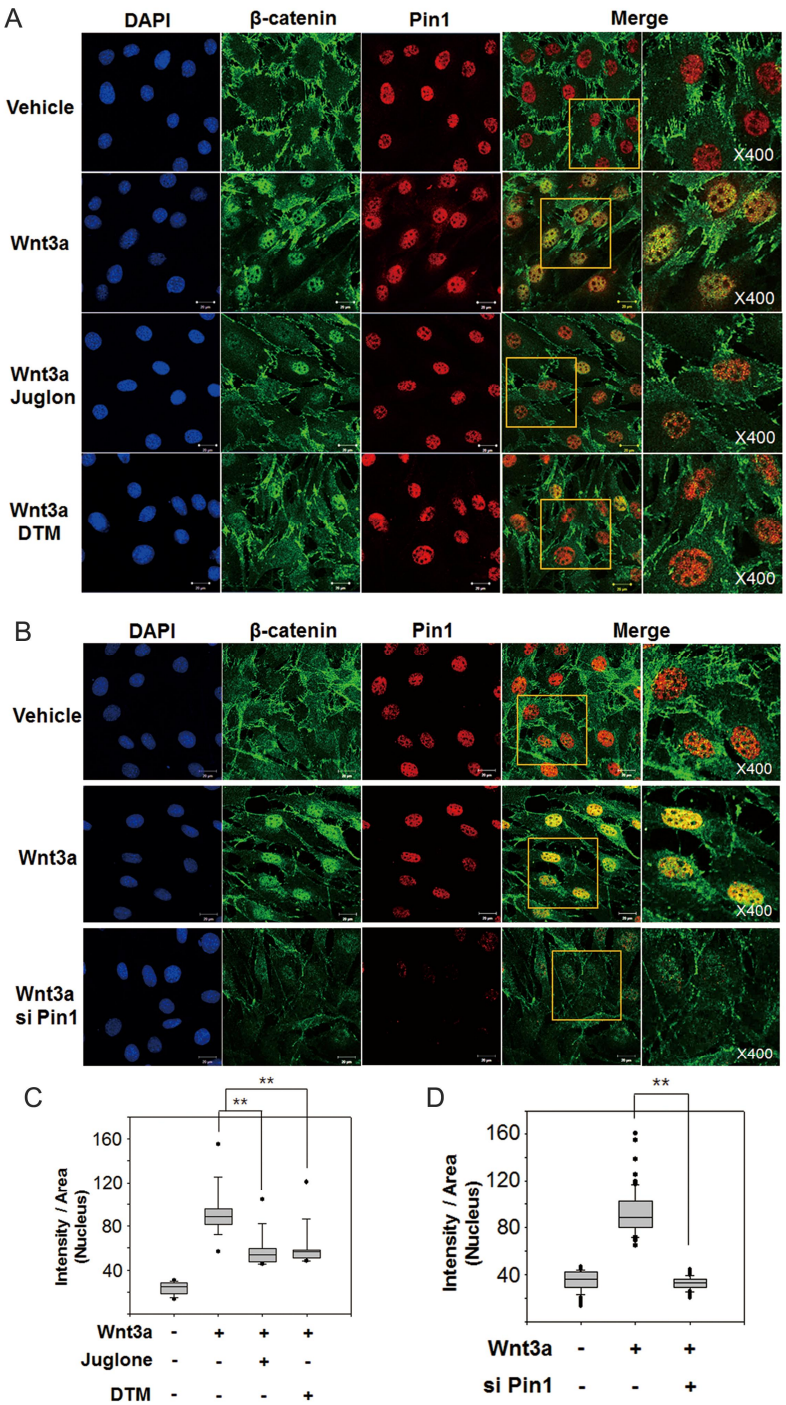
A
DAPI
β-catenin
Pin1
Merge
Vehicle
Wnt3a
Wnt3a
Juglon
Wnt3a
DTM
X400
B
DAPI
β-catenin
Pin1
Merge
Vehicle
Wnt3a
Wnt3a
si Pin1
X400
C
Intensity / Area
(Nucleus)
160
120
80
40
**
**
Wnt3a - + + +
Juglone - - + -
DTM - - - +
D
Intensity / Area
(Nucleus)
160
120
80
40
**
Wnt3a - + +
si Pin1 - - +

Figure 1.7. Pin1 is important for the nuclear localization of β-catenin in osteoblasts.

A. MC3T3-E1 cells were pretreated with 10 μM juglone and 1 uM DTM, which are Pin1 inhibitors, for 1 h and were then treated with 50ng/ml Wnt3a for an additional 24 h. **B.** Pin1 expression was inhibited by siPin1 for 24 h and then treated with 50ng/ml Wnt3a for an additional 24 h. **A-B.** Cells were fixed, and endogenous proteins were immunostained with anti-β-catenin (green) and anti-Pin1 (red) antibodies and DAPI (blue). **C-D.** Endogenous nuclear β-catenin was quantified and statistical analysis was performed by Student's t-test (n=50 in each group, ** indicates $p<0.01$).

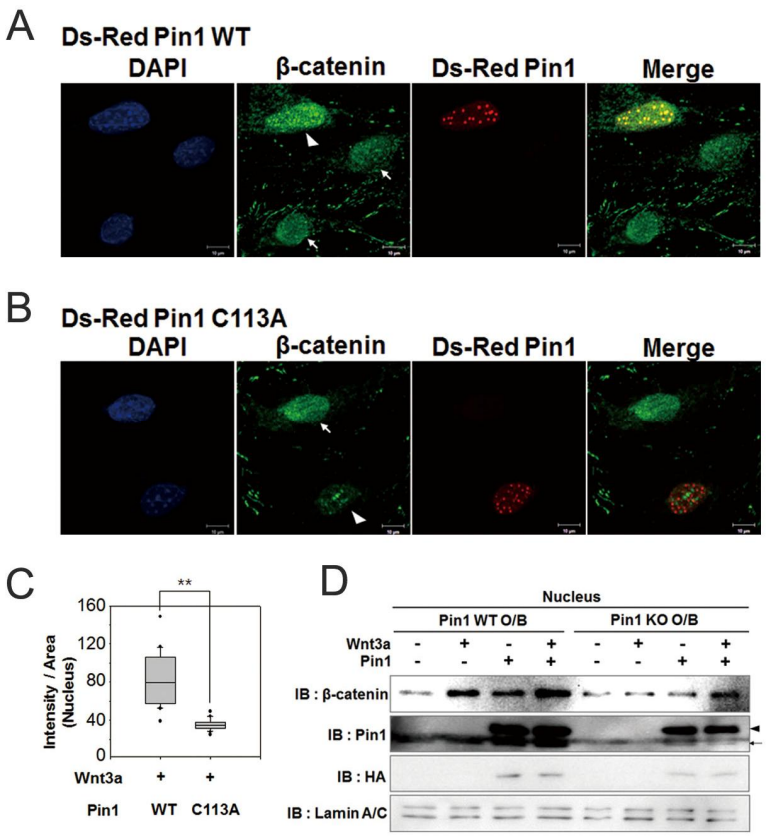

Figure 1.8. Pin1 deficiency causes a strong attenuation of nuclear β-catenin accumulation.

A, B. MC3T3-E1 cells were transfected with Ds-Red Pin1 WT (Fig. 1.8A) or C113A mutant (Fig. 1.8B) plasmids. Ds-Red Pin1 C113A has a mutant catalytic domain with dominant negative action. After 24 h of transfection, cells were fixed and stained with anti- β-catenin antibody or DAPI. **C.** Endogenous nuclear β-catenin of Ds-Red Pin1 transfected cells was quantified and statistical analysis was performed by Student's t-test (n=20 in

each group, ** indicates $p<0.01$). **D.** WT and Pin1 KO primary osteoblast cells were transfected with HA-Pin1 or pcDNA plasmids. After 24 h of transfection, cells were treated with or without 50ng/ml Wnt3a for an additional 24 h. Then, cells were harvested, and the nuclear fractions were isolated, followed by immunoblotting with marked antibodies (n=3). Arrowhead ; HA-Pin1, Arrow ; Endogenous Pin1.

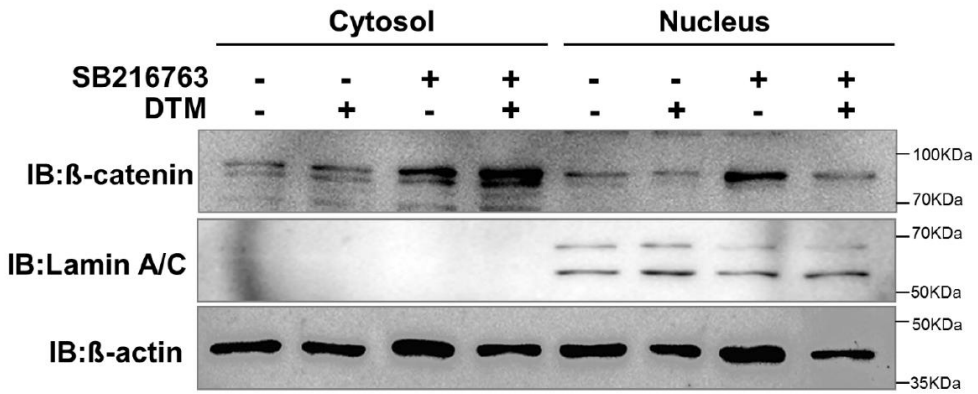

Figure 1.9. Nuclear β-catenin localization change by Pin1

HEK293 cells were pretreated for 1h with 1uM DTM, and then treated with or without 20uM SB216763 for 24h. Nuclear and cytosolic fractions were isolated from cell lysates, and were further analyzed by immunoblot analysis with anti-β-catenin, lamin A/C and β-actin antibodies.

Only β-catenin isomerized by Pin1 can be retained in the nucleus

Since Pin1 increases the accumulation of β-catenin in the nucleus, we assumed that there were two possibilities for Pin1-mediated nuclear β-catenin accumulation; that Pin1 enhances Wnt3a-induced nuclear translocation of β-catenin and that Pin1 inhibits the export of nuclear β-catenin to the cytosol. Wnt3a treatment induced nuclear translocation of β-catenin such that it was co-localized with Pin1 protein in the nucleus (Figs. 1.10A, B, second row). LMB is an inhibitor of CRM1 (Nishi et al., 1994), which is critical for the export of protein containing a NES (Kuersten et al., 2001; Watanabe et al., 1999; Wolff et al., 1997). LMB can be used to inhibit export of β-catenin from nucleus to cytoplasm because β-catenin binds to APC which has NESs near the N terminus to export its partner proteins through the CRM1 export pathway (Henderson, 2000). Wnt3a and LMB co-treatment maintained the nuclear co-localization of β-catenin and Pin1 (Figs. 1.10A, B, third row). Wnt3a and juglone, which inhibit Pin1 activity, or siPin1, which reduces Pin1 expression, significantly decreased nuclear β-catenin (Figs. 1.10A, B, fourth row). However, Wnt3a, LMB, and juglone or siPin1 co-treated cells showed strong nuclear co-localization of β-catenin and Pin1 (Figs. 1.10A, B, fifth row). These results indicate that, even in the absence of Pin1 activity or Pin1 expression, Wnt3a-induced nuclear

translocation of β-catenin occurred; juglone- or siPin1-mediated clearance of nuclear β-catenin was effectively suppressed by LMB, which is known to inhibit APC-mediated nuclear clearance of β-catenin (Henderson, 2000; Rosin-Arbesfeld et al., 2000). We also quantified the intensity of nuclear β-catenin (Figs. 1.10C, D). Consistent with the confocal images, western blotting analysis also showed that the juglone-induced decrease of Wnt-induced nuclear accumulation of β-catenin was completely recovered by LMB (Fig. 1.11A). In vivo data, we could find that β-catenin expression in WT tibia is more condensed inside the nucleus compared with Pin1 KO tibia (Fig. 12). In addition, we were more convinced with the high resolution images that nuclear β-catenin retention is regulated by Pin1 not β-catenin translocation into the nucleus because nuclear β-catenin of Pin1 KO tibia was also lightly stained (Fig. 12). Since APC protein is a critical chaperone of nuclear β-catenin to the cytosol (Ryo et al., 2001), we investigated whether Pin1-mediated structural modification of β-catenin influences the interaction between β-catenin and APC in the nucleus. Wnt3a treatment strongly increased nuclear β-catenin level (Fig. 1.11B), while it decreased β-catenin-bound APC level (Fig. 1.11B). Inhibition of Pin1 increased β-catenin-bound APC level, which was attenuated by LBM treatment both with and without Wnt3a treatment (Fig. 1.11B). Based on these results and

the constitutive nuclear localization of Pin1 protein, we suggest that Pin1 is not actively involved in the nuclear translocation of β-catenin in response to canonical Wnt signaling but plays a crucial role in the APC-mediated cytosolic export of β-catenin.

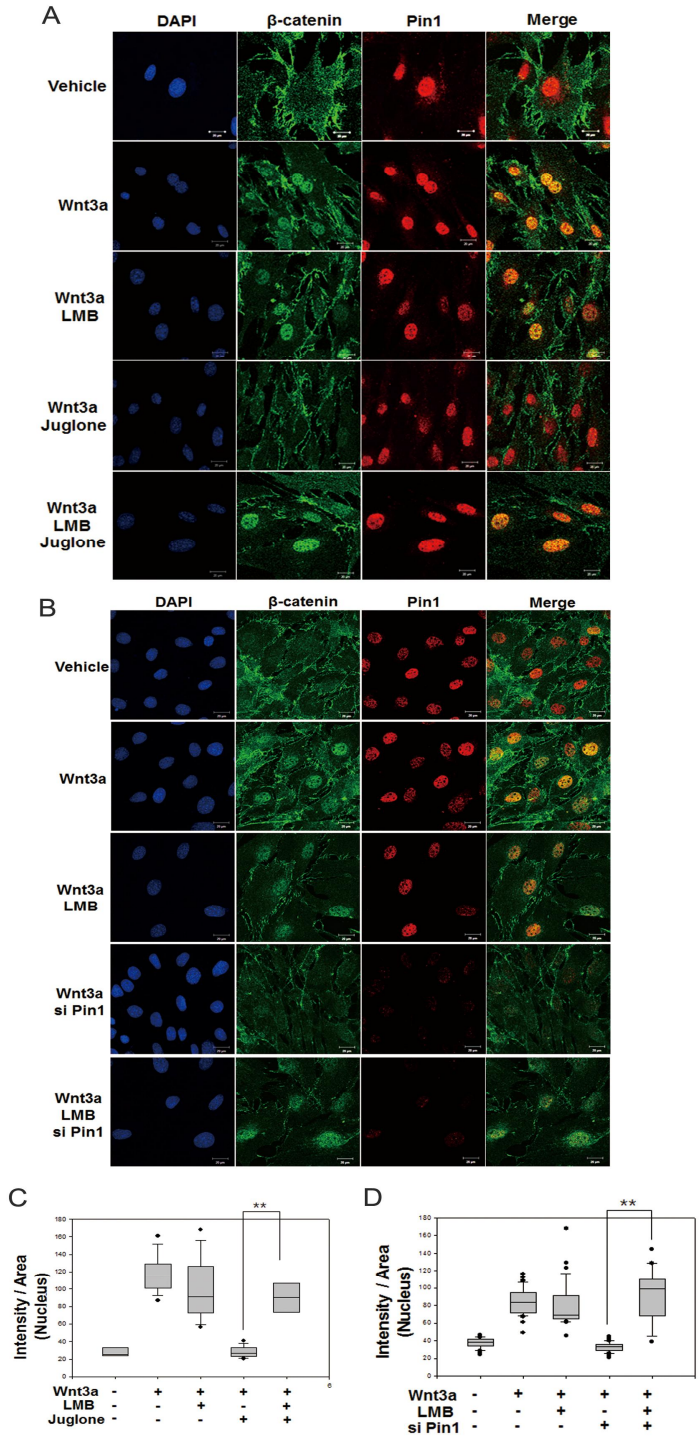
A
DAPI
β-catenin
Pin1
Merge
Vehicle
Wnt3a
Wnt3a LMB
Wnt3a Juglone
Wnt3a LMB Juglone
B
DAPI
β-catenin
Pin1
Merge
Vehicle
Wnt3a
Wnt3a LMB
Wnt3a si Pin1
Wnt3a LMB si Pin1
C
Intensity / Area (Nucleus)
**
Wnt3a
LMB
Juglone
D
Intensity / Area (Nucleus)
**
Wnt3a
LMB
si Pin1

Figure 1.10. Pin1 activity enhances the nuclear retention of β-catenin.

A. MC3T3-E1 cells were pretreated without or with 10 μM juglone and/or 100 ng/ml LMB for 1 h and then treated with 50 ng/ml Wnt3a for 24 h. Endogenous β-catenin translocation was detected using cells immunostained with anti-β-catenin, Pin1, and DAPI. LMB blocks the export system. **B.** MC3T3-E1 cells were transfected with a scramble (control) or siPin1 of siRNA. After 24 h, the same procedure was conducted. **C, D.** Endogenous nuclear β-catenin was quantified and showed as a sigma plot (n=50 in each group, ** indicates $p<0.01$).

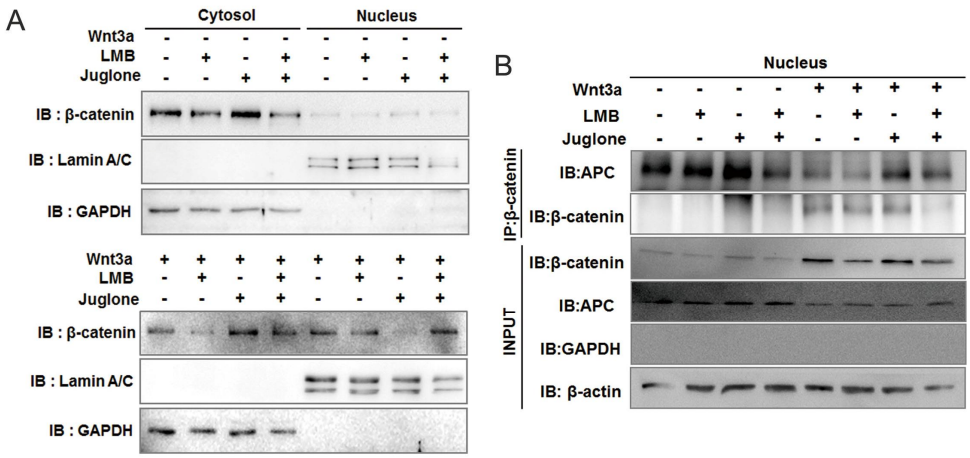

Figure 1.11. Pin1 promotes the nuclear retention of β-catenin via the dissection with APC

A. MC3T3-E1 cells were pretreated without or with 2 μM juglone and/or 100 ng/ml LMB for 1 h. Cells were treated without (upper) or with (lower) 50 ng/ml Wnt3a for 24 h. Cells were fractionated in hypotonic buffer into nuclear and cytoplasmic fractions, followed by immunoblot analysis with anti-β-catenin, anti-GAPDH, and anti-lamin A/C antibodies. Lamin A/C and GAPDH were used as a loading control for the nuclear and cytoplasmic fractions, respectively (left) (n=3). **B.** IP assay of APC and β-catenin. IP was performed with anti-β-catenin from dissociated nuclear extracts in HEK293 cells grown. APC was analyzed using immunoblot analysis with anti-APC antibody (n=3).

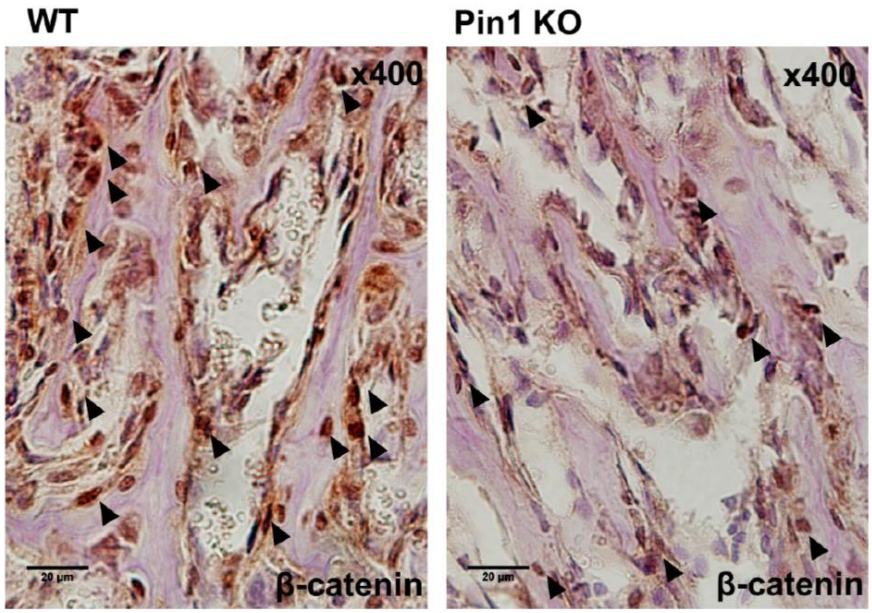

Figure 1.12. IHC for nuclear β-catenin in histological sections of the proximal tibia.

Coronal sections of the proximal tibia of P40 WT and Pin1 KO mice were stained with anti- β-catenin antibody (brown coloration). Arrowhead: nuclear β-catenin in the tibia.

β-Catenin as a substrate of Pin1 is protected by nuclear localization

Pin1 only binds to peptide bonds between pSer-Pro or pThr-Pro substrates. In silico analysis of β-catenin indicated there are three candidate target sites, Ser 191, 246, and 605 (Fig. 1.13A). We generated mutants with individual Ser to Ala substitutions, combinations of any two Ser to Ala substitution, or all three substitutions (3AP). We measured the biochemical molecular interaction by overexpression and GST-PD analysis of flag-tagged β-catenin WT or mutants with Pin1 (Fig. 1.13B). Our analysis revealed that β-catenin mutants interact, except for the 3AP mutant (Fig. 1.13B). Compared to WT β-catenin, each single substitution mutant or combination of two substitution mutants did not significantly change TOP Flash activity (data not shown). Only 3AP β-catenin showed a dramatic decrease in the TOP Flash enhancing activity of β-catenin (Fig. 1.13C). Figure 1.13. indicates that structural modification by Pin1 is critical for β-catenin nuclear retention, so we compared nuclear retention of WT β-catenin and 3AP. After 24 h overexpression of either WT or 3AP in MC3T3-E1 cells, each culture was treated with CHX for the indicated time, and then the intensity and localization of β-catenin were analyzed. Nuclear β-catenin was exported to the cytosol (Fig. 1.13D), and exported β-catenin is known to undergo proteasomal degradation (Henderson, 2000). The rate of decay of

the 3AP was faster than that of the WT (Fig. 1.13D). We quantified the intensity of the WT and 3AP nuclear β-catenin (Fig. 1.13E). Nuclear β-catenin interacts with Lef1 and enhances its transcriptional activity to stimulate osteogenesis in canonical Wnt stimulation (Behrens et al., 1996). We need to clarify whether the decrease of TOP flash enhancing activity of 3AP mutant β-catenin (Fig. 1.13C) is resulted from its decreased stability or intractability with Lef1. The interaction between Lef1 and β-catenin WT or 3AP mutant was determined by IP assay (Fig. 1.13F), which showed Flag-tagged β-catenin level is quite proportional to co-precipitated LEF1 level indicating its intractability with Lef1 was not abrogated by 3AP substitution mutation. Input protein levels of 3AP β-catenin showed a strong decrease compared to WT β-catenin (Fig. 1.13F) indicating the stability change is the main cause of decreased activity in 3AP mutant. Overexpression of 3AP mutation abrogated the stimulatory effect of β-catenin on osteogenic marker genes (Figs. 1.14A-C). These results strongly indicated that Pin1 stabilizes β-catenin and prolongs its nuclear retention which subsequently increases osteogenic marker gene expression.

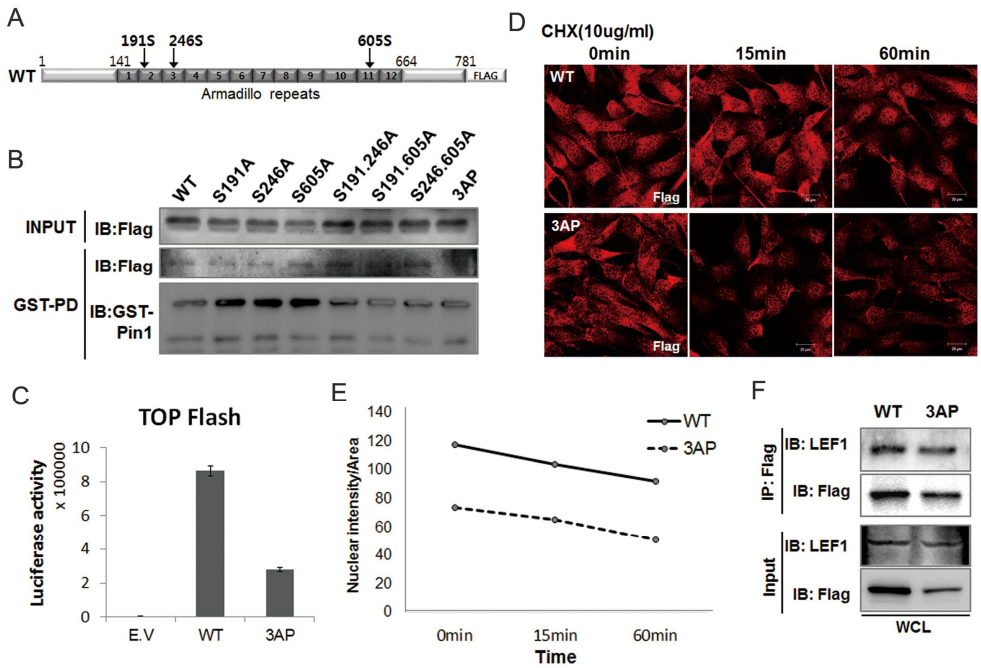

Figure 1.13. Pin1 protects against β-catenin degradation by controlling the release of β-catenin from the nucleus

A. Diagram of β-catenin structure and possible Pin1 binding sites. A mutant form of β-catenin (3AP) was generated by the site-directed mutagenesis of three Ser codons to alanine codons. **B.** HEK293 cells were transfected with the WT or mutant forms of β-catenin (single, double, or all sites mutant). After 24h, cells were treated with 50ng/ml Wnt3a for 24 h. The interaction of overexpressed β-catenin with Pin1 was determined by GST-PD (n=3). **C.** TOP Flash activity was characterized in HEK293 cells, which overexpressed the WT or 3AP (Ser191Ala, Ser246Ala, and Ser605Ala)

mutant of β-catenin or the empty vector (EV). After 24 h, luciferase activity was determined (n=3). **D.** MC3T3-E1 cells were transfected with the WT or 3AP mutant expression plasmids. After transfection for 24 h, the cells were harvested at 0 or 60 min after CHX treatment (10 μg/ml), and β-catenin was detected using IF. **E.** Nuclear β-catenin was quantified and showed a graph by time course (n=10 in each group).

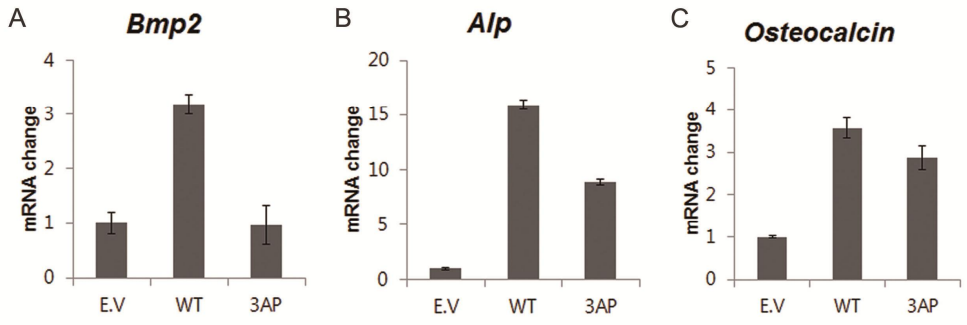

Figure 1.14. Change of bone marker genes by 3AP mutation of β-catenin

A-C. MC3T3-E1 cells were transfected with WT or 3AP mutant expression plasmids or EV. After 48 h, mRNA levels of Bmp2, Alp, and Osteocalcin were quantitatively analyzed (n=3).

Discussion

Pin1 is critical for the nuclear retention of β-catenin

In the presence of a Wnt signal, the inhibition of phosphorylation and subsequent ubiquitination of β-catenin results in its accumulation in the cytosol (Logan and Nusse, 2004). However, the mechanisms controlling the nuclear localization of β-catenin, especially entrance into and exit from the nucleus are poorly understood. Since β-catenin does not contain a NLS or NES sequence (MacDonald et al., 2009), the efficient entry and exit of β-catenin to and from the nucleus are unknown. Even though previous reports have investigated the many molecules involved in the import and export of β-catenin (Henderson, 2000; Kramps et al., 2002; Tolwinski and Wieschaus, 2001; Townsley et al., 2004), the results are quite controversial. Rigorous control of β-catenin-mediated transcription is essential to prevent the tenacious activation of Wnt target genes in the canonical Wnt signaling pathway. Export of β-catenin from the nucleus completely terminates the transcriptional function of β-catenin. Our data show that Pin1 is critical to keep β-catenin in the nucleus and is not critical to translate β-catenin from the cytosol to the nucleus (Figs. 1.10, 1.11). If Pin1 were involved in the nuclear translocation of β-catenin, β-catenin would not be present in the nucleus when cells were treated with siPin1 or juglone and LMB, as β-

catenin would have already failed to enter the nucleus due to inhibited Pin1 expression and activity. We observed that nuclear β-catenin was still highly maintained (Figs. 1.10, 1.11). This result is congruous with the results of earlier studies where Pin1-mediated conformational change determined the molecular localization in a cell (Ryo et al., 2001; Yang et al., 2012). Regulation of β-catenin retention by Pin1 affects to reductions in transcriptional activity and target gene expression when Pin1 was inhibited or absent (Figs. 1.1-4).

β-Catenin directly interacts with Pin1 in the nucleus

Among the many prolyl isomerases, Pin1 shows the narrowest target specificity for Pro-directed phosphorylation sites in a subset of proteins (Lim and Lu, 2005). In silico analysis of β-catenin indicates that it has three candidate Pin1 binding sites, Ser191, Ser246, and Ser605 (Fig. 1.13A). Previous reports have suggested that post-phosphorylation binding of Pin1 to the Ser246 of β-catenin is vital for the stability and/or subcellular localization of β-catenin (Nakamura et al., 2012; Ryo et al., 2001). Another study stresses that Ser191 and Ser605 are more critical for β-catenin nuclear localization than Ser246 (Wu et al., 2008). In the present study, we did not find any significant difference in interaction (Fig. 1.13B), transcriptional

activity and localization between the WT and any Ser to Ala single or double substitution mutants in β-catenin. Only 3AP failed to bind to Pin1 (Fig. 1.13B) and showed a significant down-regulation of its transcriptional activity (Fig. 1.13C), indicating that all three candidate sites are targets of Pin1 substrate. These results are different from those of previous reports in which the authors designated one or two specific sites for Pin1 interaction. We assume that this is because multiple signaling cascades converge on β-catenin via phosphorylation to control canonical Wnt signaling. Studies indicate that intracellular molecular mechanisms of β-catenin are tightly controlled by multiple signaling pathways in different biological contexts; in fibroblasts, Wnt3a activates ERK and plays an important role in cell proliferation (Yun et al., 2005); in differentiated osteoblasts, Wnt3a prevents apoptosis through β-catenin-dependent signaling cascades involving Src/ERK and phosphoinositide 3 kinase (PI3K)/AKT (Almeida et al., 2005); and TGFβ and Notch signaling pathways also maintain crosstalk with the Wnt signaling pathway (Attisano and Labbe, 2004; Caliceti et al., 2014; Fre et al., 2009; Warner et al., 2005). Pin1 target sequences are shared by several protein kinases, such as ERK, CDK, and GSK3a (Yoon et al., 2014a). Therefore, we suggest that the conformational change of each of the three different phosphorylation sites probably has different biological implications.

Nuclear interaction of β-catenin and APC is regulated by Pin1

Our next question addressed the mechanism by which Pin1-modified β-catenin remains in the nucleus for long periods of time. Previous reports have indicated that a nuclear-cytoplasmic shuttling protein, APC, can function as a chaperone for β-catenin export from the nucleus (Henderson, 2000; Rosin-Arbesfeld et al., 2000). Pin1 affects the interaction between β-catenin and APC (Ryo et al., 2001); therefore, we hypothesized that the conformational change of nuclear β-catenin by Pin1 does not allow for the interaction with APC, inhibiting the export of β-catenin to the cytosol from the nucleus and consequently enhancing the nuclear retention of β-catenin. We observed that the interaction between nuclear APC and β-catenin was generally reduced in the presence of Wnt ligand and increased when Pin1 activity was inhibited by juglone (Fig. 1.11B). Therefore, we suggest that the conformational change of nuclear β-catenin by Pin1 inhibits the ability of β-catenin to interact with nuclear APC and subsequent APC-guided export of β-catenin to the cytosol (Fig. 15).

Regulation of nuclear β-catenin retention by Pin1 implicates it as a drug target for bone diseases and cancer

The canonical Wnt signaling pathway is an important regulatory pathway in the osteogenic differentiation of MSCs (Holland et al., 2013; Kim et al., 2013) and bone development (Westendorf et al., 2004). Induction of the Wnt signaling pathway promotes bone formation (Gong et al., 2001; Hill et al., 2005; Little et al., 2002). Genetic studies have shown that LRP5 can control bone mass (Gong et al., 2001; Little et al., 2002) and conditional deletion of β-catenin in the embryonic limb, and head mesenchyme results in the absence of mature osteoblasts in membranous bones (Hill et al., 2005; Kolpakova and Olsen, 2005). Our previous studies have shown the importance of Pin1 in bone development (Yoon et al., 2014a; Yoon et al., 2014b; Yoon et al., 2013a). Considering this, Wnt signaling including all the components of the canonical pathway and Pin1 are deemed essential for bone formation. We demonstrated that Pin1 increases Wnt-induced osteoblast differentiation. These results are consistent with those of previous reports showing that Pin1 KO mice had low bone mineral density (Shen et al., 2013; Yoon et al., 2013a). These data identify for the first time a major function of Pin1 in osteoblast differentiation by regulating the interaction between β-catenin and APC. Therefore, Pin1 is a potential biological marker or therapeutic target that enhances Wnt-induced osteoblast differentiation. Both the Wnt signaling pathway and Pin1 have been studied in pathological

human cancers (Anastas and Moon, 2013; Driver and Lu, 2010; Lu and Zhou, 2007; Morin, 1999; Wulf et al., 2003). Pin1 plays a key role in the pathogenesis of other malignancies such as breast, colon, and prostate cancer (Chen et al., 2006; Driver and Lu, 2010; Suizu et al., 2006). In particular, unregulated activation of β-catenin is a major cause of tumorigenesis in cancers (Luu et al., 2004). In addition, Pin1 increases the transcription of several β-catenin target genes by inhibiting its interaction with APC (Ryo et al., 2001) in cancer. Thus, our novel finding that Pin1 is important for regulating the interaction between β-catenin and APC in the nucleus and the export of β-catenin to the cytosol (Fig. 1.11) can also be a useful tool in cancer therapeutics.

In conclusion, our results reveal a novel molecular mechanism whereby Pin1 promotes the nuclear retention of β-catenin through inhibition of the interaction between APC and β-catenin in the nucleus, which, in turn, up-regulates osteoblast differentiation. This mechanism is a new avenue for studying the translocation of nuclear β-catenin, and this knowledge leads to a deeper understanding of the importance of isomerized β-catenin in bone development. Although we examined the Pin1 and β-catenin relationship under physiological conditions in osteoblast differentiation, these results raise the possibility as a cancer drug target.

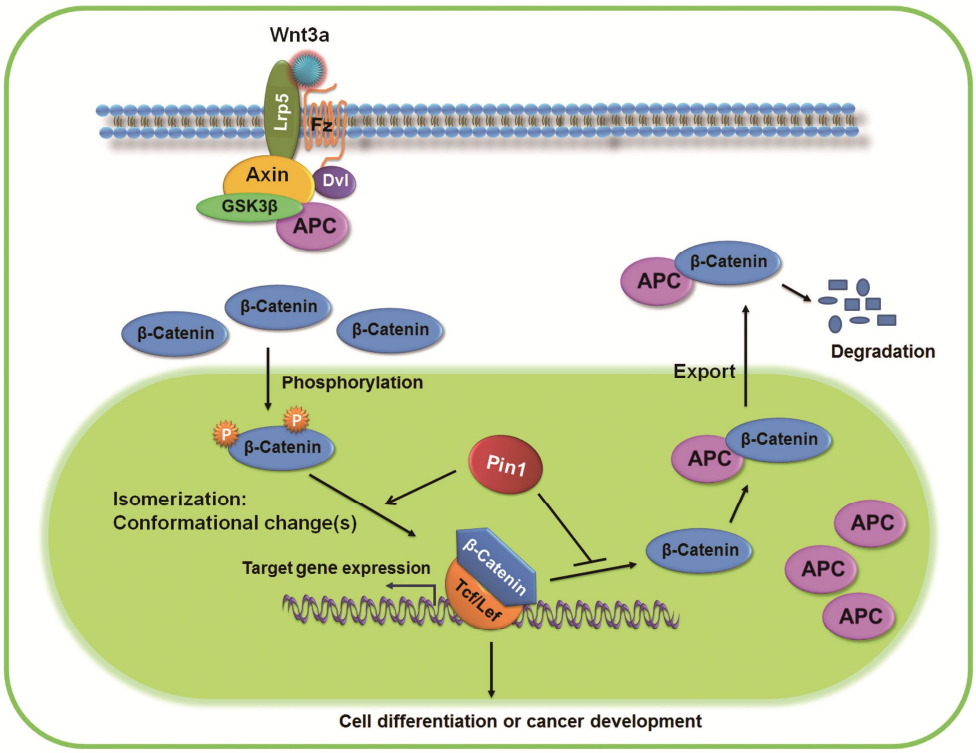

Figure 1.15. Model of Pin1-mediated nuclear retention of β-catenin.

We propose that Pin1 is critical for the retention of β-catenin to properly control transcriptional activity. After β-catenin phosphorylation through some mechanism, Pin1 recognizes the phosphorylated WW motifs and catalyzes conformational change(s) of β-catenin. The conformational change enhances nuclear retention of β-catenin by inhibiting interaction of β-catenin and APC, positively affecting the trans-acting activity of β-catenin. Taken together, our results reveal that Pin1 is a novel regulator of β-catenin localization and promotes cell differentiation like osteoblast differentiation.

Our results reveal a novel mechanism whereby Pin1 activity is needed to enhance the nuclear retention of β-catenin. This finding sheds light on the potential for novel therapeutic approaches.

V. Part 2.

Pin1 is a new therapeutic target of craniosynostosis

Abstract

Gain-of-function mutations in FGFRs cause congenital skeletal anomalies including CS, which is characterized by the premature closure of craniofacial sutures. AS is one of the severest forms of CS, and the only treatment is surgical expansion of prematurely fused sutures in infants. Previously, we demonstrated that the prolyl isomerase Pin1 plays a critical role in mediating FGFR signaling, and that *Pin1*$^{+/-}$ mice exhibit delayed closure of cranial sutures. In this study, using both genetic and pharmacologic approaches, we tested whether Pin1 modulation could be used as a therapeutic regimen against AS. In the genetic approach, we crossbred *Fgfr2*$^{S252W/+}$, a mouse model of AS, and *Pin1*$^{+/-}$ mice. Down-regulation of *Pin1* gene dosage attenuated premature cranial suture closure and other phenotypes of AS in *Fgfr2*$^{S252W/+}$ mutant mice. In the pharmacological approach, we intraperitoneally administered juglone, a Pin1 enzyme inhibitor, to pregnant *Fgfr2*$^{S252W/+}$ mutant mice, and found that this treatment successfully interrupted fetal development of AS phenotypes. Primary cultured osteoblasts from *Fgfr2*$^{S252W/+}$ mutant mice expressed high levels of FGFR2 downstream target genes, but this phenotype was attenuated by Pin1 inhibition. Post-translational stabilization and activation of Runx2 in *Fgfr2*$^{S252W/+}$ osteoblasts were also attenuated by Pin1 inhibition.

Based on these observations, we conclude that Pin1 enzyme activity is important for FGFR2-induced Runx2 activation and craniofacial suture morphogenesis. Moreover, these findings highlight that juglone or other Pin1 inhibitors represent viable alternatives to surgical intervention for treatment of CS and other hyperostotic diseases.

Introduction

CS, defined as premature fusion of one or more of the cranial sutures, occurs in approximately 1 in 2,500 live births (Johnson and Wilkie, 2011). Normally, the mammalian cranial vault consists of five major flat bones joined by structures known as cranial sutures (Clendenning and Mortlock, 2012), which play a key role in cranial growth during development (Jin et al., 2016). To permit brain growth in the early stage of life, the sutures should remain patent (Johnson and Wilkie, 2011). However, in CS, premature fusion prevents skull expansion to accommodate brain growth, potentially resulting in elevated intracranial pressure and multiple sequelae including brain dysfunction, hydrocephalus, reduced intelligence, and visual impairment due to pressure on the optic nerve (Derderian and Seaward, 2012; Johnson and Wilkie, 2011). Currently, the only treatments for these disorders involve postnatal surgery.

In a prospective analysis of a cohort presenting with CS, the genes most frequently mutated were *FGFR2* (32%), *FGFR3* (25%), *TWIST1* (19%), and *EFNB1* (7%) (Johnson and Wilkie, 2011). Heterozygous mutations of *FGFR2* cause three classical CS syndromes: Apert, Crouzon, and Pfeiffer (Bagheri-Fam et al., 2015). AS, one of the severest form of CS (Du et al., 2010; Koca, 2016), is accompanied by facial abnormalities such

as bicoronal synostosis, hypertelorism, mid-face hypoplasia, narrow arched palate, and mitten-like syndactyly of fingers and toes (Robin et al., 1993). Over 98% of cases are caused by specific missense mutations of *FGFR2*, either Ser252Trp (66%) or Pro253Arg (32%), in the linker between the IgII and IgIII domains (Ibrahimi et al., 2004; Johnson and Wilkie, 2011). These substitutions increase the affinity and broaden the specificity of FGF-ligand binding, explaining the cellular consequences of mutation including accelerated proliferation and differentiation of osteoblasts in the cranial suture; premature differentiation is probably the most important factor leading to CS (Anderson et al., 1998; Ibrahimi et al., 2004). In this study, we focused on early coronal suture closure using a mouse model of AS that harbors a targeted mutation (S252W) in *Fgfr2*.

Pin1 catalyzes post-phosphorylation conformational regulation. It binds only to specific pSer/Thr-Pro motifs, causing a cis–trans conformational change of the substrate (Nakamura et al., 2012). In a previous study, we demonstrated that *Runx2* expression is regulated by FGF2 (Kim et al., 2003), and that prolyl isomerization of Runx2 mediated by Pin1 is crucial for acetylation and stabilization of the Runx2 in FGF/FGFR2 signaling (Yoon et al., 2014a; Yoon et al., 2013a). This molecular modification is essential for proper bone development (Kim et al.,

2016; Shin et al., 2016; Yoon et al., 2014a; Yoon et al., 2015a; Yoon et al., 2013a). Excessive FGFR2 downstream signaling, including elevated Runx2 activity and stability due to *FGFR2* mutations, could be a crucial driver of CS phenotypes.

Juglone (5-hydroxy-1,4-naphthoquinone) is a brown dye isolated from walnut shells and leaves of walnut trees (genus *Juglans*) (Hennig et al., 1998). Numerous *in vitro* and *in vivo* studies have shown that juglone effectively inhibits Pin1 activity (Aithal et al., 2012; Hennig et al., 1998; Jeong et al., 2009; Reese et al., 2010). We hypothesized that suppression of Pin1 would normalize hyper-activated FGFR2 signaling, thereby rescuing the premature obliteration of coronal sutures that is the hallmark symptom of CS. To test our hypothesis, we pursued two independent approaches in *Fgfr2*$^{S252W/+}$ mice, a model for human AS: a genetic approach targeting one allele of Pin1, and a pharmacological approach in which Pin1 activity was suppressed by administration of juglone during fetal development. Both approaches successfully attenuated CS phenotypes in the disease model mice, suggesting that Pin1 represents a promising molecular target for overcoming CS without surgery.

Materials and methods

Animal experiments

Fgfr2$^{S252W/+}$ and *Pin1*-deficient mice (Fujimori et al., 1999; Shukla et al., 2007) were maintained under specific pathogen–free (SPF) conditions. The loxP-neo-loxP cassette, a blocker sequence, can be removed to stimulate the *Fgfr2*^{S252W} allele upon crossing with mice carrying a ubiquitous *Cre* transgene (*EIIA-Cre*, The Jackson Laboratory) (Lakso et al., 1996; Shukla et al., 2007). Mice carrying the *Fgfr2*^{S252W} and *EIIA-Cre* alleles were mated, and *Pin1;Fgfr2* compound mutant mice were generated by mating *Pin1*$^{+/-}$*Fgfr2*$^{Neo\text{-}S252W/+}$ mice with *Pin1*$^{+/-}$*EIIa-Cre/*+ mice. The genetic background of *Fgfr2*$^{Neo\text{-}S252W/+}$ mice is FVB (Shukla et al., 2007), and the *EIIa-Cre* transgene (B6.FVB-TgN(EIIa-cre)C5379Lm, No: 003724) was from the Jackson Laboratory. The genetic background of the *Pin1*$^{+/-}$ mice is C57BL/6 (Komori et al., 1997). Pregnant mice were injected intraperitoneally with juglone (Calbiochem, Darmstadt, Germany). The numbers of animals in experimental groups are indicated in the figure legends. Animals were housed in cages following IACUC policies. All animal studies were reviewed and approved by the Special Committee on Animal Welfare, Seoul National University, Seoul, Republic of Korea.

Skeletal staining

For skeletal staining, P0.5 mice were exenterated, skin was pareed follow by fat tissue was removed. After overnight fixation in ethanol with 95% dose, samples were stained in alcian blue solution (150mg Alcian blud, 800ml 98% ethanol, 200ml acetic acid) for 24h. After then, they were transported to 2% KOH for 24h. Overnight staining in Alizarin red solution (50mg/l Alizarin red in 2% KOH) was successively performed and then samples were cleared in solution of 1% KO with 20% glycerol and slowly increase the amount of glycerol for 2-3 weeks and saved in 100% glycerol.

Micro-CT analysis

P0.5 mice were sacrificed and fixed with 4% paraformaldehyde overnight at 4°C. Micro-CT sanning was achieved on an inspeXio SMX-100CT, and data were examined using the TriBON software (RATOC, Tokyo, Japan). The use of these methods for bone analyses was described previously (Cho et al., 2016; Ruan et al., 2016; Ruan et al., 2013). After taking 3-dimentional images of micro-CT, samples were sequentially used for immune-histochemistry or skeletal staining.

Cell culture and nuclear–cytoplasmic fractionation

Primary osteoblasts of WT and *Fgfr2*$^{S252W/+}$ mice were isolated from calvaria of P0.5 mice. Primary osteoblasts and pre-osteoblast MC3T3-E1 cells were cultured in α-MEM with 10% FBS containing 1% penicillin and streptomycin antibiotics. For osteogenic differentiation, the medium was supplemented with 5 mM β-glycerophosphate and 50 μg/ml ascorbic acid, and cells were cultured with osteogenic medium for 2-3 weeks. Nuclear–cytoplasmic fractionation was conducted using the NE-PER Nuclear and Cytoplasmic Extraction Reagent kit (Thermo Fisher Scientific, Massachusetts, USA) according to the manufacturer's protocol as Part.1 study.

Cytotoxicity test and cell proliferation assay

To test the cytotoxicity of juglone, cells were seeded at a confluence of $2x10^3$ cells in 96well plates, and treated with juglone for 24h. Water-soluble tetrazolium assay was completed for determination of the amount of viable and proliferated cells by using EZ-CyTox solution (Daeil Lab Service, Seoul, Korea). Tests were performed depending on the manufacturer's instruction. To check the rate of proliferation, culture the cells and measure the cell number from day1 to day7.

Luciferase assay

The transcriptional activity of Runx2 was determined with the 6XOSE2 luciferase reporter plasmid vector. Luciferase assay was performed as Part.1 study using the Luciferase Assay Kit (Promega, Madison, WI, USA).

Antibodies and reagents

Antibodies and reagents are described in detail in Tables 2.1 and 2.2.

Alizarin Red S staining

After primary osteoblasts were cultured in osteogenic differentiation medium for 3 weeks, matrix mineralization was checked by Alizarin red S staining. Cells were washed with Ca^{2+} free PBS for 3 times and fixed with 1% formaldehyde for 20min at 4℃. After cells were washed 5 times with PBS, cells were stained with 1% Alizarin red S solution for 5min (Sigma, St.Louis, MO, USA).

Histology analysis

For H&E staining and IHC of tissue sections, P0.5 mice were fixed in

4% paraformaldehyde for 24 h, dehydrated, and embedded in paraffin using standard procedures. Serial paraffin sections (5-μm thickness) were prepared, deparaffinized and rehydrated. The tissue sections were then stained with H&E staining as described previously (Yoon et al., 2013) or IHC using the EnVision^{TM} G|2 Doublestain System (Dako, Glostrup, Denmark) as part.1 (Bae et al., 2017a). Stained tissues were imaged on a conventional microscope equipped with a DP72 digital camera (Olympus, Tokyo, Japan). Antibodies used for these experiments are listed in Table 2.1.

Extraction of total RNAs, reverse transcription polymerase chain reaction (RT-PCR), and real-time PCR (qPCR)

Total RNA extraction from cultured cells, RT-PCR, and qPCR were performed as described Part.1 (Bae et al., 2017a; Cho et al., 2016; Shukla et al., 2007). The primer sets used for real-time PCR are listed in Tables 2.3.

IP and IF

For IP, cellular nuclear proteins from primary osteoblast were extracted using the NE-PER Nuclear and Cytoplasmic Extraction Reagent kit (Thermo Fisher Scientific, Massachusetts, USA), and proceeded with IP

as described in part.1 with a buffer which consisting of 150mM NaCl, 50mM HEPES (pH 7.5), 100mM NaF, 1mM EDTA, 0.25% sodium deoxycholate, 1mM DTT, 0.25% CHAPS, 1% Nonidet P-40, and 10% glycerol supplemented with protease and phosphatase inhibitors, including Na_3VO_4. The precipitated proteins were then analyzed by immunoblot detection with specific antibodies. For IF, cells were fixed in 4% formaldehyde for 10min at 4℃. Then, cells were stained with the primary antibody and fluorescent-conjugated secondary antibody. Visualization with a Carl Zeiss LSM700 microscope and analysis with ZEN2011 software were performed (Carl Zeiss, Oberkochen, Germany).

DNA construction and transfection

Construction of $Fgfr2^{WT}$ and $Fgfr2^{S252W}$ mutant expression vectors was described previously (Tanimoto et al., 2004). Transactivation activity of Runx2 was evaluated using the 6XOSE2-Luc reporter vector (Kim et al., 2003). The Neon transfection system (Invitrogen, San Diego, CA, USA) was used for DNA transfection of primary osteoblasts or MC3T3-E1 cells.

Statistics

All quantitative data are presented as means ± SD (*in vitro* data) or

means ± SEM (*in vivo* data). Each experiment was performed at least three times, and results from representative individual experiments are shown in the figures. Statistical analysis was performed by either unpaired two-tailed Student's t-test or one-way ANOVA followed by Bonferroni's test using the Prism 5.0 software (GraphPad Software, San Diego, CA, USA). $P < 0.05$ was considered significant.

Study approval

The Seoul National University institutional animal care and use committees approved the animal study (Approval No.SNU-160121-1).

Table 2.1. Antibodies used in this study.

Antigen	Clone	Cat.#	Host	Appl.	Source
Runx2	8G5	D130-3	M, mAb	WB, IP, IC,IH	MBL
RNA Pol II	N-20	#G2914	Rb, pAb	WB, IP, IF	Santa Cruz
Acetyl-lysine	-	#9441	Rb, pAb	WB, IP, IHC,IF	Cell signaling
Lamin A/C	N-18	Sc-6215	G, pAb	WB,IP,IF	Santa Cruz

M, mouse; Rb, rabbit; G, goat
mAb, monoclonal antibody; pAb, polyclonal antibody

Table 2.2. Chemical reagents used in this study.

Chemical reagents	Application	Source
Juglone	Pin1 inhibitor	Calbiochem
CHX	Protein synthesis inhibitor	Sigma-Aldrich
Alizarin Red S	The staining of cartilage and bone Checking the calcium deposites	Sigma-Aldrich
Alcian Blue 8GX	The staining and precipitation of glycosaminoglycans	MENTOS
CHX	Protein synthesis inhibitor	Sigma-Aldrich

Juglone, 5-hydroxy-1,4-naphthalenedione; CHX, Cycloheximide;

Table 2.3. Primer list used in this study

For Real-time PCR	
Name	Oligonucleotide Sequence
Spry2(forward)	***5'- GGC CTC GGA GCA GTA CAA GG-3'***
Spry2(reverse)	***5'- GTA GGC ATG CAG ACC AAA T -3'***
Spry3(forward)	***5'- TCT GAT TGG TCC CTG GCT AC-3'***
Spry3(reverse)	***5'- GGG TTC TGA TGA TGG ACT GG -3'***
Dusp6(forward)	***5'- CGA GTC GTC ACA CAT CGA AT-3'***
Dusp6(reverse)	***5'- TCG CTG CTA TTC TCG TCG TA -3'***
ß-catenin(forward)	***5'-ATGGAGCCGGACAGAAAAGC -3'***
ß-catenin (reverse)	***5'-CTTGCCACTCAGGGAAGGA -3'***
c-Myc(forward)	***5'-CAG ATC AGC AAC AAC CGA AA--3'***
c-Myc(reverse)	***5'-GGC CTT TTC ATT GRR TTC CA -3'***
Pcna(forward)	***5'-TTTGAGGCACGCCTGATCC -3'***
Pcna(reverse)	***5'-GGAGACGTGAGACGAGTCCAT -3'***
Mapk(forward)	***5'-CAGGTGTTCGACGTAGGGC -3'***
Mapk(reverse)	***5'-TCTGGTGCTCAAAAGGACTGA -3'***
Collagen1α1(forward)	***5'- GCTCCTCTTAGGGGCCACT - 3'***
Collagen1α1 (reverse)	***5'- CCACGTCTCACCATTGGGG -3'***
Osteocalcin (forward)	***5'- CTG ACA AAG CCT TCA TGT CCA A -3'***
Osteocalcin (reverse)	***5'- GCG CCG GAG TCT GTT CAC TA -3'***

Results

Inactivation of Pin1 prevents premature fusion of coronal suture in AS model mice

Pin1 is crucial for osteoblast differentiation mediated by FGF/FGFR2 signaling (Yoon et al., 2014a; Yoon et al., 2013a). To further investigate the relationship between Pin1 and skeletal abnormalities in our AS mouse model, we reduced the dose of Pin1 by crossing *Pin1*$^{+/-}$*Fgfr2*$^{Neo-S252W/+}$ with *Pin1*$^{+/-}$*EIIA-Cre*$^{+/-}$ (*Pin1*$^{+/-}$*;Fgfr2*$^{S252W/+}$) to generate compound mutant mice. These genetic manipulations resulted in significantly different overall phenotypes. *Fgfr2*$^{S252W/+}$ mice exhibited abnormalities including a dome-shaped skull, shortened skull length (Fig. 2.1A), and smaller body length (Fig. 2.3), as described previously (Shukla et al., 2007). As a reference, a schematic diagram (Wang et al., 2010) is shown in Fig. 2.1B. Micro-CT scans were performed on P0.5 mice to observe mineralized tissues (Fig. 2.1C, D). *Fgfr2*$^{S252W/+}$ mice had CS of coronal suture, but this phenotype was rescued in *Pin1*$^{+/-}$*;Fgfr2*$^{S252W/+}$ mice (Fig. 2.1C, D, yellow arrows). In comparison with *Fgfr2*$^{S252W/+}$ mice, these mice had a longer skull (Fig. 2.1E) and nasal region (Fig. 2.1F) and smaller skull height (Fig. 2.1G) and intercanthal distance (Fig. 2.1H). To observe histological changes, we

prepared sagittal sections of calvaria. As reported previously, *Fgfr2*$^{S252W/+}$ coronal sutures were completely fused (Fig. 2.2). By contrast, *Pin1*$^{+/-}$*;Fgfr2*$^{S252W/+}$ coronal sutures remained in the differentiated state, and were not yet completely fused (Fig. 2.2). These results were also observed by walking through the suture on the micro-CT analysis (Fig. 2.4). The fused coronal sutures of *Fgfr2*$^{S252W/+}$ mice were completely mineralized, with no space between the frontal (F) and parietal (P) bones (Fig. 2.4A). However, this was not observed in *Pin1*$^{+/-}$*Fgfr2*$^{S252W/+}$ mice, in which the distance between the frontal and parietal bones was increased comparable to that in WT mice (Fig. 2.4A, B). These differences were statistically significant. The incidence of coronal and frontal–nasal suture fusion depended on genotype (Table. 2.4). Reduced body length in *Fgfr2*$^{S252W/+}$ mice was also restored by genetic deletion of one allele of *Pin1*; this effect was statistically significant (Fig. 2.3). These observations suggest that inactivation of Pin1 prevents CS of coronal sutures in *Fgfr2*$^{S252W/+}$ mice.

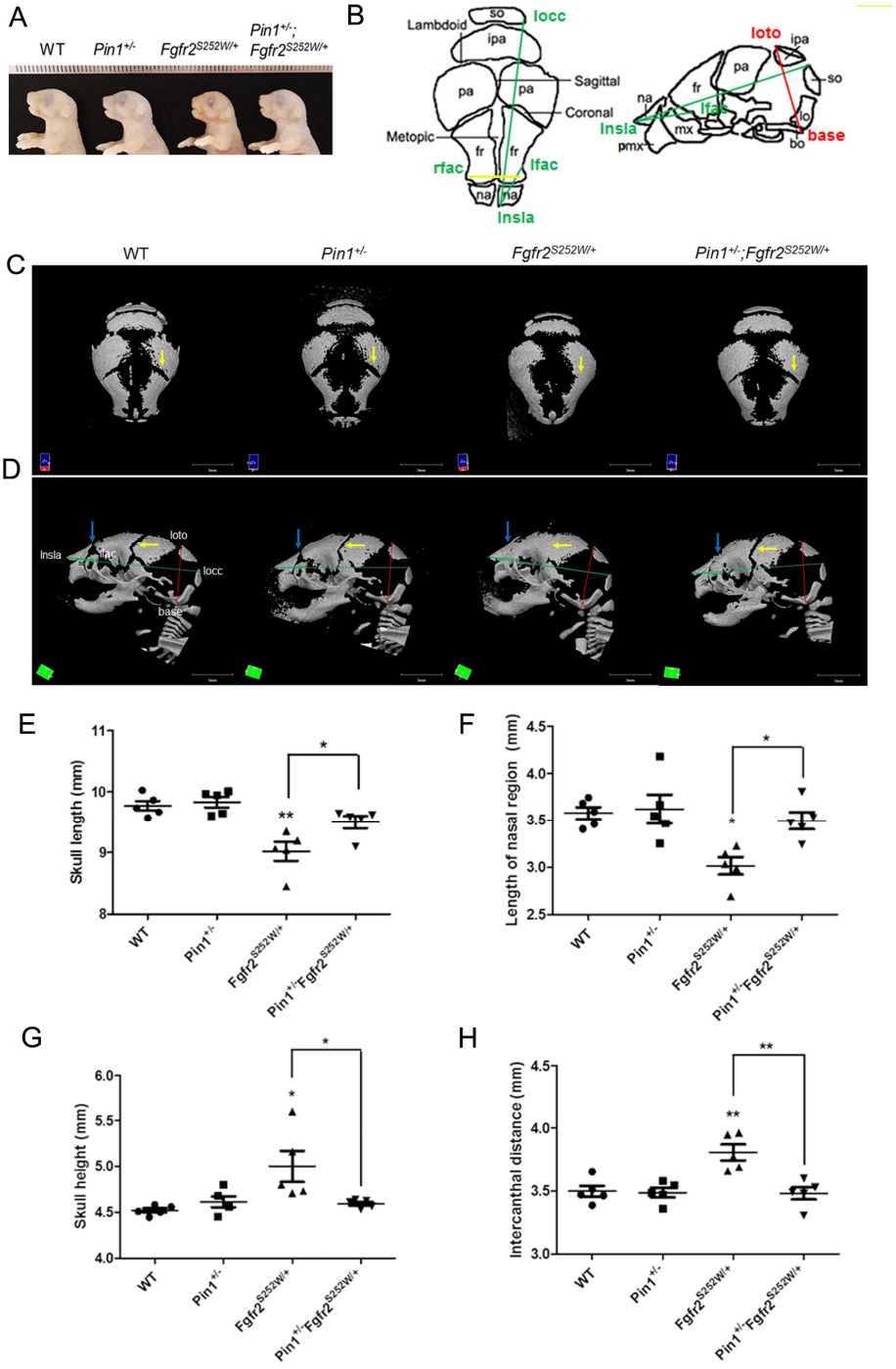
A
WT
Pin1+/-
Fgfr2S252W/+
Pin1+/-; Fgfr2S252W/+
B
Lambdoid
so
locc
ipa
Sagittal
pa
Coronal
Metopic
fr
rfac
lfac
na
Insla
loto
base
mx
pmx
bo
lo
C
D
E
Skull length (mm)
F
Length of nasal region (mm)
G
Skull height (mm)
H
Intercanthal distance (mm)

Figure 2.1. Rescue of premature fusion of coronal suture in *Fgfr2*$^{S252W/+}$ mice by removal of one allele of *Pin1*.

A. P0.5 skull of WT, *Pin1*$^{+/-}$, *Fgfr2*$^{Neo\text{-}S252W/+}$ *E2A-Cre*$^{+/-}$(*Fgfr2*$^{S252W/+}$), and *Pin1*$^{+/-}$;*Fgfr2*$^{Neo\text{-}S252W/+}$*EIIA-Cre*$^{+/-}$(*Pin1*$^{+/-}$;*Fgfr2*$^{S252W/+}$) mice. **B.** Schematic diagram and landmarks of mouse skull vault. The mouse skull consists of paired frontal bones (fr), paired parietal bones (pa), and the interparietal bone (ipa), intervened by the coronal, sagittal, metopic, and lambdoid sutures. **C, D.** Representative micro-CTs of skulls from WT, *Pin1*$^{+/-}$, Fgfr2$^{S252W/+}$, and *Pin1*$^{+/-}$;*Fgfr2*$^{S252W/+}$ mice (n=3). Superior views (C) and lateral views (D) of skull calvaria. Removal of one allele of *Pin1* rescued premature fusion of coronal suture (yellow arrows), a CS calvarial phenotype, and the frontal–nasal suture (blue arrows). The 3D coordinates of specific craniofacial landmarks, shown in Fig. 2.1B and 2.1D, were used for morphometric analyses of the skulls. Green lines represent linear distances corresponding to the length of the nasal region (lnsla–lflac) and the skull length (rnsla–rocc). Red line indicates skull height (lpto–bas). Yellow lines, indicating intercanthal distance (lflac–rflac), show linear distances corresponding to facial width. **E–H**. Representative micro-CT results of skulls, shown as bar graphs (n=5 in each group; *$p < 0.05$; **$p < 0.005$; ***$p < 0.001$).

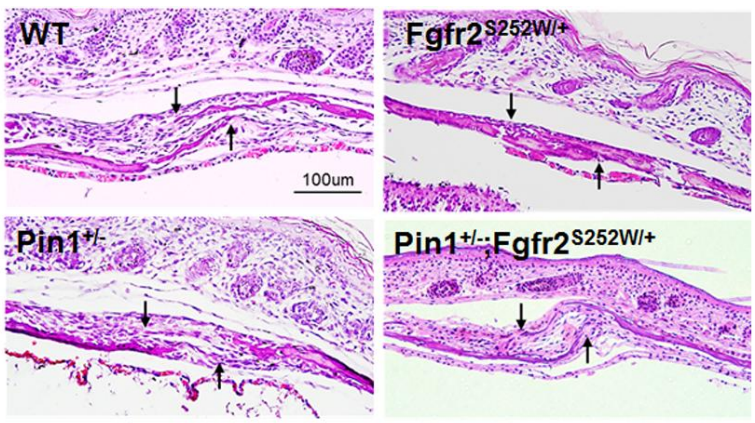

Figure 2.2. Histological change of premature fusion of coronal suture

Histological sections of coronal sutures in P0.5 mice. Arrows indicate growing fronts of frontal and parietal bones.

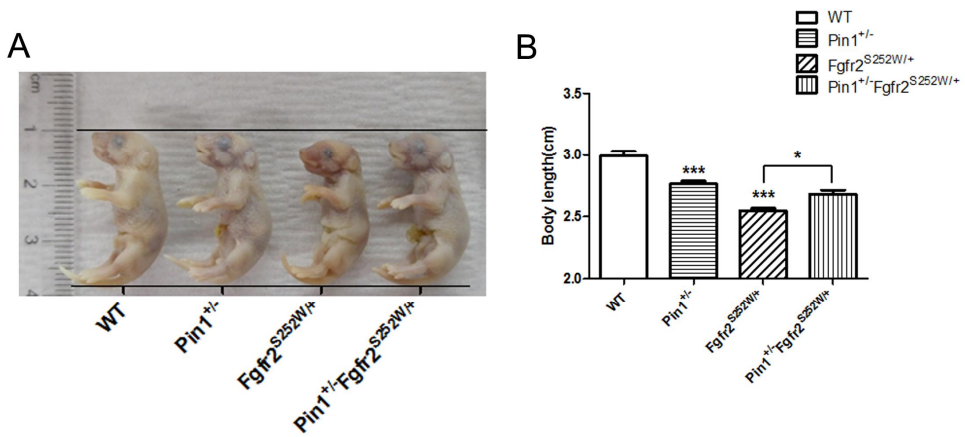

Figure 2.3. Changes in body length according to mice genetic modification. A. The gross appearance shows the rescue of the smaller body size of *Fgfr*$^{2S252W/+}$ mice by the reduction of Pin1 dosage. **B.** The results with statistical significance are shown by the graph. (n=5 in each group, *indicates $p<0.05$, **indicates $p<0.005$, ***indicates $p<0.001$).

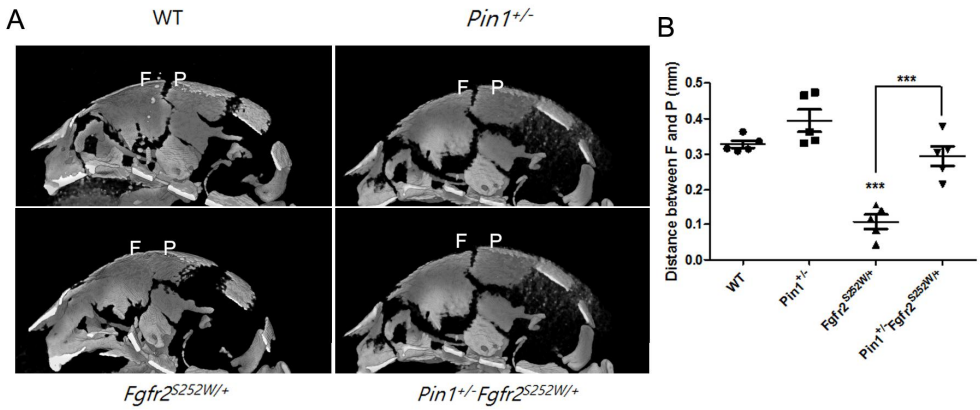

Fig. 2.4. The analysis of the fused coronal suture. **A.** Mice calvaria were analyzed by the suture slice by slice on the micro-CT analysis. We measured the distance between the frontal (F) and parietal (P) bone. **B.** The results with statistical significance are shown by the graph. (n=5 in each group, *indicates $p<0.05$, **indicates $p<0.005$, ***indicates $p<0.001$).

Table 2.4. Suture closure of mice used in each genotype

Genotype	Coroanl suture fusion (between frontal and parietal bone)	Ratio(%)	Frontal-nasal suture fusion (between nasal and frontal bone)	Ratio(%)
WT (n=5)	0/5	0	0/5	0
Pin1$^{+/-}$ *(n=5)*	0/5	0	0/5	0
Fgfr2$^{S252W/+}$ *(n=5)*	5/5	100	5/5	100
Pin1$^{+/-}$ *Fgfr2*$^{S252W/+}$ *(n=5)*	0/5	0	2/5	40

Restoration of craniofacial skeletal abnormalities in juglone-treated Fgfr2$^{S252W/+}$ mice

To assess the relevance of these findings to patients, we treated our model mice with juglone, a pharmacological inhibitor of Pin1 (Hennig et al., 1998). Prior to these experiments, we optimized the dose of juglone based on toxicity tests (Figure 2.5). For this purpose, pregnant mice were injected once daily with juglone (0, 0.01, 0.1, 1, or 2.5 mg/kg) from E14.5 to E18.5; dynamic skeletogenesis of the calvaria occurs around E12.5 (Rice, 2008). P0.5 mice were sacrificed and examined to determine the highest concentration that did not decrease the number of littermates (Fig. 2.5A, B) or significantly affect the skeletal phenotype (Fig. 2.5C); based on the results of this analysis, we set the concentration of juglone to 1 mg/kg.

The level of skull development was evaluated by embryonic skeletal staining and histological analysis (Figs. 2.6A-C). As in the experiments described above, *Fgfr2*$^{S252W/+}$ mice exhibited multiple abnormalities, including a dome-shaped skull (Fig. 2.6A), shortened skull length (Figs. 2.6A, B), widely spaced eyes (Fig. 2.6B, yellow line), and premature closure of the coronal suture (Fig. 2.6A, white arrowhead; Fig. 2.6B, arrow) and nasal suture (Fig. 2.6A, black arrowhead), whereas juglone-treated *Fgfr2*$^{S252W/+}$ mice were similar to WT mice. Next, we made

histological observations of the coronal sections in sagittal sections of calvaria (Fig. 2.6C). *Fgfr2*$^{S252W/+}$ mice exhibited premature closure of coronal sutures, whereas closure occurred normally in juglone-treated *Fgfr2*$^{S252W/+}$ mice despite expression of the mutant *Fgfr2*^{S252W} allele (Fig. 2.6C). To quantify restoration of CS calvaria phenotypes by juglone treatment, we obtained micro-CT scans of skulls from each group and littermate controls at birth (Figs. 2.6D, E). Images from the top (Fig. 2.6D) and the side (Fig. 2.6E) of *Fgfr2*$^{S252W/+}$ mice calvaria showed that coronal (yellow arrow) and nasal (blue arrow) sutures were completely overlapping and calcified. By contrast, juglone-treated *Fgfr2*$^{S252W/+}$ mice had calvarial phenotypes similar to those of WT mice. The incidence of coronal and frontal–nasal suture fusion depended on genotype (Table. 2.5). These results were also observed by walking through the suture on the micro-CT analysis (Fig. 2.7A). *Fgfr2*$^{S252W/+}$ mice had no space between the frontal (F) and parietal (P) bones because the coronal sutures were already fused and mineralized (Fig. 2.7A), but the distance between the frontal and parietal bones was greater in juglone-treated *Fgfr2*$^{S252W/+}$ mice (Fig. 2.7B).

We then looked for morphological differences in specific craniofacial features between groups, in comparison with WT littermate mice (Figs. 2.6D, E), using Fig. 1B and reference landmarks (Maga et al.,

2015; Wang et al., 2010). The lengths of the skull and nasal region were significantly shorter in *Fgfr2*$^{S252W/+}$ mice than in WT mice (Figs. 2.6F, G). In addition, cranial height and inter-ocular distance were larger in *Fgfr2*$^{S252W/+}$ mice than in WT mice, likely due to brain development under size limitations (Figs. 2.6H, I); this difference was statistically significant. The reduced body length of *Fgfr2*$^{S252W/+}$ mice was rescued by juglone treatment (Figure 2.8A, B), and the overall phenotypes of juglone-treated *Fgfr2*$^{S252W/+}$ mice were similar to those of WT mice. Together, these results indicate that juglone attenuates abnormal calvaria bone formation in *Fgfr2*$^{S252W/+}$ mice.

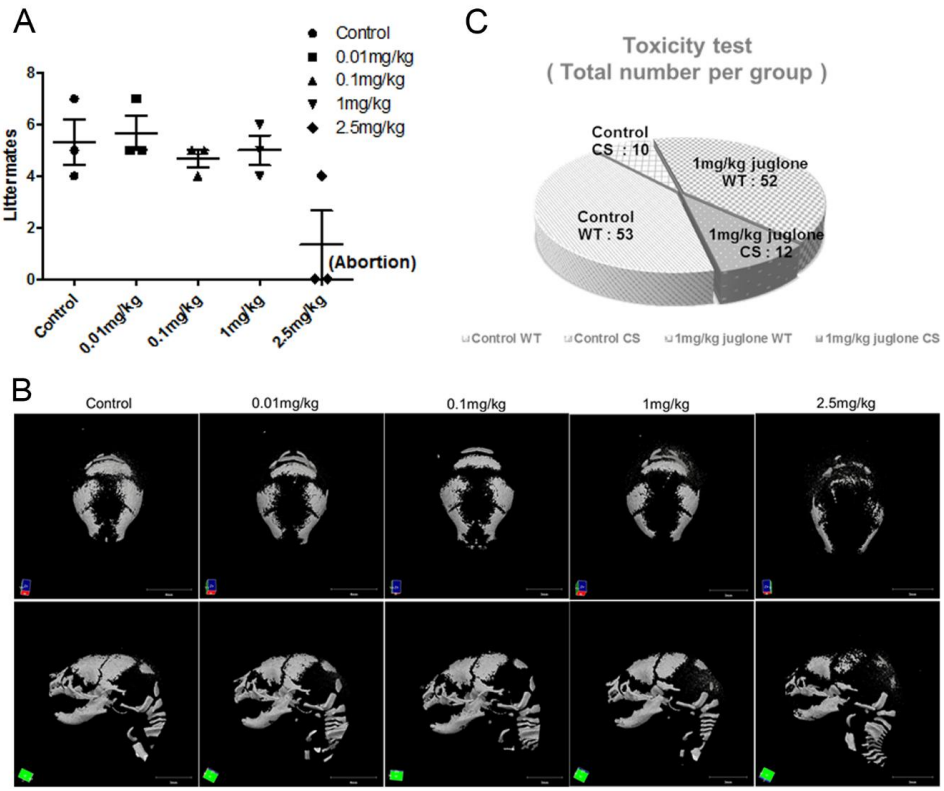

Figure 2.5. The toxicity test of juglone in pregnant mice. **A.** The graph shows the number of littermates by the toxicity test in which pregnant mice were administered juglone at a concentration of 0, 0.01, 0.1, 1 and 2.5mg/kg once daily from E14.5 to E18.5 (n=3). **B.** The overall skull phenotypes were analyzed by micro-CT depending on dose of injected juglone. **C.** The graph shows the total number per mice group.

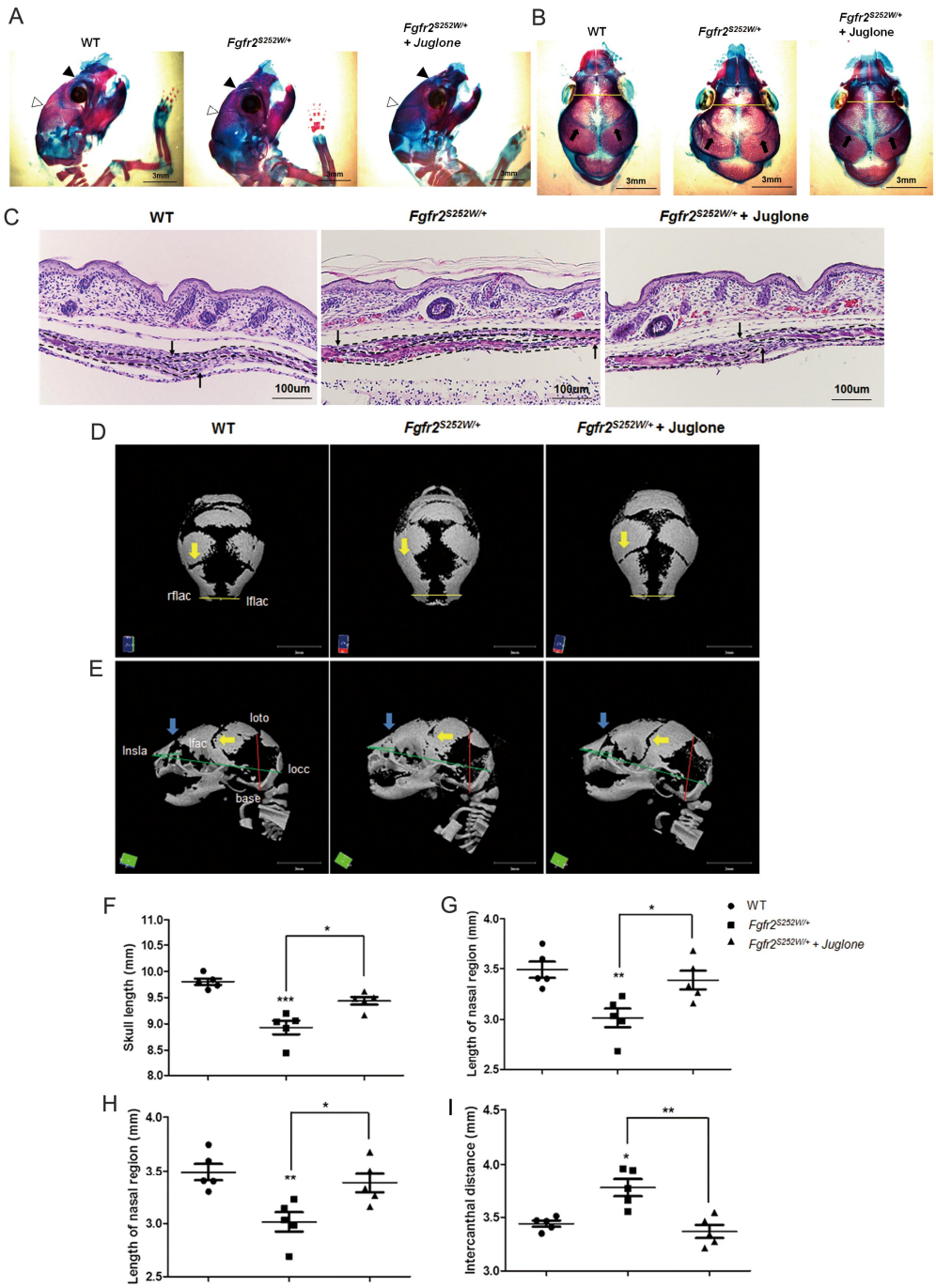
A
WT
Fgfr2S252W/+
Fgfr2S252W/+ + Juglone
3mm
B
WT
Fgfr2S252W/+
Fgfr2S252W/+ + Juglone
3mm
C
WT
Fgfr2S252W/+
Fgfr2S252W/+ + Juglone
100um
D
WT
Fgfr2S252W/+
Fgfr2S252W/+ + Juglone
rflac
lflac
E
loto
lnsla
lfac
locc
base
F
Skull length (mm)
11.0
10.5
10.0
9.5
9.0
8.5
8.0
*
***
G
Length of nasal region (mm)
4.0
3.5
3.0
2.5
*
**
WT
Fgfr2S252W/+
Fgfr2S252W/+ + Juglone
H
Length of nasal region (mm)
4.0
3.5
3.0
2.5
*
**
I
Intercanthal distance (mm)
4.5
4.0
3.5
3.0
**
*

Figure 2.6. CS phenotypes in AS model mice are rescued by treatment with the Pin1 inhibitor juglone.

Pregnant mice were intraperitoneally injected with 1 mg/kg juglone (*Fgfr2*$^{S252W/+}$ + Juglone) or vehicle (*Fgfr2*$^{S252W/+}$) once a day from E14.5 to E18.5. WT and *Fgfr2*$^{S252W/+}$ mice were sacrificed at birth. **A, B.** Mouse calvaria were examined after Alizarin red S and Alcian blue staining. Black arrowheads, frontonasal suture; white arrowheads, coronal suture (A). Both sutures were already closed in *Fgfr2*$^{S252W/+}$ mice, whereas those of WT and *Fgfr2*$^{S252W/+}$ + juglone mice remained open. Coronal views of the heads of the same animals are shown in B. Intercanthal distance (yellow lines) was significantly wider in *Fgfr2*$^{S252W/+}$ mice than in control mice. Arrows indicate a coronal suture that is almost overlapping in *Fgfr2*$^{S252W/+}$, whereas sutures in the other group remain open. **C.** Histological sections of coronal sutures in P0.5 mice. Arrows indicate growing fronts of frontal and parietal bones. Note that suture overlap is much more pronounced in *Fgfr2*$^{S252W/+}$ mice than in the other groups. **D, E.** Representative micro-CTs of skulls from WT, *Fgfr2*$^{S252W/+}$, and juglone-treated *Fgfr2*$^{S252W/+}$ mice (n=5). Superior views (D) and lateral views (F) of skull calvaria. Yellow arrows indicate rescue of early fusion of coronal suture, and blue arrows indicate rescue of the distorted frontal–nasal suture of mutant mice by juglone. Red lines

represent linear distances corresponding to the lengths of the nasal region and the skull. Green line indicates skull height, whereas the yellow lines, such as the neurocranial width at intercanthal distance (lflac–rflac), indicate linear distances corresponding to facial width. **F–I.** Representative micro-CT results of skulls are shown in bar graphs (n=5 in each group; *$p < 0.05$; **$p < 0.005$; ***$p < 0.001$). Statistically significant differences indicate rescue of the CS calvarial phenotype.

Table 2.5. Suture closure of mice used in each experimental group

Genotype	Coroanl suture fusion (between frontal and parietal bone)	Ratio(%)	Frontal-nasal suture fusion (between nasal and frontal bone)	Ratio(%)
WT (n=5)	0/5	0	0/5	0
Fgfr2$^{S252W/+}$ *(n=5)*	5/5	100	5/5	100
Fgfr2$^{S252W/+}$ + Juglone (n=5)	1/5	20	3/5	60

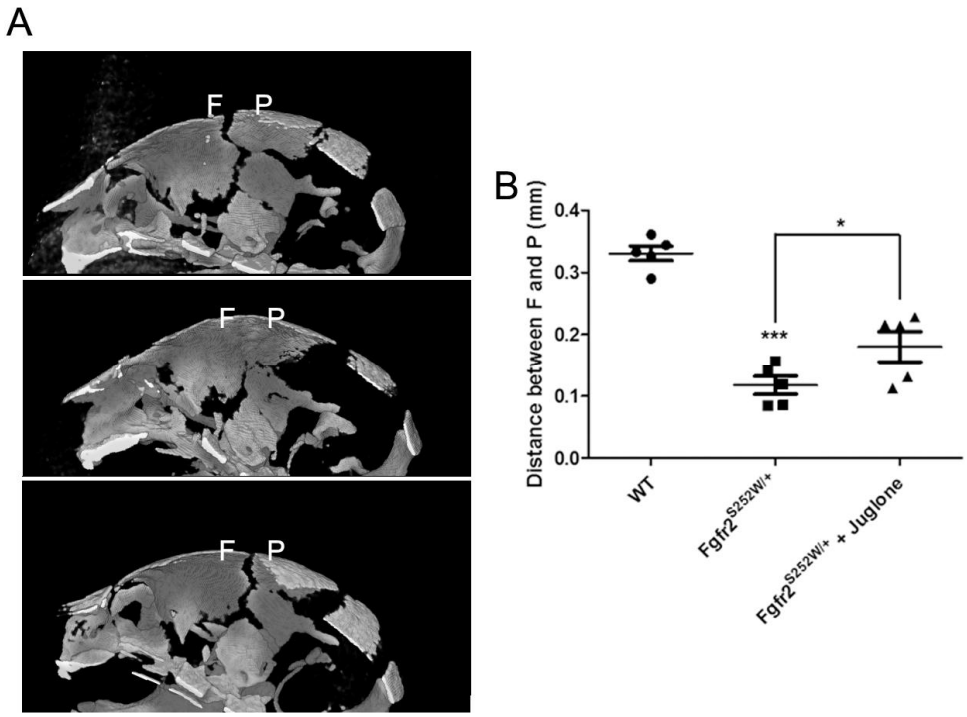

Figure 2.7. The change of the fused coronal suture by treatment of juglone. **A.** Mice calvaria were analyzed by the suture slice by slice on the micro-CT analysis. We measured the distance between the frontal (F) and parietal (P) bone. **B.** The results with statistical significance are shown by the graph. (n=5 in each group, *indicates $p<0.05$, **indicates $p<0.005$, ***indicates $p<0.001$).

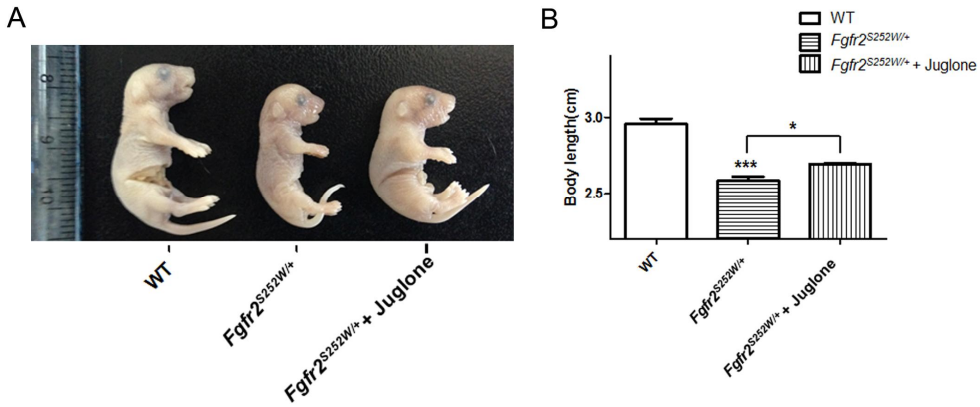

Figure 2.8. Changes in body length. A. The gross appearance shows the rescue of the smaller body size of *Fgfr*$^{2S252W/+}$ mice by the treatment of Pin1 inhibitor, juglone. **B.** The results with statistical significance are shown by the graph. (n=5 in each group, *indicates $p<0.05$, **indicates $p<0.005$, ***indicates $p<0.001$).

Juglone affects expression of genes downstream of FGF/FGFR2

Previously, we found links between FGF/FGFR2 signaling and Pin1 in cell culture (Islam et al., 2016; Yoon et al., 2014a). Therefore, we examined whether rescue by juglone which the IC50 value is 13.55μM in primary osteoblasts (Fig. 2.9) affected expression modulators and downstream genes of FGFR signaling, including *Dusp6* and two genes in the Sprouty family, *Spry2* and *Spry3* (Shukla et al., 2007). ERK1/2 activation triggers the transcription of *Dusp6* mRNA, and the Dusp6 protein inactivates ERK1/2, resulting in a negative feedback loop activated by FGF during somite development (Smith et al., 2005). Similarly, members of the Sprouty family antagonize FGF and FGFR signaling (Faedo et al., 2010). To assess the effect of juglone on FGF/FGFR2 signaling, we measured mRNA expression of *Dusp6, Spry2*, and *Spry3* by RT-PCR. Expression of all three genes was elevated in primary mouse calvarial cells from *Fgfr2*$^{S252W/+}$ mice (Figs. 2.10A, B) and MC3T3-E1 cells overexpressing *Fgfr*^{S252W} from a plasmid (Figs. 2.10C-E), in which FGF/FGFR2 signaling was hyper-activated in comparison with WT primary mouse calvarial cells and *Fgfr2*^{WT}-overexpressing MC3T3-E1 cells. After juglone treatment, expression of these genes decreased in a dose-dependent manner (Figs. 2.10A–E). These observations indicate that juglone inhibits the downstream

genes of FGF/FGFR2 signaling.

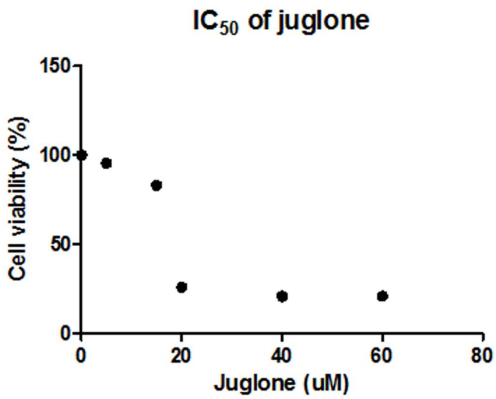

Figure 2.9. IC50 of juglone. Quantitation of the IC50 of juglone in primary osteoblasts. The IC50 for the inhibitory effect of julgone was determined by cell proliferation assay.

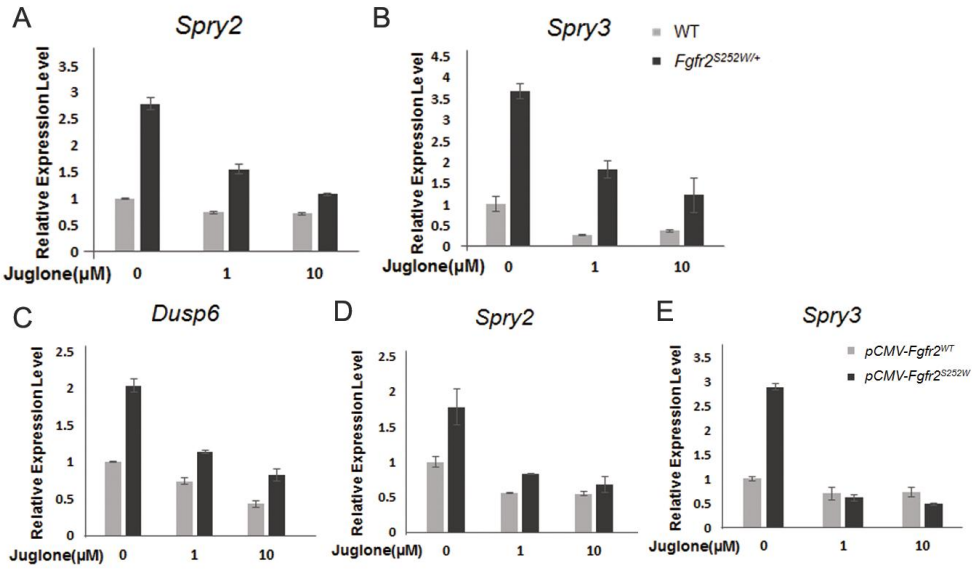

Figure 2.10. Expression of target genes changes upon treatment with juglone.

A, B. Relative expression levels of FGFR2 signaling modulators and downstream genes, based on qPCR analysis of WT and *Fgfr2*$^{S252W/+}$ calvaria cells (n=3) following treatment with different dosages of juglone for 1 day. **C–E.** Confluent MC3T3-E1 cells were transfected with *Fgfr2*^{WT} or *Fgfr2*^{S252W} mutant expression plasmids. After 24 h, cells were treated with 0, 1, and 10 μM of juglone for 1 day. mRNA levels of FGFR signaling modulators and downstream genes, such as *Dusp6* (C) and the *Sprouty* family genes *(Spry2, 3)* (D, E), were analyzed quantitatively (n=3). The level of each mRNA was normalized to that of *Gapdh* in the same sample.

Juglone restores Runx2 protein hyperstability in *Fgfr2*$^{S252W/+}$ mouse calvarial cells by decreasing acetylation of Runx2

Runx2, a key transcription factor in osteoblast differentiation, triggers MSCs to differentiate into osteoblasts (Xu et al., 2015). The importance of Runx2 protein in mammalian skeletal development has been clearly demonstrated by the observation that *Runx2* KO mice lack both mature osteoblasts and a mineralized skeleton, including the calvaria (Komori et al., 1997). In addition, *Runx2* expression is localized to the critical area of cranial suture closure (Park et al., 2001). To determine the mechanism underlying restoration of the calvarial phenotype of *Fgfr2*$^{S252W/+}$ mice by juglone, we assessed endogenous Runx2 expression in WT and *Fgfr2*$^{S252W/+}$ primary mouse calvarial cells by IF analysis (Fig. 2.11A). In WT cells, we observed weak staining for endogenous Runx2 in the nucleus (Fig. 2.11A, first row). After treatment of WT cells with juglone, the level of endogenous Runx2 protein was slightly reduced (Fig. 2.11A, second row). By contrast, *Fgfr2*$^{S252W/+}$ cells had more endogenous Runx2 in the nucleus than WT cells (Fig. 2.11A, third row). Juglone treatment decreased nuclear overexpression of Runx2 caused by *Fgfr2* mutation (Fig. 2.11A, fourth row), and Runx2 protein (green) expression in *Fgfr2*$^{S252W/+}$ primary mouse calvarial cells was significantly attenuated by juglone treatment (Fig. 2.11B).

Similar patterns were observed in the levels of endogenous Runx2 protein in the nuclear fraction (Fig. 2.12A).

We showed previously that PTM is important for Runx2 stabilization (Islam et al., 2016; Yoon et al., 2014a; Yoon et al., 2013a). In particular, Pin1-mediated structural modification of Runx2 is an indispensable step connecting phosphorylation, acetylation, and transcriptional activation of Runx2 by FGF signaling (Yoon et al., 2014a). To determine the mechanism by which juglone restored nuclear Runx2 protein to WT level, we examined the acetylation of Runx2. IP assays revealed that acetylation of Runx2 was higher in $Fgfr2^{S252W/+}$ mouse calvarial cells than in WT cells (Fig. 2.12B). By contrast, the acetylated Runx2 level returned to normal in juglone-treated $Fgfr2^{S252W/+}$ mouse calvarial cells (Fig. 2.12B).

Next, we investigated whether juglone affects the stability of the Runx2 protein. FGF signaling promotes *Runx2* expression in osteoblasts (Kim et al., 2003); however, we wanted to test the effects of juglone on PTM of Runx2, as this affects the stability of the Runx2 protein. To this end, we transfected *Runx2* plasmid into WT and $Fgfr2^{S252W/+}$ mouse calvarial cells and monitored the stability of exogenous Runx2 (Fig. 2.12C, black arrow). Exogenous Runx2 was stable in $Fgfr2^{S252W/+}$ mouse calvarial cells

for almost 18 h after treatment with CHX, an inhibitor of protein synthesis, whereas in WT cells, the level of Runx2 protein gradually decreased with time (Fig. 2.12C). However, when *Fgfr2*$^{S252W/+}$ mouse calvarial cells were treated with juglone, the stability of Runx2 protein was similar to that in WT cells (Fig. 2.12C). Endogenous Runx2 protein exhibited the same patterns (Fig. 2.12C, white arrow). We quantified the changes in Runx2 expression over time (Fig. 2.12D). These results strongly indicate that isomerization of Runx2 by Pin1, which is critical for Runx2 stabilization through acetylation, is inhibited by juglone, thereby restoring Runx2 stability to a near-normal level and reversing the effects of the *Fgfr2*^{S252W} mutation and the associated stabilization of Runx2. Using IHC, we confirmed that elevated Runx2 protein levels in *Fgfr2*$^{S252W/+}$ mouse coronal sutures were attenuated by juglone treatment (Fig. 2.13). Together, these results suggest that *Fgfr2* mutation in osteoblasts alters the amount of Runx2 protein, but juglone can restore Runx2 protein to WT levels.

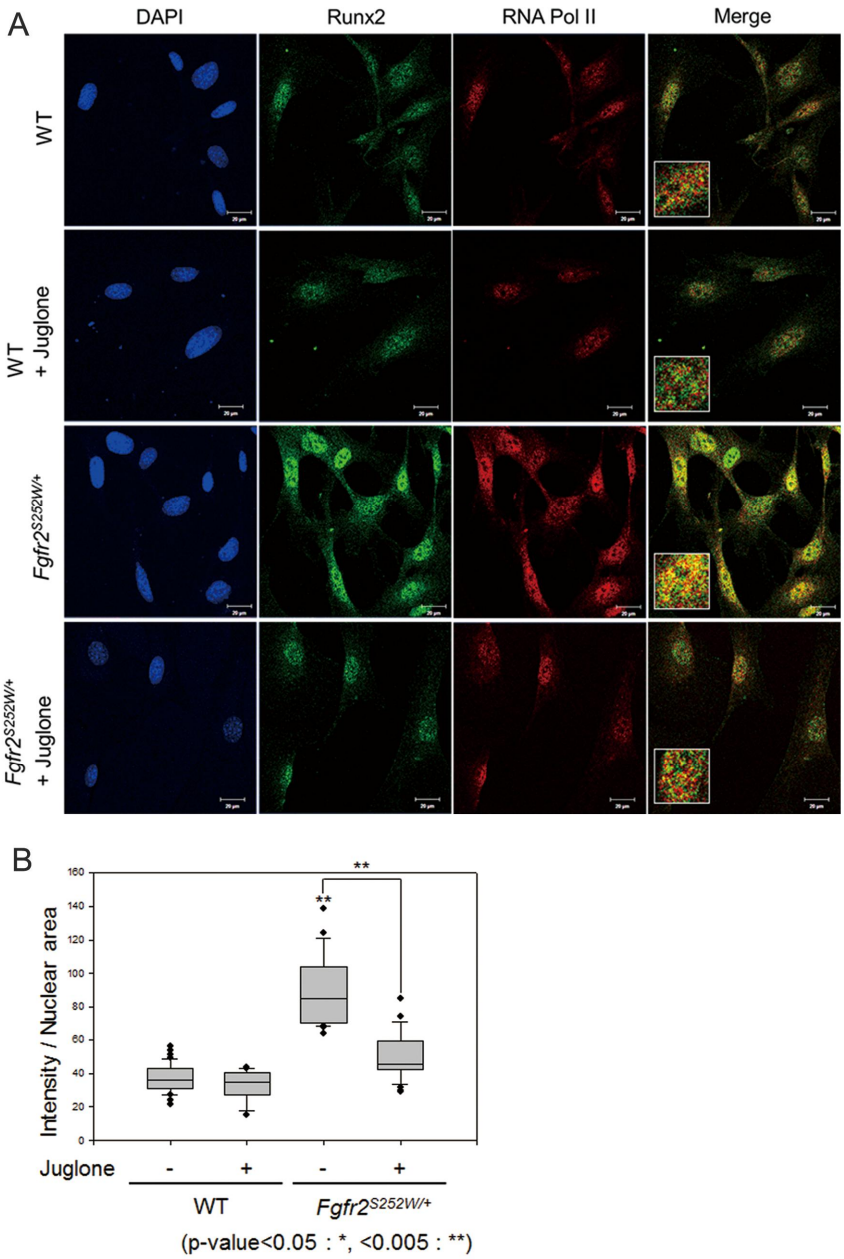

Figure 2.11. Increased nuclear Runx2 in *Fgfr2*$^{S252W/+}$ mice attenuated by juglone treatment.

A. Endogenous Runx2 protein was detected by IF and immunocytochemistry. Primary mouse calvarial cells from WT and *Fgfr2*$^{S252W/+}$ mice were treated with 5 μM juglone for 24 h. Cells were fixed, and endogenous proteins were immunostained with anti-Runx2 (green) and anti-RNA Pol II (red) antibodies, as well as DAPI (blue). In the merged image, Runx2 and RNA Pol II co-localization (yellow) was observed as foci, particularly in *Fgfr2*^{S252W} mutant-expressing cells. **B.** Endogenous intranuclear Runx2 was quantified, and results are shown as a sigma plot (n=20 in each group; *$p < 0.01$; **$p < 0.001$).

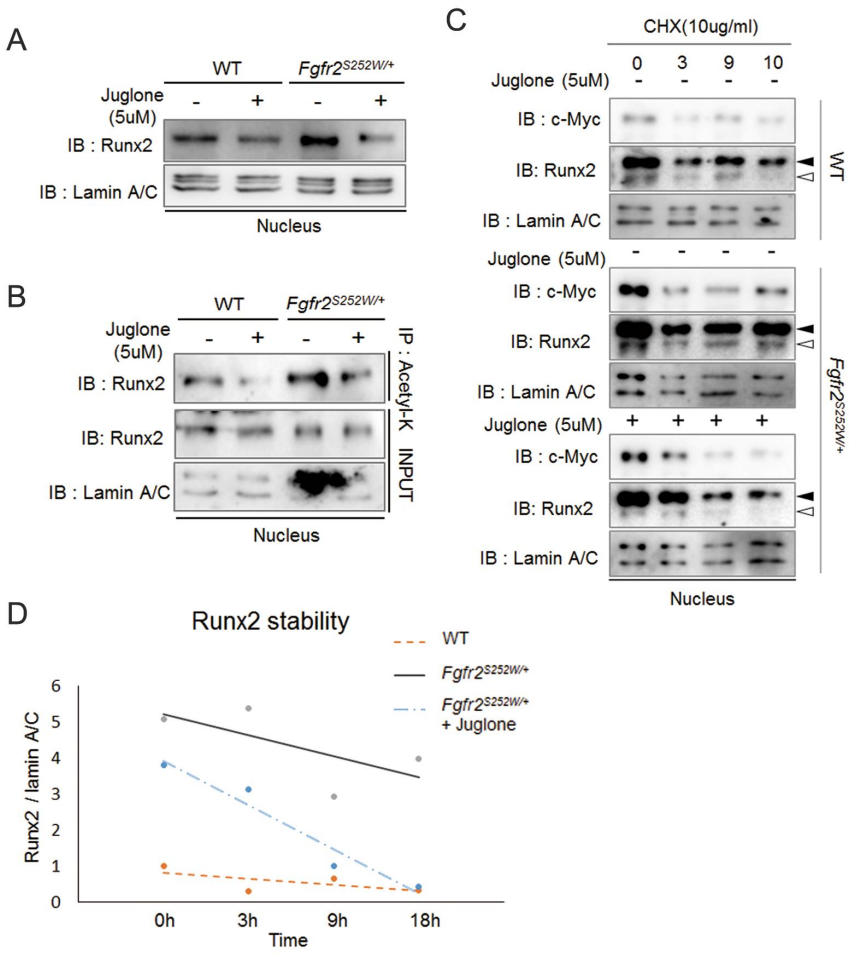

Figure 2.12. Runx2 is over-activated in *Fgfr2*$^{S252W/+}$ mice, and juglone destabilizes Runx2 by decreasing acetylation.

A. Abundance of endogenous Runx2 protein in dissociated nuclear extracts, as determined by immunoblot assay. **B.** Degree of acetylation of Runx2 protein, as determined by IP with anti-acetyl-lysine antibody from dissociated nuclear extracts. **C, D.** Runx2 protein stability analysis. *Runx2*

plasmid was transfected into primary mouse calvaria cells. After 24 h, cells were pretreated with or without 5 μM juglone for 1 h, and then treated with 10 μg/ml CHX for the indicated times. Cells were harvested and nuclear fractions were isolated, followed by immunoblotting with the indicated antibodies. Black arrow indicates overexpressed Runx2, and white arrow indicates endogenous Runx2. Lamin A/C was used as a loading control for the nuclear fractions. **D.** Nuclear Runx2 was quantified, and levels are shown as a function of time.

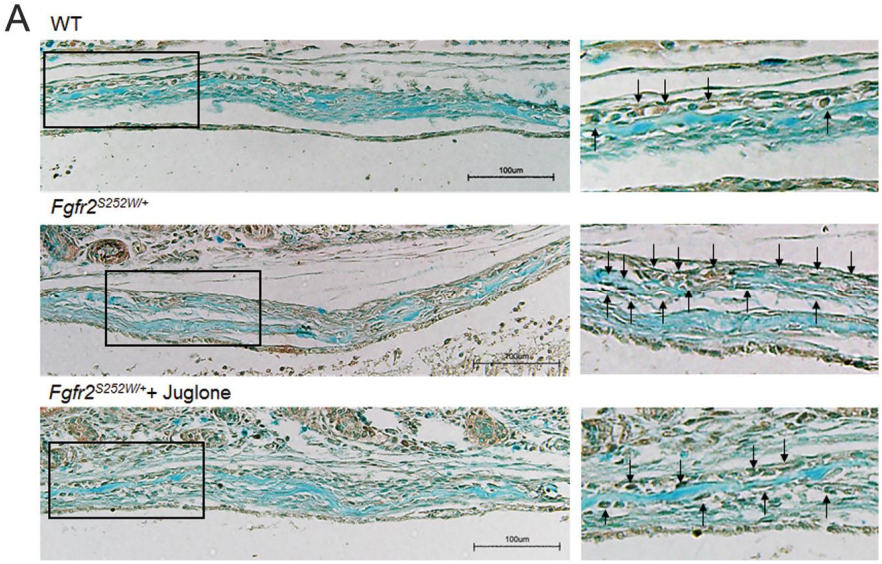

Figure 2.13. Runx2 in coronal sutures. Runx2 in calvaria tissue from coronal sutures of P0.5 mice was detected by IHC.

Juglone attenuates *Fgfr2* mutation-induced osteoblast proliferation and differentiation in CS

As shown in Fig. 4, juglone prevented excessive Runx2 acetylation and stabilization. Because acetylated and stabilized Runx2 has transactivation activity and regulates cell proliferation and differentiation (Galindo et al., 2005; Komori, 2010), we examined the *in vitro* effects of juglone on osteoblast differentiation. Runx2 activity was assessed in a reporter assay using 6XOSE2, a construct that contains six tandem repeats of osteoblast-specific cis-element 2 (Kim et al., 2003). Primary mouse calvarial cells of $Fgfr2^{S252W/+}$ mice exhibited approximately 2.5-fold higher levels of Runx2 activity than those of WT mice (Fig. 2.14A). However, the elevated Runx2 activity caused by $Fgfr2^{S252W}$ mutation decreased in a dose-dependent manner following juglone treatment (Fig. 2.14A); this observation has important implications for cell proliferation and differentiation, which are regulated by Runx2. The FGF/FGFR2 signaling pathway is critical for proliferation in skeletogenesis (Su et al., 2014). To determine the effects of juglone on osteoblast proliferation and differentiation, we performed a proliferation assay and assessed the mRNA levels of marker genes in WT and $Fgfr2^{S252W/+}$ primary mouse calvarial cells. Cell growth (Fig. 2.15A) and expression of proliferation marker genes such

as *CyclinD1, Cdk2, Cdk4* and *PCNA* were higher in *Fgfr2*$^{S252W/+}$ calvarial cells than in WT cells (Figs. 2.15B-E). Administration of juglone decreased cell growth (Fig. 2.15A), as well as the expression of proliferation marker genes (Figs. 2.15B-E), in a dose-dependent manner. Transcript levels of bone marker genes followed a similar pattern (Figs. 2.16A, B). Suppression of Pin1 by juglone almost completely abrogated the higher expression of specific genes induced by *Fgfr2*^{S252W} mutation. During osteoblast maturation, *Fgfr2*$^{S252W/+}$ calvarial cells exhibited enhanced production of mineralized bone matrix compared with WT cells, as detected by Alizarin red staining (Fig. 2.16C); juglone rescued this phenotype in a concentration-dependent manner (Fig. 2.16C). Together, these data suggest that juglone reduces the transcriptional activity of Runx2 and abrogates the effects of *Fgfr2* mutation, namely, excessive osteoblast differentiation resulting in CS.

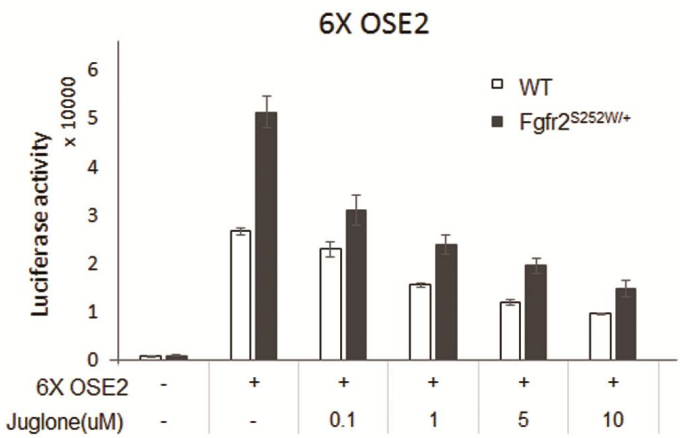

Figure 2.14. Transacting activity change depended on treatment of juglone in *Fgfr2*$^{S252W/+}$ mouse calvarial cells.

Relative Runx2 transacting activity was assessed using a 6XOSE2 luciferase reporter construct. Following transfection with the 6XOSE2 reporter gene, cells were treated with juglone at various concentrations for 24 h. Luciferase assays were performed on both WT and *Fgfr2*$^{S252W/+}$ mouse calvarial cells.

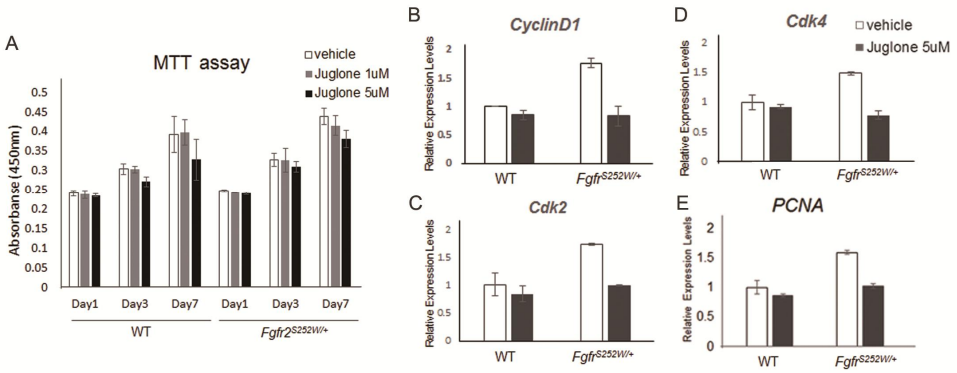

Figure 2.15. Effects of juglone treatment on osteoblast proliferation

A. Proliferation of WT and *Fgfr2*$^{S252W/+}$ mouse calvarial cells following treatment with various doses of juglone for 1, 3, and 7 days. Cell proliferation was assessed by water-soluble tetrazolium assay. **B–E.** Relative expression of proliferation-related genes in WT and *Fgfr2*$^{S252W/+}$ mouse calvarial cells, as determined by qPCR.

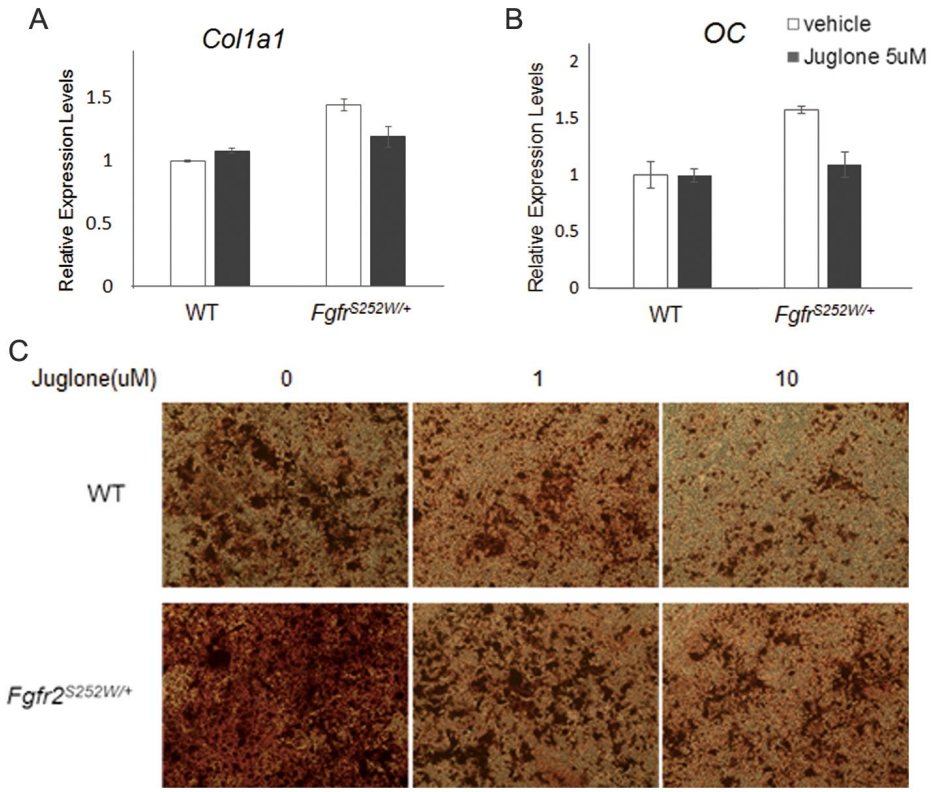

Figure 2.16. Effects of juglone treatment on osteoblast differentiation.

A, B. Relative expression of osteoblast differentiation markers in both genotypes of primary mouse calvarial cells, as determined by qPCR. Cells were cultured with vehicle or 5 μM juglone for 24 h before mRNA isolation. Expression of each marker gene was normalized against that of *Gapdh* in the same sample. **C.** Late-stage primary osteoblast differentiation was confirmed by Alizarin red S staining. Both genotypes of primary calvarial cells were cultured for 3 weeks in osteogenic media after 48 h culture with

the indicated concentrations of juglone.

Discussion

The majority of severe CS cases are due to *de novo* mutations, and are therefore usually unanticipated (Johnson and Wilkie, 2011). Currently, the only way to treat CS patients is surgical intervention, involving creation of an expanded but rigid skull vault to accommodate further increases in brain growth, with some additional remodeling of the inner surface of the calvaria (Johnson and Wilkie, 2011). However, recent developments in prenatal diagnostic testing for mutations in amniotic fluid, especially *FGFR2* mutations, raise the possibility of early diagnosis (Phupong et al., 2004; Twigg and Wilkie, 2015). Detection of CS during pregnancy could allow premature closure of the cranial suture to be prevented by inhibiting excessive growth at the developmental stage of the fetus using a drug. This approach is promising in that it not only alleviates the burden of surgery in infants, but could also prevent mental retardation caused by delayed surgery or surgery sequela arising during brain growth.

In this study, we generated *Pin1;Fgfr2* compound mutant mice and investigated the effects of juglone, an inhibitor of Pin1, on the recovery of CS phenotypes such as early suture closure in $Fgfr2^{S252W/+}$ mice (Figs. 2.1, 2.2, 2.4, 2.6 and 2.7). Previously, Shukla et al. reported that U0126, which suppresses ERK/MAPK signaling, prevents premature cranial suture closure

in *Fgfr2*$^{S252W/+}$ mice (Shukla et al., 2007). Usually, the ERK/MAPK enzyme action products are shared with a substrate for the Pin1 enzyme, because Pin1 binds to only pSer/Thr-Pro motif (Hsu et al., 2001; Yoon et al., 2014a). Therefore, inhibition of Pin1 disrupts signaling downstream of the ERK/MAP kinase pathway, and it is possible to reduce the non-specific effects than using ERK-MAP kinase inhibitors. In addition, in our genetic approach, we demonstrated that targeting the *Pin1* gene in *Fgfr2*$^{S252W/+}$ mice leads to AS phenotype recovery (Fig. 2.1, 2.2), supporting the conclusion drawn from our pharmacological approach that juglone-mediated rescue is indeed due to inhibition of Pin1. Accordingly, we propose that Pin1-targeted therapy would be valuable for treatment of CS.

Juglone is one of the most well-known Pin1 inhibitors, the IC50 values are reported differently depending on the cell type (Avci et al., 2016; Chao et al., 2001; Zhang et al., 2015). In primary osteoblasts, we found that the IC50 value is 13.55 μM (Fig. 2.9). In addition, juglone passes the placenta barrier, as demonstrated by the observation that high concentration of juglone could induce abortion (Fig. 2.5). Juglone undergoes biotransformation in the liver to yield various metabolites, which are detected primarily in the urine (Saling et al., 2011), indicating that the compound has access to liver cells (Chen et al., 2005; Saling et al., 2011)

These observations imply that juglone has the potential to regulate liver function and could also be used for medicinal purpose in other parts of the body (Chen et al., 2005; Hennig et al., 1998; Saling et al., 2011). We established the appropriate concentration of juglone through toxicity testing in pregnant mice, and determined a dose that did not affect the number of littermates or overall skull phenotypes (Fig. 2.5). We confirmed that development of the abnormal phenotype of *Fgfr2*$^{S252W/+}$ mice (small, shortened skull and premature fusion of the coronal suture) could be prevented by juglone treatment (Fig. 2.6). Also, although many previous studies have reported that the survival rate of AS is very low (Park et al., 1995; Slaney et al., 1996; Wang et al., 2005; Yang et al., 2008), the optimized concentration of juglone did decrease litter size, and instead increased the number of littermates in comparison with the control group (average control litter: 5.25 pups; average litter of juglone-injected mother: 7.11 pups). This observation suggests that juglone improves the survival of P0.5 mice with the *Fgfr2*$^{S252W/+}$ mutation.

Together, these genetic and pharmacological approaches using juglone indicate that Pin1 is the target for juglone-mediated attenuation of hyper-activated FGF/FGFR signaling in *Fgfr2*$^{S252W/+}$ mice. However, pure juglone is used only for research purposes, and is categorized as an

'Unapproved Herb' in the German Commission E monograph due to its probably mutagenic and carcinogenic properties (Chen et al., 2005). In addition, it has been designated as a potentially toxic natural product by the National Toxicology Program in USA (Chen et al., 2005; Saling et al., 2011). Therefore, for clinical use, it would be important to develop Pin1 inhibitors that are both effective and safe.

This approach could also be applied to alleviating other phenotypes associated with FGFR-related CS. These phenotypes differ slightly different depending on the type of *FGFR* mutation (Robin et al., 1993; Teven et al., 2014). The *FGFR S252W* mutation, as in AS, causes premature fusion of the coronal suture with syndactyly of the hands or feet, mid-face hypoplasia, and dwarfism (Chen et al., 2003; Johnson and Wilkie, 2011; Wang et al., 2005). As described previously (Shukla et al., 2007; Wang et al., 2010; Wang et al., 2005), we also observed abnormalities in endochondral bone formation, as evidenced by shorter body length (Fig. 2.3 and 2.8) and shortening of the skull (Figs. 2.1 and 2.6) in $Fgfr2^{S252W}$ mutant mice. In addition to fusion of the calvarial sutures, mid-face growth is also an important factor affecting skull length (Morriss-Kay and Wilkie, 2005), and these phenotypes are caused by increased endochondral ossification due to gain-of-function mutation in *FGFR*s (Chen et al., 2014). We found that

inactivation of Pin1 by genetic manipulation or drug treatment restored body size (Fig. 2.3 and 2.8) and skull length (Figs. 2.1 and 2.6). These effects of Pin1 targeting might also be applied to endochondral ossification processes. Furthermore, these bone phenotypes are similar to those in patients with AS and achondroplasia, the most common genetic dwarfism in humans, which is caused by mutation in *FGFR3* (Lee et al., 2017). CS can be classified as syndromic based on *FGFR* gene mutations and associated phenotypes. Although we only used the $Fgfr2^{S252W/+}$ CS mouse model in this study, CS is also caused by mutations in other *FGFRs,* including *FGFR1, FGFR2* or *FGFR3* (Johnson and Wilkie, 2011; Robin et al., 1993). Some of these mutations, like $FGFR^{S252W}$, increase the affinity of the receptor for ligand, whereas others cause excessive signaling via ligand-independent receptor activation (Robin et al., 1993; Teven et al., 2014). However, we found that early fused cranial sutures are restored by targeting Pin1, thereby suppressing hyper-activated downstream signaling, which is a common result of most mutation in *FGFR*s. Therefore, we propose that this approach is applicable to the recovery of CS symptoms due to gain-of-function mutations in other *FGFR*s.

It is widely accepted that Pin1 is a molecular switch that determines the fate of numerous osteogenic transcription factors, especially those

related to stabilization of substrate proteins (Islam et al., 2017; Shin et al., 2016; Yoon et al., 2014a; Yoon et al., 2015a; Yoon et al., 2013a). In addition, direct delivery of Pin1 protein into mesenchymal cells stimulates their osteogenic differentiation (Kim et al., 2017). We previously suggested that Fgf2 induces PTMs of Runx2. In particular, we showed that Runx2 is acetylated by p300 (Jeon et al., 2006), and that FGF2-induced phosphorylation(Kim et al., 2003; Kim et al., 2004) and subsequent acetylation (Park et al., 2010) of Runx2 stimulates its *in vitro* transactivation activity by stabilizing the protein. Also, we reported that prolyl isomerization of Runx2 alters the conformation to an acetylation-friendly structure, resulting in stabilization and activation Runx2 (Yoon et al., 2014a). In this study, we found that $Fgfr2^{S252W}$ mutation increased the Runx2 level by promoting these PTMs, which in turn increased the nuclear Runx2 protein level in $Fgfr2^{S252W/+}$ primary calvarial cells or tissues (Fig. 2.11 and 2.12). This increase in Runx2 protein level, in addition to elevation of general FGFR signaling, resulted in excessive osteoblast proliferation and differentiation (Fig. 2.15 and 2.16), which may be the molecular mechanism underlying premature closure of the coronal sutures in CS. Moreover, we showed that the Pin1 inhibitor juglone decreased excessive Runx2 stabilization by inhibiting its isomerization and consequent acetylation (Figs.

2.12 and 2.14), confirming the importance of Pin1 in the Runx2 PTM process *in vivo*.

In this study, we showed that recovery of coronal suture fusion was only due to excessive stabilization of Runx2, which is affected by Pin1 regulation via the FGF/FGFR signaling pathway. Many previous studies using AS mouse models reported that phosphorylation levels of ERK1/2, AKT and p38 are elevated in the calvaria by gain-of-function mutations of FGFR2 such as S252W and P253R (Holmes et al., 2009; Shukla et al., 2007; Wang et al., 2010; Yin et al., 2008). In addition, inhibition of ERK, an important mediator of FGF signaling, restores the phenotype of AS mouse (Shukla et al., 2007). In a previous study, we showed that Pin1 is crucial for regulation of the FGF/FGFR signaling pathway (Islam et al., 2017; Yoon et al., 2014a), and that FGF target genes are affected by juglone (Fig. 2.10). In addition, the hallmark skull abnormality in *Runx2*$^{+/-}$ mice is a wider sagittal suture resulting from delayed development of the parietal bone (Bae et al., 2017b). Because the mixed developmental origin of the mammalian skull vault (Senarath-Yapa et al., 2013), this area is developmentally distinct from the coronal suture or frontal bone: the frontal and sagittal suture are neural crest–derived, whereas the parietal bone and coronal suture are of mesodermal origin. Therefore, we suspect that restoration of CS phenotypes

via alteration of Runx2 PTMs represents only one of many potential mediators downstream of the FGF signaling pathway.

In summary, our results indicate that Pin1 is a new therapeutic target for CS. Rescue of CS by juglone was associated with alterations in Pin1 activity and Runx2 stability (Fig. 2.17). Administration of the Pin1 inhibitor juglone during pregnancy significantly suppressed CS phenotypes, especially premature fusion of the coronal suture, in a *Fgfr2*^{S252W} mutant mouse model. These data clearly establish the regulatory role of Pin1 in abnormalities associated with FGF/FGFR2 hyper-activation, and highlight the feasibility of developing specific targeted prevention and therapeutic strategies for CS.

Acknowledgments: We thank C.X. Deng (University of Macau, China) for providing the *Fgfr2*^{S252W} knock-in mouse; S.C. Bae (Chungbuk National University, Cheongju, Korea) for providing valuable advice of pharmacokinetics. We also thank the American Society of Bone and Mineral Research for selecting the abstract related to this work for the Young Investigator Award at the ASBMR 2016 annual meeting.

Author roles: H.R. Shin, designed and performed all experiments, analyzed the data, and wrote the manuscript. H.S. Bae, B.S. Kim, and W.J. Kim contributed to animal management, analysis of mice genotypes, and histomorphometric analysis. Y.D. Cho and K.Y. Choi performed primary cell culture and edited the manuscript. Y.S. Lee, K.M. Woo, and J.H. Baek participated in the *in vivo* study and analyzed the data. H.M. Ryoo designed all experiments, provided supervisory support, and wrote the paper.

Data and materials availability: All mice and plasmid constructs mentioned in this research article are available via material transfer agreement.

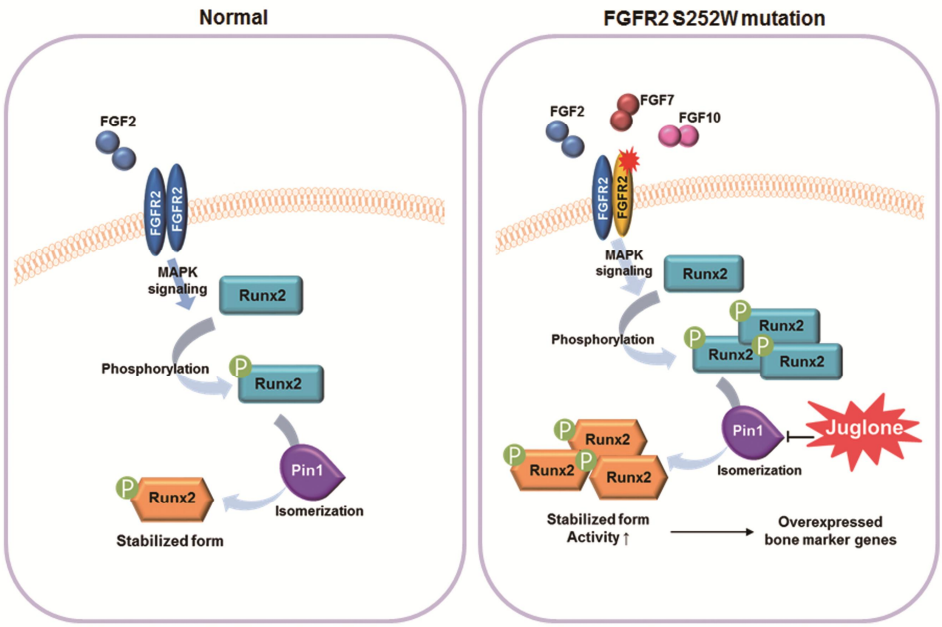

Fig. 2.17. Mechanisms underlying restoration of the normal phenotype by juglone in calvaria with gain-of-function mutations in *FGFR2*.

Juglone treatment lowers abnormally elevated Runx2 protein levels in *Fgfr2*$^{S252W/+}$ mice by inhibiting Runx2 isomerization, thereby restoring proper downstream transcriptional activity (Ibrahimi et al., 2004; Yu et al., 2000). The *S252W* mutation of *FGFR2* increases ligand affinity and alters ligand specificity, resulting in hyperactive FGF signaling. In this genetic background, Runx2, one of the targets of FGF signaling, undergoes excessive post-translational modification, such as isomerization and acetylation. Repression of Runx2 isomerization by juglone, a Pin1 inhibitor, decreases the Runx2 protein level and normalizes the expression of Runx2

target genes, thereby rescuing the abnormal calvaria phenotypes of *Fgfr2*$^{S252W/+}$ mice.

VI. Conclusion

In this study, we focused on PTM action of osteoblast differentiation regulators by Pin1. In the part I, we tried to demonstrate the novel molecular mechanism of Pin1 in Wnt/β-catenin signaling pathway. Pin1 directly interacts with β-catenin, and whereby Pin1 promotes the nuclear retention of β-catenin through inhibition of the interaction between APC and β-catenin in the nucleus, which, in turn, up-regulates osteoblast differentiation. In the part II, I tried animal experiment to examine whether Pin1 is a new therapeutic target or not in CS using *Fgfr2*$^{S252W/+}$ mice. With these results, we suggest that a regulatory role for Pin1 in abnormalities associated with FGF/FGFR2 over-activation and highlight the feasibility of developing specific targeted prevention and therapeutic strategies for CS.

Pin1 is a critical and unique enzyme among PPIases. Controlling of Pin1 has been a major concern in the clinical field such as cancer. In addition, this study suggests that the regulation of Pin1 in the osteoblast differentiation process is also clinically valuable. However, in Part I, we showed the importance of Pin1 to promote osteoblast differentiation. Conversely, in Part II, we demonstrated the importance of inhibiting of Pin1 which is one of the mediators in the hyper-activated signaling pathway. Therefore, to prove practical value of these studies, further studies should be

conducted with applying to Pin1 to be regulated by cell or tissue type specific.

VII. References

Aithal, K. B., Kumar, S., Rao, B. N., Udupa, N., and Rao, S. B. (2012). Tumor growth inhibitory effect of juglone and its radiation sensitizing potential: in vivo and in vitro studies. Integr Cancer Ther *11*, 68-80.

Akram, A., McKnight, M. M., Bellardie, H., Beale, V., and Evans, R. D. (2015). Craniofacial malformations and the orthodontist. Br Dent J *218*, 129-141.

Almeida, M., Han, L., Bellido, T., Manolagas, S. C., and Kousteni, S. (2005). Wnt proteins prevent apoptosis of both uncommitted osteoblast progenitors and differentiated osteoblasts by beta-catenin-dependent and -independent signaling cascades involving Src/ERK and phosphatidylinositol 3-kinase/AKT. The Journal of biological chemistry *280*, 41342-41351.

Anastas, J. N., and Moon, R. T. (2013). WNT signalling pathways as therapeutic targets in cancer. Nature reviews Cancer *13*, 11-26.

Anderson, J., Burns, H. D., Enriquez-Harris, P., Wilkie, A. O., and Heath, J. K. (1998). Apert syndrome mutations in fibroblast growth factor receptor 2 exhibit increased affinity for FGF ligand. Human molecular genetics *7*, 1475-1483.

Attisano, L., and Labbe, E. (2004). TGFbeta and Wnt pathway cross-talk. Cancer metastasis reviews *23*, 53-61.

Avci, E., Arikoglu, H., and Erkoc Kaya, D. (2016). Investigation of juglone effects on metastasis and angiogenesis in pancreatic cancer cells. Gene *588*, 74-78.

Bae, H. S., Yoon, W. J., Cho, Y. D., Islam, R., Shin, H. R., Kim, B. S., Lim, J. M., Seo, M. S., Cho, S. A., Choi, K. Y., *et al.* (2017a). An HDAC Inhibitor, Entinostat/MS-275, Partially Prevents Delayed Cranial Suture Closure in Heterozygous Runx2 Null Mice. Journal of bone and mineral research : the official journal of the American Society for Bone and Mineral Research.

Bae, H. S., Yoon, W. J., Cho, Y. D., Islam, R., Shin, H. R., Kim, B. S., Lim, J. M., Seo, M. S., Cho, S. A., Choi, K. Y., *et al.* (2017b). An HDAC Inhibitor, Entinostat/MS-275, Partially Prevents Delayed Cranial Suture Closure in Heterozygous Runx2 Null Mice. J Bone Miner Res *32*, 951-961.

Bagheri-Fam, S., Ono, M., Li, L., Zhao, L., Ryan, J., Lai, R., Katsura, Y., Rossello, F. J., Koopman, P., Scherer, G., *et al.* (2015). FGFR2

mutation in 46,XY sex reversal with craniosynostosis. Human molecul ar genetics *24*, 6699-6710.
Balastik, M., Lim, J., Pastorino, L., and Lu, K. P. (2007). Pin1 in Al zheimer's disease: multiple substrates, one regulatory mechanism? Bioc him Biophys Acta *1772*, 422-429.
Behrens, J., von Kries, J. P., Kuhl, M., Bruhn, L., Wedlich, D., Gross chedl, R., and Birchmeier, W. (1996). Functional interaction of beta-ca tenin with the transcription factor LEF-1. Nature *382*, 638-642.
Bell, A., Wernli, B., and Franklin, R. M. (1994). Roles of peptidyl-pr olyl cis-trans isomerase and calcineurin in the mechanisms of antimala rial action of cyclosporin A, FK506, and rapamycin. Biochem Pharma col *48*, 495-503.
Belludi, A., Belludi, S., Bhardwaj, A., and Dilliwal, S. (2012). Crouzo n syndrome--A case report. Gen Dent *60*, e162-165.
Bikkavilli, R. K., Feigin, M. E., and Malbon, C. C. (2008). p38 mito gen-activated protein kinase regulates canonical Wnt-beta-catenin signal ing by inactivation of GSK3beta. Journal of cell science *121*, 3598-36 07.
Brognard, J., and Hunter, T. (2011). Protein kinase signaling networks in cancer. Curr Opin Genet Dev *21*, 4-11.
Caliceti, C., Nigro, P., Rizzo, P., and Ferrari, R. (2014). ROS, Notch, and Wnt signaling pathways: crosstalk between three major regulators of cardiovascular biology. BioMed research international *2014*, 31871 4.
Chao, S. H., Greenleaf, A. L., and Price, D. H. (2001). Juglone, an i nhibitor of the peptidyl-prolyl isomerase Pin1, also directly blocks tran scription. Nucleic Acids Res *29*, 767-773.
Chen, L., Li, D., Li, C., Engel, A., and Deng, C. X. (2003). A Ser25 2Trp [corrected] substitution in mouse fibroblast growth factor receptor 2 (Fgfr2) results in craniosynostosis. Bone *33*, 169-178.
Chen, L. J., Lebetkin, E. H., and Burka, L. T. (2005). Metabolism an d disposition of juglone in male F344 rats. Xenobiotica *35*, 1019-1034.
Chen, P., Zhang, L., Weng, T., Zhang, S., Sun, S., Chang, M., Li, Y., Zhang, B., and Zhang, L. (2014). A Ser252Trp mutation in fibroblast growth factor receptor 2 (FGFR2) mimicking human Apert syndrome reveals an essential role for FGF signaling in the regulation of endo chondral bone formation. PLoS One *9*, e87311.
Chen, S. Y., Wulf, G., Zhou, X. Z., Rubin, M. A., Lu, K. P., and Ba lk, S. P. (2006). Activation of beta-catenin signaling in prostate cancer by peptidyl-prolyl isomerase Pin1-mediated abrogation of the androge

n receptor-beta-catenin interaction. Molecular and cellular biology *26*, 929-939.
Cho, Y. D., Bae, H. S., Lee, D. S., Yoon, W. J., Woo, K. M., Baek, J. H., Lee, G., Park, J. C., Ku, Y., and Ryoo, H. M. (2016). Epigenetic Priming Confers Direct Cell Trans-Differentiation From Adipocyte to Osteoblast in a Transgene-Free State. Journal of cellular physiology *231*, 1484-1494.
Cho, Y. D., Yoon, W. J., Kim, W. J., Woo, K. M., Baek, J. H., Lee, G., Ku, Y., van Wijnen, A. J., and Ryoo, H. M. (2014). Epigenetic modifications and canonical wingless/int-1 class (WNT) signaling enable trans-differentiation of nonosteogenic cells into osteoblasts. The Journal of biological chemistry *289*, 20120-20128.
Chocarro-Calvo, A., Garcia-Martinez, J. M., Ardila-Gonzalez, S., De la Vieja, A., and Garcia-Jimenez, C. (2013). Glucose-induced beta-catenin acetylation enhances Wnt signaling in cancer. Molecular cell *49*, 474-486.
Ciurea, A. V., and Toader, C. (2009). Genetics of craniosynostosis: review of the literature. J Med Life *2*, 5-17.
Clendenning, D. E., and Mortlock, D. P. (2012). The BMP ligand Gdf6 prevents differentiation of coronal suture mesenchyme in early cranial development. PloS one *7*, e36789.
Cohen, M. M., Jr. (1993). Pfeiffer syndrome update, clinical subtypes, and guidelines for differential diagnosis. Am J Med Genet *45*, 300-307.
Cong, F., and Varmus, H. (2004). Nuclear-cytoplasmic shuttling of Axin regulates subcellular localization of beta-catenin. Proceedings of the National Academy of Sciences of the United States of America *101*, 2882-2887.
Creese, A. J., and Cooper, H. J. (2016). Separation of cis and trans Isomers of Polyproline by FAIMS Mass Spectrometry. J Am Soc Mass Spectrom *27*, 2071-2074.
Cunningham, M. L., Seto, M. L., Ratisoontorn, C., Heike, C. L., and Hing, A. V. (2007). Syndromic craniosynostosis: from history to hydrogen bonds. Orthod Craniofac Res *10*, 67-81.
Delashaw, J. B., Persing, J. A., Broaddus, W. C., and Jane, J. A. (1989). Cranial vault growth in craniosynostosis. J Neurosurg *70*, 159-165.
Derderian, C., and Seaward, J. (2012). Syndromic craniosynostosis. Semin Plast Surg *26*, 64-75.
Driver, J. A., and Lu, K. P. (2010). Pin1: a new genetic link between Alzheimer's disease, cancer and aging. Current aging science *3*, 158-

165.
Du, X., Weng, T., Sun, Q., Su, N., Chen, Z., Qi, H., Jin, M., Yin, L., He, Q., and Chen, L. (2010). Dynamic morphological changes in the skulls of mice mimicking human Apert syndrome resulting from gain -of-function mutation of FGFR2 (P253R). J Anat *217*, 97-105.
Duan, G., and Walther, D. (2015). The roles of post-translational modi fications in the context of protein interaction networks. PLoS Comput Biol *11*, e1004049.
Faedo, A., Borello, U., and Rubenstein, J. L. (2010). Repression of F gf signaling by sprouty1-2 regulates cortical patterning in two distinct regions and times. J Neurosci *30*, 4015-4023.
Filtz, T. M., Vogel, W. K., and Leid, M. (2014). Regulation of transcr iption factor activity by interconnected post-translational modifications. Trends Pharmacol Sci *35*, 76-85.
Fre, S., Pallavi, S. K., Huyghe, M., Lae, M., Janssen, K. P., Robine, S., Artavanis-Tsakonas, S., and Louvard, D. (2009). Notch and Wnt si gnals cooperatively control cell proliferation and tumorigenesis in the i ntestine. Proceedings of the National Academy of Sciences of the Uni ted States of America *106*, 6309-6314.
Fujimori, F., Takahashi, K., Uchida, C., and Uchida, T. (1999). Mice l acking Pin1 develop normally, but are defective in entering cell cycle from G(0) arrest. Biochem Biophys Res Commun *265*, 658-663.
Galindo, M., Pratap, J., Young, D. W., Hovhannisyan, H., Im, H. J., Choi, J. Y., Lian, J. B., Stein, J. L., Stein, G. S., and van Wijnen, A. J. (2005). The bone-specific expression of Runx2 oscillates during th e cell cycle to support a G1-related antiproliferative function in osteob lasts. The Journal of biological chemistry *280*, 20274-20285.
Gong, Y., Slee, R. B., Fukai, N., Rawadi, G., Roman-Roman, S., Regi nato, A. M., Wang, H., Cundy, T., Glorieux, F. H., Lev, D., *et al.* (2 001). LDL receptor-related protein 5 (LRP5) affects bone accrual and eye development. Cell *107*, 513-523.
Greenwood, J., Flodman, P., Osann, K., Boyadjiev, S. A., and Kimoni s, V. (2014). Familial incidence and associated symptoms in a populat ion of individuals with nonsyndromic craniosynostosis. Genet Med *16*, 302-310.
Hanes, S. D. (2015). Prolyl isomerases in gene transcription. Biochim Biophys Acta *1850*, 2017-2034.
Hansen, A. S., and O'Shea, E. K. (2015). Limits on information trans duction through amplitude and frequency regulation of transcription fa

ctor activity. Elife *4*.
Henderson, B. R. (2000). Nuclear-cytoplasmic shuttling of APC regulates beta-catenin subcellular localization and turnover. Nature cell biology *2*, 653-660.
Hennig, L., Christner, C., Kipping, M., Schelbert, B., Rucknagel, K. P., Grabley, S., Kullertz, G., and Fischer, G. (1998). Selective inactivation of parvulin-like peptidyl-prolyl cis/trans isomerases by juglone. Biochemistry *37*, 5953-5960.
Heuze, Y., Boyadjiev, S. A., Marsh, J. L., Kane, A. A., Cherkez, E., Boggan, J. E., and Richtsmeier, J. T. (2010). New insights into the relationship between suture closure and craniofacial dysmorphology in sagittal nonsyndromic craniosynostosis. J Anat *217*, 85-96.
Hill, T. P., Spater, D., Taketo, M. M., Birchmeier, W., and Hartmann, C. (2005). Canonical Wnt/beta-catenin signaling prevents osteoblasts from differentiating into chondrocytes. Dev Cell *8*, 727-738.
Holland, J. D., Klaus, A., Garratt, A. N., and Birchmeier, W. (2013). Wnt signaling in stem and cancer stem cells. Current opinion in cell biology *25*, 254-264.
Holmes, G., Rothschild, G., Roy, U. B., Deng, C. X., Mansukhani, A., and Basilico, C. (2009). Early onset of craniosynostosis in an Apert mouse model reveals critical features of this pathology. Dev Biol *328*, 273-284.
Hsu, T., McRackan, D., Vincent, T. S., and Gert de Couet, H. (2001). Drosophila Pin1 prolyl isomerase Dodo is a MAP kinase signal responder during oogenesis. Nat Cell Biol *3*, 538-543.
Huber, O., Korn, R., McLaughlin, J., Ohsugi, M., Herrmann, B. G., and Kemler, R. (1996). Nuclear localization of beta-catenin by interaction with transcription factor LEF-1. Mechanisms of development *59*, 3-10.
Ibrahimi, O. A., Zhang, F., Eliseenkova, A. V., Itoh, N., Linhardt, R. J., and Mohammadi, M. (2004). Biochemical analysis of pathogenic ligand-dependent FGFR2 mutations suggests distinct pathophysiological mechanisms for craniofacial and limb abnormalities. Human molecular genetics *13*, 2313-2324.
Inoue, T., Kagawa, T., Fukushima, M., Shimizu, T., Yoshinaga, Y., Takada, S., Tanihara, H., and Taga, T. (2006). Activation of canonical Wnt pathway promotes proliferation of retinal stem cells derived from adult mouse ciliary margin. Stem Cells *24*, 95-104.
Islam, R., Bae, H. S., Yoon, W. J., Woo, K. M., Baek, J. H., Kim, H. H., Uchida, T., and Ryoo, H. M. (2014a). Pin1 regulates osteoclast

fusion through suppression of the master regulator of cell fusion DC-STAMP. J Cell Physiol *229*, 2166-2174.
Islam, R., Yoon, W. J., and Ryoo, H. M. (2016). Pin1, the Master Or chestrator of Bone Cell Differentiation. Journal of cellular physiology.
Islam, R., Yoon, W. J., and Ryoo, H. M. (2017). Pin1, the Master Or chestrator of Bone Cell Differentiation. J Cell Physiol *232*, 2339-2347.
Islam, R., Yoon, W. J., Woo, K. M., Baek, J. H., and Ryoo, H. M. (2014b). Pin1-mediated prolyl isomerization of Runx1 affects PU.1 exp ression in pre-monocytes. J Cell Physiol *229*, 443-452.
Jensen, O. N. (2006). Interpreting the protein language using proteomi cs. Nat Rev Mol Cell Biol *7*, 391-403.
Jeon, E. J., Lee, K. Y., Choi, N. S., Lee, M. H., Kim, H. N., Jin, Y. H., Ryoo, H. M., Choi, J. Y., Yoshida, M., Nishino, N., *et al.* (200 6). Bone morphogenetic protein-2 stimulates Runx2 acetylation. J Biol Chem *281*, 16502-16511.
Jeong, H. G., Pokharel, Y. R., Lim, S. C., Hwang, Y. P., Han, E. H., Yoon, J. H., Ahn, S. G., Lee, K. Y., and Kang, K. W. (2009). Nove l role of Pin1 induction in type II collagen-mediated rheumatoid arthri tis. Journal of immunology *183*, 6689-6697.
Jian, H., Shen, X., Liu, I., Semenov, M., He, X., and Wang, X. F. (2 006). Smad3-dependent nuclear translocation of beta-catenin is required for TGF-beta1-induced proliferation of bone marrow-derived adult hu man mesenchymal stem cells. Genes & development *20*, 666-674.
Jin, S. W., Sim, K. B., and Kim, S. D. (2016). Development and Gro wth of the Normal Cranial Vault : An Embryologic Review. J Korean Neurosurg Soc *59*, 192-196.
Johnson, D., and Wilkie, A. O. (2011). Craniosynostosis. Eur J Hum Genet *19*, 369-376.
Kannan, K., and Givol, D. (2000). FGF receptor mutations: dimerizati on syndromes, cell growth suppression, and animal models. IUBMB L ife *49*, 197-205.
Kim, H. J., Kim, J. H., Bae, S. C., Choi, J. Y., Kim, H. J., and Ryo o, H. M. (2003). The protein kinase C pathway plays a central role i n the fibroblast growth factor-stimulated expression and transactivation activity of Runx2. J Biol Chem *278*, 319-326.
Kim, H. J., Park, H. D., Kim, J. H., Cho, J. Y., Choi, J. Y., Kim, J. K., Kim, H. J., Shin, H. I., and Ryoo, H. M. (2004). Establishment and characterization of a stable cell line to evaluate cellular Runx2 ac tivity. J Cell Biochem *91*, 1239-1247.
Kim, J. H., Liu, X., Wang, J., Chen, X., Zhang, H., Kim, S. H., Cui,

J., Li, R., Zhang, W., Kong, Y., *et al.* (2013). Wnt signaling in bone formation and its therapeutic potential for bone diseases. Therapeutic advances in musculoskeletal disease *5*, 13-31.
Kim, W. J., Islam, R., Kim, B. S., Cho, Y. D., Yoon, W. J., Baek, J. H., Woo, K. M., and Ryoo, H. M. (2016). Direct Delivery of Recombinant Pin1 Protein Rescued Osteoblast Differentiation of Pin1 Deficient Cells. Journal of cellular physiology.
Kim, W. J., Islam, R., Kim, B. S., Cho, Y. D., Yoon, W. J., Baek, J. H., Woo, K. M., and Ryoo, H. M. (2017). Direct Delivery of Recombinant Pin1 Protein Rescued Osteoblast Differentiation of Pin1-Deficient Cells. J Cell Physiol *232*, 2798-2805.
Kimonis, V., Gold, J. A., Hoffman, T. L., Panchal, J., and Boyadjiev, S. A. (2007). Genetics of craniosynostosis. Semin Pediatr Neurol *14*, 150-161.
Kirkbride, K. C., Townsend, T. A., Bruinsma, M. W., Barnett, J. V., and Blobe, G. C. (2008). Bone morphogenetic proteins signal through the transforming growth factor-beta type III receptor. J Biol Chem *283*, 7628-7637.
Koca, T. T. (2016). Apert syndrome: A case report and review of the literature. North Clin Istanb *3*, 135-139.
Kolpakova, E., and Olsen, B. R. (2005). Wnt/beta-catenin--a canonical tale of cell-fate choice in the vertebrate skeleton. Dev Cell *8*, 626-627.
Komori, T. (2010). Regulation of osteoblast differentiation by Runx2. Adv Exp Med Biol *658*, 43-49.
Komori, T., Yagi, H., Nomura, S., Yamaguchi, A., Sasaki, K., Deguchi, K., Shimizu, Y., Bronson, R. T., Gao, Y. H., Inada, M., *et al.* (1997). Targeted disruption of Cbfa1 results in a complete lack of bone formation owing to maturational arrest of osteoblasts. Cell *89*, 755-764.
Kramps, T., Peter, O., Brunner, E., Nellen, D., Froesch, B., Chatterjee, S., Murone, M., Zullig, S., and Basler, K. (2002). Wnt/wingless signaling requires BCL9/legless-mediated recruitment of pygopus to the nuclear beta-catenin-TCF complex. Cell *109*, 47-60.
Kreiborg, S., and Cohen, M. M., Jr. (2010). Ocular manifestations of Apert and Crouzon syndromes: qualitative and quantitative findings. J Craniofac Surg *21*, 1354-1357.
Kuersten, S., Ohno, M., and Mattaj, I. W. (2001). Nucleocytoplasmic transport: Ran, beta and beyond. Trends Cell Biol *11*, 497-503.
Lakso, M., Pichel, J. G., Gorman, J. R., Sauer, B., Okamoto, Y., Lee, E., Alt, F. W., and Westphal, H. (1996). Efficient in vivo manipulati

on of mouse genomic sequences at the zygote stage. Proceedings of t he National Academy of Sciences of the United States of America *93*, 5860-5865.
Lee, Y. C., Song, I. W., Pai, Y. J., Chen, S. D., and Chen, Y. T. (20 17). Knock-in human FGFR3 achondroplasia mutation as a mouse mo del for human skeletal dysplasia. Sci Rep *7*, 43220.
Lim, J., and Lu, K. P. (2005). Pinning down phosphorylated tau and t auopathies. Biochimica et biophysica acta *1739*, 311-322.
Lindner, U., Kramer, J., Rohwedel, J., and Schlenke, P. (2010). Mesen chymal Stem or Stromal Cells: Toward a Better Understanding of The ir Biology? Transfus Med Hemother *37*, 75-83.
Liou, Y. C., Zhou, X. Z., and Lu, K. P. (2011). Prolyl isomerase Pin 1 as a molecular switch to determine the fate of phosphoproteins. Tre nds in biochemical sciences *36*, 501-514.
Little, R. D., Carulli, J. P., Del Mastro, R. G., Dupuis, J., Osborne, M., Folz, C., Manning, S. P., Swain, P. M., Zhao, S. C., Eustace, B., *et al.* (2002). A mutation in the LDL receptor-related protein 5 gene results in the autosomal dominant high-bone-mass trait. Am J Hum Genet *70*, 11-19.
Logan, C. Y., and Nusse, R. (2004). The Wnt signaling pathway in d evelopment and disease. Annual review of cell and developmental biol ogy *20*, 781-810.
Long, F., and Ornitz, D. M. (2013). Development of the endochondral skeleton. Cold Spring Harb Perspect Biol *5*, a008334.
Lu, K. P., Finn, G., Lee, T. H., and Nicholson, L. K. (2007). Prolyl c is-trans isomerization as a molecular timer. Nat Chem Biol *3*, 619-629.
Lu, K. P., Hanes, S. D., and Hunter, T. (1996). A human peptidyl-pro lyl isomerase essential for regulation of mitosis. Nature *380*, 544-547.
Lu, K. P., and Zhou, X. Z. (2007). The prolyl isomerase PIN1: a piv otal new twist in phosphorylation signalling and disease. Nat Rev Mol Cell Biol *8*, 904-916.
Lu, Z., and Hunter, T. (2014). Prolyl isomerase Pin1 in cancer. Cell Res *24*, 1033-1049.
Luu, H. H., Zhang, R., Haydon, R. C., Rayburn, E., Kang, Q., Si, W., Park, J. K., Wang, H., Peng, Y., Jiang, W., and He, T. C. (2004). W nt/beta-catenin signaling pathway as a novel cancer drug target. Curre nt cancer drug targets *4*, 653-671.
MacDonald, B. T., Tamai, K., and He, X. (2009). Wnt/beta-catenin sig naling: components, mechanisms, and diseases. Developmental cell *17*, 9-26.

Maga, A. M., Navarro, N., Cunningham, M. L., and Cox, T. C. (201 5). Quantitative trait loci affecting the 3D skull shape and size in mo use and prioritization of candidate genes in-silico. Front Physiol *6*, 92.
Moazen, M., Peskett, E., Babbs, C., Pauws, E., and Fagan, M. J. (20 15). Mechanical properties of calvarial bones in a mouse model for cr aniosynostosis. PLoS One *10*, e0125757.
Mohan, R. S., Vemanna, N. S., Verma, S., and Agarwal, N. (2012). C rouzon syndrome: clinico-radiological illustration of a case. J Clin Ima ging Sci *2*, 70.
Molenaar, M., van de Wetering, M., Oosterwegel, M., Peterson-Madur o, J., Godsave, S., Korinek, V., Roose, J., Destree, O., and Clevers, H. (1996). XTcf-3 transcription factor mediates beta-catenin-induced axis formation in Xenopus embryos. Cell *86*, 391-399.
Morin, P. J. (1999). beta-catenin signaling and cancer. BioEssays : ne ws and reviews in molecular, cellular and developmental biology *21*, 1021-1030.
Morriss-Kay, G. M., and Wilkie, A. O. (2005). Growth of the normal skull vault and its alteration in craniosynostosis: insights from human genetics and experimental studies. J Anat *207*, 637-653.
Nakamura, K., Kosugi, I., Lee, D. Y., Hafner, A., Sinclair, D. A., Ry o, A., and Lu, K. P. (2012). Prolyl isomerase Pin1 regulates neuronal differentiation via beta-catenin. Molecular and cellular biology *32*, 29 66-2978.
Neufeld, K. L., Zhang, F., Cullen, B. R., and White, R. L. (2000). A PC-mediated downregulation of beta-catenin activity involves nuclear s equestration and nuclear export. Embo Rep *1*, 519-523.
Nishi, K., Yoshida, M., Fujiwara, D., Nishikawa, M., Horinouchi, S., and Beppu, T. (1994). Leptomycin B targets a regulatory cascade of c rm1, a fission yeast nuclear protein, involved in control of higher ord er chromosome structure and gene expression. The Journal of biologic al chemistry *269*, 6320-6324.
Ornitz, D. M., and Marie, P. J. (2015). Fibroblast growth factor signal ing in skeletal development and disease. Genes Dev *29*, 1463-1486.
Park, M. H., Shin, H. I., Choi, J. Y., Nam, S. H., Kim, Y. J., Kim, H. J., and Ryoo, H. M. (2001). Differential expression patterns of Ru nx2 isoforms in cranial suture morphogenesis. Journal of bone and mi neral research : the official journal of the American Society for Bone and Mineral Research *16*, 885-892.
Park, M. S., Yoo, J. E., Chung, J., and Yoon, S. H. (2006). A case o f Pfeiffer syndrome. J Korean Med Sci *21*, 374-378.

Park, O. J., Kim, H. J., Woo, K. M., Baek, J. H., and Ryoo, H. M. (2010). FGF2-activated ERK mitogen-activated protein kinase enhances Runx2 acetylation and stabilization. J Biol Chem *285*, 3568-3574.
Park, W. J., Theda, C., Maestri, N. E., Meyers, G. A., Fryburg, J. S., Dufresne, C., Cohen, M. M., Jr., and Jabs, E. W. (1995). Analysis o f phenotypic features and FGFR2 mutations in Apert syndrome. Am J Hum Genet *57*, 321-328.
Phupong, V., Srichomthong, C., and Shotelersuk, V. (2004). Prenatal e xclusion of Crouzon syndrome by mutation analysis of FGFR2. South east Asian J Trop Med Public Health *35*, 977-979.
Reese, S., Vidyasagar, A., Jacobson, L., Acun, Z., Esnault, S., Hullett, D., Malter, J. S., and Djamali, A. (2010). The Pin 1 inhibitor juglon e attenuates kidney fibrogenesis via Pin 1-independent mechanisms in the unilateral ureteral occlusion model. Fibrogenesis Tissue Repair *3*, 1.
Rice, D. P. (2008). Craniofacial sutures. Development, disease and trea tment. Preface. Front Oral Biol *12*, xi.
Robin, N. H., Falk, M. J., and Haldeman-Englert, C. R. (1993). FGF R-Related Craniosynostosis Syndromes. In GeneReviews(R), R.A. Pago n, M.P. Adam, H.H. Ardinger, S.E. Wallace, A. Amemiya, L.J.H. Bea n, T.D. Bird, N. Ledbetter, H.C. Mefford, R.J.H. Smith, and K. Steph ens, eds. (Seattle (WA)).
Rosin-Arbesfeld, R., Townsley, F., and Bienz, M. (2000). The APC tu mour suppressor has a nuclear export function. Nature *406*, 1009-1012.
Ruan, M. Z., Cerullo, V., Cela, R., Clarke, C., Lundgren-Akerlund, E., Barry, M. A., and Lee, B. H. (2016). Treatment of osteoarthritis usin g a helper-dependent adenoviral vector retargeted to chondrocytes. Mol Ther Methods Clin Dev *3*, 16008.
Ruan, M. Z., Dawson, B., Jiang, M. M., Gannon, F., Heggeness, M., and Lee, B. H. (2013). Quantitative imaging of murine osteoarthritic c artilage by phase-contrast micro-computed tomography. Arthritis Rheum *65*, 388-396.
Ryo, A., Nakamura, M., Wulf, G., Liou, Y. C., and Lu, K. P. (2001). Pin1 regulates turnover and subcellular localization of beta-catenin by inhibiting its interaction with APC. Nature cell biology *3*, 793-801.
Saling, S. C., Comar, J. F., Mito, M. S., Peralta, R. M., and Bracht, A. (2011). Actions of juglone on energy metabolism in the rat liver. Toxicol Appl Pharmacol *257*, 319-327.
Samatha, Y., Vardhan, T. H., Kiran, A. R., Sankar, A. J., and Ramakr ishna, B. (2010). Familial Crouzon syndrome. Contemp Clin Dent *1*,

277-280.
Senarath-Yapa, K., Li, S., Meyer, N. P., Longaker, M. T., and Quarto, N. (2013). Integration of multiple signaling pathways determines differences in the osteogenic potential and tissue regeneration of neural crest-derived and mesoderm-derived calvarial bones. Int J Mol Sci *14*, 5978-5997.
Shen, Z. J., Hu, J., Ali, A., Pastor, J., Shiizaki, K., Blank, R. D., Kuro-o, M., and Malter, J. S. (2013). Pin1 null mice exhibit low bone mass and attenuation of BMP signaling. PloS one *8*, e63565.
Shin, H. R., Islam, R., Yoon, W. J., Lee, T., Cho, Y. D., Bae, H. S., Kim, B. S., Woo, K. M., Baek, J. H., and Ryoo, H. M. (2016). Pin1-mediated Modification Prolongs the Nuclear Retention of beta-Catenin in Wnt3a-induced Osteoblast Differentiation. J Biol Chem *291*, 5555-5565.
Shukla, V., Coumoul, X., Wang, R. H., Kim, H. S., and Deng, C. X. (2007). RNA interference and inhibition of MEK-ERK signaling prevent abnormal skeletal phenotypes in a mouse model of craniosynostosis. Nat Genet *39*, 1145-1150.
Slaney, S. F., Oldridge, M., Hurst, J. A., Moriss-Kay, G. M., Hall, C. M., Poole, M. D., and Wilkie, A. O. (1996). Differential effects of FGFR2 mutations on syndactyly and cleft palate in Apert syndrome. Am J Hum Genet *58*, 923-932.
Smith, T. G., Sweetman, D., Patterson, M., Keyse, S. M., and Munsterberg, A. (2005). Feedback interactions between MKP3 and ERK MAP kinase control scleraxis expression and the specification of rib progenitors in the developing chick somite. Development *132*, 1305-1314.
Snider, N. T., and Omary, M. B. (2014). Post-translational modifications of intermediate filament proteins: mechanisms and functions. Nat Rev Mol Cell Biol *15*, 163-177.
Su, N., Jin, M., and Chen, L. (2014). Role of FGF/FGFR signaling in skeletal development and homeostasis: learning from mouse models. Bone Res *2*, 14003.
Suizu, F., Ryo, A., Wulf, G., Lim, J., and Lu, K. P. (2006). Pin1 regulates centrosome duplication, and its overexpression induces centrosome amplification, chromosome instability, and oncogenesis. Molecular and cellular biology *26*, 1463-1479.
Suzuki, H., Suda, N., Shiga, M., Kobayashi, Y., Nakamura, M., Iseki, S., and Moriyama, K. (2012). Apert syndrome mutant FGFR2 and its soluble form reciprocally alter osteogenesis of primary calvarial osteoblasts. J Cell Physiol *227*, 3267-3277.

Tanimoto, Y., Yokozeki, M., Hiura, K., Matsumoto, K., Nakanishi, H., Matsumoto, T., Marie, P. J., and Moriyama, K. (2004). A soluble form of fibroblast growth factor receptor 2 (FGFR2) with S252W mutation acts as an efficient inhibitor for the enhanced osteoblastic differentiation caused by FGFR2 activation in Apert syndrome. The Journal of biological chemistry *279*, 45926-45934.

Teven, C. M., Farina, E. M., Rivas, J., and Reid, R. R. (2014). Fibroblast growth factor (FGF) signaling in development and skeletal diseases. Genes Dis *1*, 199-213.

Thorpe, J. R., Morley, S. J., and Rulten, S. L. (2001). Utilizing the peptidyl-prolyl cis-trans isomerase pin1 as a probe of its phosphorylated target proteins. Examples of binding to nuclear proteins in a human kidney cell line and to tau in Alzheimer's diseased brain. J Histochem Cytochem *49*, 97-108.

Tolwinski, N. S., and Wieschaus, E. (2001). Armadillo nuclear import is regulated by cytoplasmic anchor Axin and nuclear anchor dTCF/Pan. Development *128*, 2107-2117.

Townsley, F. M., Cliffe, A., and Bienz, M. (2004). Pygopus and Legless target Armadillo/beta-catenin to the nucleus to enable its transcriptional co-activator function. Nat Cell Biol *6*, 626-633.

Twigg, S. R., and Wilkie, A. O. (2015). A Genetic-Pathophysiological Framework for Craniosynostosis. American journal of human genetics *97*, 359-377.

Vogels, A., and Fryns, J. P. (2006). Pfeiffer syndrome. Orphanet J Rare Dis *1*, 19.

Wang, Y., Sun, M., Uhlhorn, V. L., Zhou, X., Peter, I., Martinez-Abadias, N., Hill, C. A., Percival, C. J., Richtsmeier, J. T., Huso, D. L., and Jabs, E. W. (2010). Activation of p38 MAPK pathway in the skull abnormalities of Apert syndrome Fgfr2(+P253R) mice. BMC Dev Biol *10*, 22.

Wang, Y., Xiao, R., Yang, F., Karim, B. O., Iacovelli, A. J., Cai, J., Lerner, C. P., Richtsmeier, J. T., Leszl, J. M., Hill, C. A., *et al.* (2005). Abnormalities in cartilage and bone development in the Apert syndrome FGFR2(+/S252W) mouse. Development *132*, 3537-3548.

Warner, D. R., Greene, R. M., and Pisano, M. M. (2005). Cross-talk between the TGFbeta and Wnt signaling pathways in murine embryonic maxillary mesenchymal cells. FEBS letters *579*, 3539-3546.

Watanabe, M., Fukuda, M., Yoshida, M., Yanagida, M., and Nishida, E. (1999). Involvement of CRM1, a nuclear export receptor, in mRNA export in mammalian cells and fission yeast. Genes Cells *4*, 291-297.

Westendorf, J. J., Kahler, R. A., and Schroeder, T. M. (2004). Wnt si gnaling in osteoblasts and bone diseases. Gene *341*, 19-39.
Widelitz, R. (2005). Wnt signaling through canonical and non-canonica l pathways: recent progress. Growth Factors *23*, 111-116.
Wolff, B., Sanglier, J. J., and Wang, Y. (1997). Leptomycin B is an i nhibitor of nuclear export: inhibition of nucleo-cytoplasmic translocatio n of the human immunodeficiency virus type 1 (HIV-1) Rev protein a nd Rev-dependent mRNA. Chemistry & biology *4*, 139-147.
Wu, X., Tu, X., Joeng, K. S., Hilton, M. J., Williams, D. A., and Lo ng, F. (2008). Rac1 activation controls nuclear localization of beta-cate nin during canonical Wnt signaling. Cell *133*, 340-353.
Wulf, G., Ryo, A., Liou, Y. C., and Lu, K. P. (2003). The prolyl iso merase Pin1 in breast development and cancer. Breast cancer research : BCR *5*, 76-82.
Xu, J., Li, Z., Hou, Y., and Fang, W. (2015). Potential mechanisms u nderlying the Runx2 induced osteogenesis of bone marrow mesenchym al stem cells. Am J Transl Res *7*, 2527-2535.
Yang, F., Wang, Y., Zhang, Z., Hsu, B., Jabs, E. W., and Elisseeff, J. H. (2008). The study of abnormal bone development in the Apert sy ndrome Fgfr2+/S252W mouse using a 3D hydrogel culture model. Bo ne *43*, 55-63.
Yang, W., Zheng, Y., Xia, Y., Ji, H., Chen, X., Guo, F., Lyssiotis, C. A., Aldape, K., Cantley, L. C., and Lu, Z. (2012). ERK1/2-dependent phosphorylation and nuclear translocation of PKM2 promotes the War burg effect. Nature cell biology *14*, 1295-1304.
Yin, L., Du, X., Li, C., Xu, X., Chen, Z., Su, N., Zhao, L., Qi, H., Li, F., Xue, J., *et al.* (2008). A Pro253Arg mutation in fibroblast gro wth factor receptor 2 (Fgfr2) causes skeleton malformation mimicking human Apert syndrome by affecting both chondrogenesis and osteoge nesis. Bone *42*, 631-643.
Yoon, W. J., Cho, Y. D., Kim, W. J., Bae, H. S., Islam, R., Woo, K. M., Baek, J. H., Bae, S. C., and Ryoo, H. M. (2014a). Prolyl isome rase Pin1-mediated conformational change and subnuclear focal accum ulation of Runx2 are crucial for fibroblast growth factor 2 (FGF2)-ind uced osteoblast differentiation. J Biol Chem *289*, 8828-8838.
Yoon, W. J., Islam, R., Cho, Y. D., Ryu, K. M., Shin, H. R., Woo, K. M., Baek, J. H., and Ryoo, H. M. (2014b). Pin1 Plays a Critical Role as a Molecular Switch in Canonical BMP Signaling. Journal of cellular physiology.
Yoon, W. J., Islam, R., Cho, Y. D., Ryu, K. M., Shin, H. R., Woo,

K. M., Baek, J. H., and Ryoo, H. M. (2015a). Pin1 plays a critical r ole as a molecular switch in canonical BMP signaling. J Cell Physiol *230*, 640-647.
Yoon, W. J., Islam, R., Cho, Y. D., Ryu, K. M., Shin, H. R., Woo, K. M., Baek, J. H., and Ryoo, H. M. (2015b). Pin1 Plays a Critical Role as a Molecular Switch in Canonical BMP Signaling. Journal of cellular physiology *230*, 640-647.
Yoon, W. J., Islam, R., Cho, Y. D., Woo, K. M., Baek, J. H., Uchida, T., Komori, T., van Wijnen, A., Stein, J. L., Lian, J. B., *et al.* (201 3a). Pin1-mediated Runx2 modification is critical for skeletal develop ment. J Cell Physiol *228*, 2377-2385.
Yoon, W. J., Islam, R., Cho, Y. D., Woo, K. M., Baek, J. H., Uchida, T., Komori, T., van Wijnen, A., Stein, J. L., Lian, J. B., *et al.* (201 3b). Pin1-Mediated Runx2 Modification Is Critical for Skeletal Develo pment. Journal of cellular physiology *228*, 2377-2385.
Yu, K., Herr, A. B., Waksman, G., and Ornitz, D. M. (2000). Loss of fibroblast growth factor receptor 2 ligand-binding specificity in Apert syndrome. Proceedings of the National Academy of Sciences of the United States of America *97*, 14536-14541.
Yun, M. S., Kim, S. E., Jeon, S. H., Lee, J. S., and Choi, K. Y. (20 05). Both ERK and Wnt/beta-catenin pathways are involved in Wnt3a-induced proliferation. Journal of cell science *118*, 313-322.
Zhang, M., Wang, M., Tan, X., Li, T. F., Zhang, Y. E., and Chen, D. (2010). Smad3 prevents beta-catenin degradation and facilitates beta-c atenin nuclear translocation in chondrocytes. The Journal of biological chemistry *285*, 8703-8710.
Zhang, W., Li, Y., Luo, J., Lu, X., Chen, M., Zhu, W., and Jiang, Y. (2015). [Juglone inhibits proliferation and induces apoptosis of human cervical squamous cancer SiHa cells]. Xi Bao Yu Fen Zi Mian Yi X ue Za Zhi *31*, 186-189.

국문초록

뼈 형성에서 Pin1 매개 이성질화의 역할

서울대학교 대학원 치의과학과 분자유전학전공
(지도교수 류 현 모)
신 혜 림

단백질의 인산화, 아세틸화, 또는 유비퀴틴화와 같은 다양한 합성 후 수식 과정은 단백질의 구조와 기능까지 변화시키는 매우 중요한 과정이다. 특히, 세포에서 가장 많이 일어난다고 보고된 합성 후 수식은 인산화로, 이러한 인산화 된 잔기를 인식하여 이성질화를 통한 단백질의 구조적 변환을 야기하는 효소로 Pin1이 있다. Pin1은 pavuylin family에 속하는 이성질화 효소로, 오직 인산화 된 세린/트레오닌 다음에 프롤린 잔기가 오는 자리만을 인식하여 단백질 구조 변화를 유도한다. 최근 연구에서는 Pin1의 null mice가 뼈 발달 과정이 제대로 일어나지 못하는 것을 밝혔고, 뼈를 만드는 조골세포를 조절하는 신호전달 과정인 FGF, BMP 그리고 PTH 신호전달에서 모두 Pin1에 의한 이성질화가 조골세포 분화를 위한 신호전달 과정에 꼭 필요하다는 것을 밝혔다.

또 다른 조골세포 분화 과정에 필요한 신호전달인 Wnt/β-catenin 신호전달 과정, 특히나 β-catenin이 핵 속으로 이동하거나 빠져나오는 과정은 매우 중요한 단계임에도 불구하고 뼈 발달 과정에서의 Wnt/β-catenin 신호전달 과정과 Pin1의 연관성은 잘 알려져 있지 않고 그 정확한 기작에 대해서도 모호하다. 따라서 우리는 먼저 Pin1 null 마우스 tibia 조직의 조골세포에서 β-catenin의 단백질 양이 정상 마우스에 비해 확연히 감소됨을 확인하였고, 이러한 in vivo 데이터를 시작으로 MC3T3-E1 조골세포주에 si Pin1와 Pin1 억제제를 이용하여 Pin1을 불활성화 시켰을 때, 핵 내 beta-catenin 수준, Wnt/β-catenin의 전사 활성, 그에 따른 타겟 유전자 발현이 모두 감소함을 확인 할 수 있었다. 이는 Pin1과 β-catenin이 직접적으로 상호작용하여, Wnt 신호전달에 의해 핵 내로 들어온 β-catenin이 Pin1에 의해 이성질화가 일어나야지만 핵 내에 유지되며 전사활성에 관여하는 인자로 작용할 수 있고, 이성질화가 되지 못할 경우 β-catenin의 export를 관여하는 APC와 함께 세포질로 빠져나가 분해되어 그 안정화 수준이 감소됨을 증명하였다. 이러한 결과는 Pin1이 Wnt/β-catenin 신호전달에 의해 조절 받는 뼈 형성 과정을 관장할 수 있는 매우 중요한 인자 임을 보여준다.

나아가 part2에서는 뼈 형성 과정에서 Pin1의 중요성을

두개봉합 조기유합증 (Craniosynostosis; 이하 CS) 질병 동물 모델을 통해서 확인하였다. CS는 두개골 봉합선이 정상인보다 일찍 유합되어 나타나는 병으로 이러한 기형은 외부의 이상은 물론 두개 용적의 감소로 두뇌 발육 부전과 뇌수종 같은 심각한 이상을 동반한다. CS는 주로 fibroblast growth factor receptor 2 (FGFR2) 유전자의 돌연변이에 의해 상염색체 우성 유전되며, 본 연구에서는 에이퍼트 신드롬을 야기하는 FGFR2 S252W knock-in 마우스를 사용하여 주요 표현형 중 하나인 관상 봉합 유합증의 변화에 초점을 두고 연구를 진행하였다. 따라서 본 연구는 그 동안 본 연구팀이 밝힌 FGF 신호에 의한 Runx2의 합성 후 수식 과정에서 Pin1에 의한 Runx2의 이성질화 부분을 억제함으로써 과 활성 된 FGF 신호에 의한 질병을 치료하고자 하는 목적으로 시작되었다. 그 결과 CS 표현형을 나타내는 FGFR2S252W/+ 유전형과 Pin1+/- 유전형이 동시에 존재할 경우, 두개골의 관상봉합 유합증이 정상 형질에 가깝게 회복되는 것을 확인하였고 이는 약물 치료로 발전하기 위해 FGFR2S252W/+ 마우스의 태아에 Pin1 억제제인 juglone을 투약하였 때에도 같은 치료 효과를 보였다.

본 논문에서는 beta-catenin과 Pin1의 직접적인 상호작용을 통한 β-catenin의 이성질화가 핵 내 β-catenin 유지와 그 안정성을

조절하는 중요 인자임을 보여준다. 또한 또 다른 조골세포 분화 신호전달 중 하나인 FGF 신호가 과도함에 따라 야기된 질병인 CS 질병 동물 모델을 통하여 Pin1의 불활성화가 질병의 회복을 야기하는 것을 증명하였다. 이는 CS 질병의 약물 타겟을 제시함과 동시에 FGF/FGFR를 통한 Runx2 단백질 PTM 과정에서 Pin1에 의한 이성질화의 중요성을 in vivo에서 증명한 의의를 가진다.

주요어 : 이성질화, Pin1, Wnt/β-catenin 신호전달, FGFR, 뼈 형성, 두개조기유합증

학 번 : 2011-23826